(-)-Δ^9-tetrahydrocannabinol and pregnancy: transporter-mediated tissue distribution and drug interactions

Xin Chen

A dissertation
submitted in partial fulfillment of the
requirements for the degree of

Doctor of Philosophy

University of Washington
2025

Reading Committee

Jashvant D. Unadkat, Chair
Julia Y. Cui
Yvonne S. Lin

Program Authorized to Offer Degree

Pharmaceutics

University of Washington

Abstract

(-)-Δ^9-tetrahydrocannabinol and pregnancy: transporter-mediated tissue distribution and drug interactions

Xin Chen

Chair of the Supervisory Committee

Jashvant D. Unadkat

Department of Pharmaceutics

As cannabis use during pregnancy increases [1], it is important to understand the mechanisms and extent of placental transfer of (-)-*trans*-Δ^9-tetrahydrocannabinol (THC), the primary intoxicating constitute of cannabis, along with its circulating major metabolites [2,3]. In a nonhuman primate study, the fetal plasma exposure to THC is about 30% of the maternal exposure [4]. Similarly, in a human study of daily cannabis smokers, the average THC umbilical vein-to-maternal serum concentration ratio at delivery was 0.26 ± 0.10 (n = 3) [5]. This reduced fetal exposure to THC in nonhuman primates and humans is likely attributed to the placenta's ability to limit fetal exposure to xenobiotics. However, the exact mechanisms behind this protection are not fully understood. Since many transporters on both the maternal and fetal side of the syncytiotrophoblast are expressed in the placenta, we hypothesized that the reduced fetal exposure to THC could be attributed to apical (maternal-facing) efflux transporters [*i.e.*, P-glycoprotein (P-gp) and/or breast cancer resistance protein (BCRP)], or basal (fetal-facing) uptake transporters [*i.e.*, organic anion transporting polypeptide 2B1 (OATP2B1), organic cation transporter (OCT3), and/or organic anion transporter 4 (OAT4)], or both [6]. Therefore, we evaluated, *in vitro* and *in vivo,* whether THC and its major metabolites, 11-hydroxy-THC (11-

OH-THC), 11-*nor*-9-carboxy-THC (THC-COOH) are substrates of key placental efflux and uptake transporters at their pharmacologically relevant concentrations (**Chapters 2, 3, and 4**).

Cannabinoid-drug interactions may occur if the cannabinoid, at its pharmacologically relevant plasma concentrations, is a significant inhibitor of the transporter involved in the drug's tissue distribution or clearance. Therefore, we also investigated if THC and its major metabolites, 11-OH-THC and THC-COOH, are inhibitors of key placental/hepatic efflux and uptake transporters at their pharmacologically relevant concentrations (**Chapters 2 and 4**).

To test the above hypotheses, we examined in **Chapter 2**, if THC and its major metabolites interact with key placental efflux transporters using cell lines that overexpress human P-gp or BCRP. At pharmacologically relevant concentrations, neither THC nor 11-OH-THC were substrates or inhibitors of P-gp or BCRP. THC-COOH, however, showed weak substrate and inhibitory activity for BCRP but not P-gp. Therefore, the placental efflux transporters P-gp and BCRP are unlikely to cause the reduced fetal-to-maternal exposure ratio of THC observed in humans or non-human primates. Moreover, THC and its metabolites are unlikely to produce cannabinoid-drug interactions at pharmacologically relevant concentrations. These findings contrast with earlier rodent studies which suggest that THC is a substrate of P-gp and Bcrp [7,8], suggesting species-specific differences in transport of THC.

THC and its major metabolites are highly lipophilic with extensive nonspecific binding. Therefore, the above studies may be confounded by our inability to detect cannabinoid transport in the background of high non-specific binding. Others, using P-gp knock-out mice, have found that THC is a substrate of P-gp when it is administered orally [8]. Therefore, in **Chapter 3**, we investigated maternal-fetal THC distribution and disposition in P-gp and/or Bcrp knockout pregnant mice. However, no significant changes in fetal-to-maternal area under the plasma concentration-time (AUC) ratios of THC or its metabolites were observed among all genotypes. Surprisingly, P-gp-deficient pregnant mice had significantly lower maternal brain/maternal plasma AUC ratios of THC compared to the wild type pregnant mice, suggesting an interaction of P-gp knock-out with other unknown transporters or brain fatty acid binding proteins (FABPs) to which THC binds [9].

Since the above studies indicated that placental efflux transporters cannot explain the reduced fetal exposure to THC observed in human and non-human primates, in **Chapter 4**, we investigated if placental basal uptake transporters (*i.e.*, OATP2B1, OCT3, OAT4) could be

responsible for these observations. Given that THC and its metabolites are cleared by the liver [10], we also investigated if THC and its metabolites were substrates or inhibitors of the hepatic uptake transporters [OATP1B1, OATP1B3, OCT1, OAT4, sodium taurocholate cotransporter protein (NTCP)]. None of the cannabinoids interacted with these transporters, except for hepatic OCT1, which transported both THC and THC-COOH at their pharmacologically relevant concentrations. However, at these concentrations, they were not inhibitors of OCT1. Therefore, OATP2B1, OCT3, and OAT4 are also unlikely to be responsible for the reduced fetal exposure to THC. Also, this suggests that co-administration of OCT1 inhibitors with THC or THC-COOH could reduce the *in vivo* hepatic distribution of these cannabinoids provided OCT1 plays a significant role (vis-à-vis passive diffusion) in their distribution.

In summary, our research indicates that the major placental efflux and uptake transporters, in humans or mice, are not responsible for limiting the observed fetal THC exposure in human and nonhuman primates, pointing to other placental transporters or alternative mechanisms. The identification of hepatic OCT1 as a transporter for THC and THC-COOH suggests possible OCT1-based drug interactions in their *in vivo* disposition. These findings lay the groundwork for future studies on cannabinoid pharmacokinetics, including during pregnancy, and highlight the importance of considering species differences when extrapolating from preclinical data to humans.

Acknowledgements

The journey of graduate research would not have been possible without the support, guidance, and encouragement of many wonderful people.

First and foremost, I would like to express my deepest gratitude to my advisors, Jashvant D. Unadkat and the late Qingcheng Mao. I still vividly recall our first meeting in 2019. Having such outstanding advisors has been not only a tremendous fortune during my graduate studies but also a lifelong gift. From you, I learned not only the beauty of science but also invaluable lessons about life and philosophy. Your dedicated mentorship and warm support enabled me to explore the world of transporters and pregnancy pharmacology. The sudden passing of Qingcheng Mao in 2023 was a profound shock, but it also taught me resilience and maturity in facing life's hardships and challenges. Thank you both for your patience and unwavering dedication, which have been instrumental in my personal and academic growth.

I am also deeply grateful to my committee members: Julia Y. Cui, Edward J. Kelly, Yvonne S. Lin, and Libin Xu, for their constructive feedback, insightful comments, and the resources they provided, all of which greatly improved my dissertation and experimental work. My sincere thanks go to all past and present members of the Unadkat and Mao labs, and all of my collaborators. Your support during difficult times has been invaluable, and I wish each of you a bright future ahead.

To my friends and roommates, both near and far, past and present, thank you for your companionship and encouragement. Special thanks to Xia Su for introducing me to powerlifting and to Maochuan Zhang for bringing me into the world of badminton. Another special thank goes to Zezhou Wang for enlightening me with the beautiful world of geological landscapes, rocks, and volcanoes. I am also grateful to Zhanjiang Cao, Hsuan-hao Chen, Tuochao Chen, Xiang Chen, Zuxin Chen, Tianyi Huang, Linxing Jiang, Yu Li, Chaofeng Liu, Daogao Liu, Haiyang Liu, Sirui Lu, Yince Ma, Jingwei Ma, Ning Rui, Zekun Shao, Hugo Khiyad Shih, Xinyan Li, Huajun Xu, Heng Wan, Bingxin Wang, Zihan Wang, and Tong Zhu (alphabetically listed by the last name with no particular ranking) for the memorable times we shared in Seattle. I am also grateful for my friends and roommates during my time in Nanjing, Yunjun Cao, Hanyu Chen, Yining Chen, Jiawei Ji, Han Li, Kejiang Lin, Dongzhen Pan, Xianjin Qin, Rui Shi, Boheng Wan, Ruihan Wang, Fan Xu, Xiao Xu, Dejin Xun, Yong Yang, Yang You, Zihan Yu, Mingxiang Zhang, Likun Zhang, Shuwan Zhang, Zihao Zhu (alphabetically listed by the last

name with no particular ranking). My appreciation also goes to Fanze Kong for your support during my time in Vancouver in 2025, and to Olena Anoshchenko, Xinyue Chen, Mayur Ladumor, Jong-hua Lee, Michael Liao, Naveen Neradugomma, Hongjie Qian, Shuai Shao, Claire Steinbronn, Flavia Storelli, Xiaofan Tian, Zeyuan Wang, Sijia Yu, Yichao Yu, Guo Zhong, Lin Zhou, and Michael Zientek for your guidance and encouragement during my career and job search.

I would like to thank my mentors during my internship at Boehringer Ingelheim in 2023, Ash Sharma and Fenglei Huang, as well as my roommates there, Haote Li and Jin-gyu Kim, for their support and camaraderie.

Thank you to the Husky Taekwondo Club at the University of Washington for entrusting me with the role of treasurer and for all the wonderful experiences we shared in kicking and fighting. I am especially grateful for the guidance of Jeremy Fredericks, Catherine Tong, Patricia Ma, and Anthony Shin.

Last but not least, I wish to express my heartfelt gratitude to my parents, Ennian Chen and Cuirong Zhou, whose unwavering support made the journey of me as a first-generation college student possible, I could not have reached this point or seen such a broad world without your devotion. Special thanks to my uncle, Jinqiao Zhou, for his support of my study and for being there during my father's illness. Finally, I would like to thank my love, Mengqun Yu, for bringing light into my world and the rest of my life.

Table of Contents

Chapter 1
Introduction

1.1 Specific aims

With increased legalization and social acceptance, the recreational use of cannabis by pregnant women is increasing[1]. This increase has raised concerns about the potential short- and long-term consequences for fetal development from prenatal exposure to cannabis's primary intoxicating phytocannabinoid, (-)-*trans*-Δ^9-tetrahydrocannabiol (THC) as well as its primary intoxicating circulating metabolite, 11-hydroxy-THC (11-OH-THC) [2,3]. In humans, 11-OH-THC is further metabolized to the circulating non-intoxicating metabolite, 11-*nor*-9-carboxy-THC (THC-COOH) [3]. Therefore, it is important to understand the extent and mechanisms of fetal exposure to THC and its major metabolites, 11-OH-THC and THC-COOH. A nonhuman primate study has demonstrated reduced fetal-to-maternal plasma exposure (area under the curve, AUC) ratio (~30%) of THC [4]. Similarly, in a human study of daily cannabis smokers, the average THC umbilical vein-to-maternal serum concentration ratio at delivery was 0.26 ± 0.10 ($n = 3$) [5]. These macaque and human data suggest placental efflux of THC. However, the mechanisms underlying this reduced fetal exposure to THC are poorly understood. The human placenta expresses various transporters on both the apical side (maternal-facing) and the basal side (fetal-facing) of the syncytiotrophoblast [6] (**Figure 1.1)**. Therefore, the reduced fetal exposure to THC could be attributed to the efflux transporters on the apical side, or the uptake transporters on the basal side, or both, allowing vectorial transport of THC in the fetal-to-maternal direction.

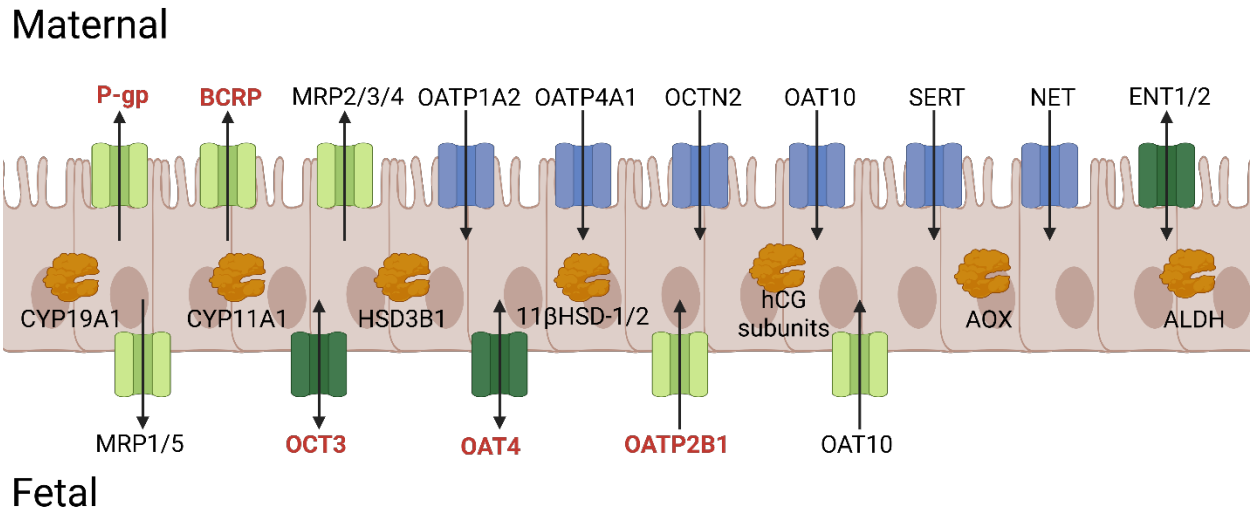

Figure 1.1 Placental transporters with their localization and directionality of transport. Placental transporters with their localization and directionality of transport. The placental transporters investigated in this dissertation are highlighted in bold and indicated in red. ALDH, aldehyde dehydrogenases; AOX, aldehyde oxidase; BCRP, breast cancer resistance protein; CYP11A1, cytochrome P450 11A1; CYP19A1, cytochrome P450 19A1; ENT, equilibrative nucleoside transporter; hCG, human chorionic gonadotropin; 11βHSD-1/2, 11β-hydroxysteroid dehydrogenase; HSD3B1, 3β-hydroxysteroid dehydrogenase; MRP, multidrug resistance associated protein; NET, norepinephrine transporter.; OAT, organic anion transporter; OATP, organic anion transporting peptide; OCT, organic cation transporter; OCTN, organic cation/carnitine transporter; P-gp, P-glycoprotein; SERT, serotonin transporter. This figure was created in biorender.com.

Previous rodent studies have indicated that THC is a substrate of P-glycoprotein (P-gp) and/or breast cancer resistance protein (Bcrp) [7,8], efflux transporters that are highly expressed on the apical membrane of the syncytiotrophoblast [11,12] **(Figure 1.1)**. Therefore, it is reasonable to hypothesize that human P-gp and/or BCRP contribute to the reduced fetal exposure to cannabinoids in human and nonhuman primates. Organic anion transporting polypeptides 2B1 (OATP2B1), organic cation transporter 3 (OCT3), organic anion transporter 4 (OAT4) are primarily expressed on the basal side of the syncytiotrophoblast [13] **(Figure 1.1)**. These basal uptake transporters could also contribute to the efflux of THC by working in tandem with the apical efflux transporters or independently, allowing vectorial transport of THC in the fetal-to-maternal direction. However, no systemic analysis of whether THC and its major metabolites are substrates or inhibitors of these placental efflux and uptake transporters has been conducted. The latter is important as cannabinoid-drug interactions may also occur if the cannabinoid, at its pharmacologically relevant plasma concentrations, is a significant inhibitor of the placental transporter of drugs consumed by the pregnant individual. Therefore, we will determine whether THC and its major metabolites are inhibitors of these efflux and uptake transporters, at their pharmacologically relevant concentrations.

To fill the above gaps in knowledge, in **Aim 1**, we will use *in vitro* cell lines/vesicles overexpressing human P-gp or BCRP, to investigate whether THC and its major metabolites are substrates or inhibitors of the highly expressed placental apical efflux transporters, P-gp and BCRP. To confirm our findings from **Aim 1**, in **Aim 2**, we will quantify the fetal-to-maternal plasma, placenta-to-maternal plasma, maternal brain-to-maternal plasma exposure (area under the curve, AUC) ratios of THC and its major metabolites in pregnant wild-type, *P-gp*$^{-/-}$, *Bcrp*$^{-/-}$, or *P-gp*$^{-/-}$/*Bcrp*$^{-/-}$ pregnant mice. Parenthetically, we note that P-gp and Bcrp are highly expressed at the mouse blood-brain barrier [14]. In **Aim 3a**, we will investigate the role of the basal placental uptake transporters (*i.e.*, OATP2B1, OCT3, OAT4) in the reduced fetal exposure to cannabinoids, and the potency of these cannabinoids to inhibit these transporters, at their pharmacologically relevant concentrations. Since THC and its metabolites are highly bound to plasma proteins, we hypothesize that they will not be inhibitors of these transporters at their pharmacologically relevant plasma concentrations.

THC and its metabolites are primarily cleared by metabolism in the liver [10], and therefore may cause cannabinoid-drug interactions provided the victim drug is significantly transported

into the liver. Therefore, to determine the risk of cannabinoid-drug interactions, we will investigate if THC and its major metabolites as substrates or inhibitors of hepatic uptake transporters not expressed in the placenta (**Aim 3b, Chapter 4)**, *i.e.*, OATP1B1, OATP1B3, OCT1, OAT2, and the sodium taurocholate cotransporter protein (NTCP).

Based on the above data and gaps in knowledge, our hypotheses are: 1) THC and its major metabolites are substrates but not inhibitors of the major human placental apical efflux transporters (*i.e.*, P-gp, BCRP), and/or major human placental basal uptake transporters (*i.e.*, OATP2B1, OCT3, OAT4) at their pharmacologically relevant plasma concentrations; 2) THC and its major metabolites are substrates of mouse P-gp/Bcrp that will result in enhanced fetal-to-maternal plasma, placenta-to-maternal plasma, maternal brain-to-maternal plasma exposure ratios of THC and its major metabolites; 3) THC and its major metabolites are substrates but not inhibitors of the major hepatic uptake transporters not expressed in the placenta (*i.e.*, OATP1B1, OATP1B3, OCT1, OAT2, NTCP) at their pharmacologically relevant plasma concentrations.

To test our hypotheses, we will pursue these specific aims:

Aim 1

To determine whether THC and its major metabolites are substrates and/or inhibitors of P-gp and BCRP at pharmacologically relevant concentrations, using transporter-expressing cells and membrane vesicles.

Aim 2

To determine if P-gp and Bcrp limit fetal, placental, and brain exposure to THC, 11-OH-THC, and THC-COOH, using pregnant FVB wild-type, *P-gp*- and/or *Bcrp*-knockout mice.

Aim 3

To determine whether THC and its major metabolites are substrates and/or inhibitors of placental **(Aim 3a)** and hepatic **(Aim 3b)** solute/drug carrier transporters (not studied above) at their pharmacologically relevant concentrations, using transporter-expressing cells.

1.2 Cannabis use during pregnancy

1.2.1 Prevalence

The prevalence of cannabis use during pregnancy is on the rise globally, influenced by changing legal landscapes and societal attitudes toward cannabis. In the United States, the prevalence of prenatal cannabis use has increased from 3.4% in 2002 to 7.0% in 2017, and further studies have shown rates rising to 8.14% during the COVID-19 pandemic [1,15]. Higher prevalence rates are often observed in populations with low income, less education, and single marital status [16]. Strikingly, among young women in Nunavut, cannabis use rates in the past year were as high as 70% of females between 15 to 19 years and 50% of females between 25 to 44 years [17]. The prevalence of past-month cannabis use also differs among different trimesters. Up to 2017, daily or near-daily cannabis use during the first (from conception to the end of 12 gestational weeks), second (from 13 weeks to the end of 27 weeks), and third trimesters (from 28 weeks to the end of 40 weeks or until birth) (T1, T2, and T3) were 5.3%, 2.5%, and 2.5%, respectively [1].

1.2.2 Cannabis and cannabinoids

Cannabis (also known as marijuana) is an annual flowering plant from the *Cannabaceae* family and originated from Central Asia [18]. Cannabis contains more than 100 phytocannabinoids. Among these, (-)-*trans*-Δ^9-tetrahydrocannabinolic acid (THCA) serves as the precursor to the intoxicating (-)-*trans*-Δ^9-tetrahydrocannbinol (THC), while (-)-cannabidiolic acid (CBDA) is the precursor to the nonintoxicating (-)-*trans*-cannabidiol (CBD)[19,20] (**Figure 1.2**). Three main species of the cannabis are: *Cannabis sativa*, *Cannabis indica*, and *Cannabis ruderalis*, each containing different concentrations of THC and CBD [21]. Specifically, *C. sativa* contains higher THC while *C. indica* contains more CBD [22], while *C. ruderalis* contains very low THC and is rarely grown for recreational use [23]. The United States Food and Drug Administration has approved Dronabinol (synthetic THC) and Nabilone for chemotherapy-induced nausea/vomiting and acquired immune deficiency syndrome (AIDS)-related weight loss, and Epidolex (CBD) for treating rare, severe forms of epilepsy [24–26].

THC is a tricyclic 21-carbon terpene with two chiral centers in trans-configuration (molecular weight = 314.45 g/mol) (**Figure 1.2**) [27,28]. THC is a volatile viscous oil with low

stability when exposed to air, heat, or light [27,29]. As a highly lipophilic (pK_a = 10.6, Log P = 6.97) compound with low aqueous solubility (2.8 mg/L or 8.9 μM) **(Table 1.1)**, THC also has a high degree of nonspecific binding [30]. In humans, THC is primarily metabolized in the liver to the intoxicating 11-hydroxy-THC (11-OH-THC), which is further metabolized to the nonintoxicating 11-*nor*-9-carboxy-THC (THC-COOH) [31] (see **Section 1.4.3, Table 1.1**, and **Figure 1.2**).

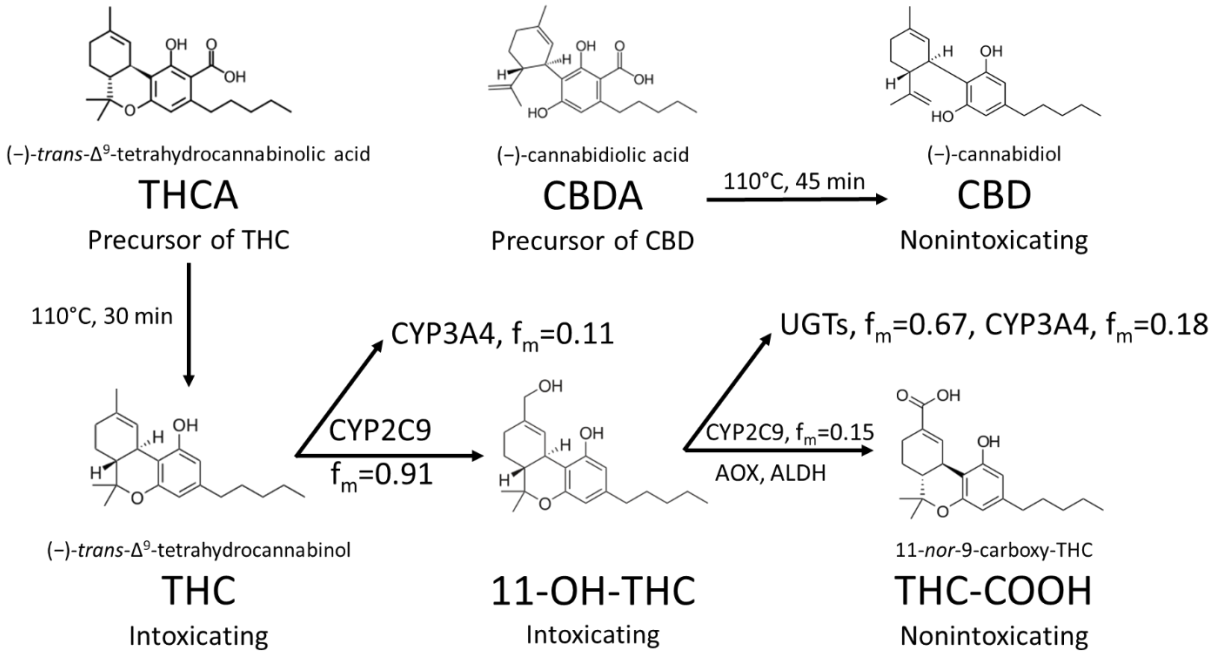

Figure 1.2 Structure of THCA, CBDA, CBD, THC, and THC metabolic profile. ALDH, aldehyde dehydrogenases; AOX, aldehyde oxidase; CYP, cytochrome P450; f_m, fraction of metabolism; UGT, uridine-5'-diphospho-glucuronosyltransferase.

Table 1.1 Physiochemical properties of THC and its major metabolites

	THC	11-OH-THC	THC-COOH	References
Molecular weight (g/mol)	314.45	330.47	344.45	PubChem
Water solubility (mg/L)	2.8	9.34	8.39	ALOGPS and [30]
pK_a	10.6	9.34	4.02	Chemaxon
LogP	6.97	5.33	5.14	Chemaxon and [32]
Blood to plasma ratio	0.71	0.73	0.65	[33]
Plasma unbound fraction ($f_{u,p}$)	0.011	0.012	0.08	[34] and [35]

1.2.3 Typical routes, frequencies, and doses

Cannabis use during pregnancy occurs through various routes with smoking as the most common route for French (60%) [36] and American women (42%), followed by edibles (16%), vaping (16%), and other routes [37]. During pregnancy, it has been reported that approximately 6% of individuals who used cannabis stopped using it, while about 11% reduced their cannabis consumption during gestation [36]. Strikingly, among pregnant cannabis users, 7.5-9.5% report using cannabis at least 10 times per day during pregnancy [36]. Accurate quantification of prenatal cannabis exposure remains challenging due to reliance on self-reported data for both dose and frequency, as well as substantial heterogeneity in cannabis products across different regions. Nonetheless, it is generally estimated that a single cannabis joint contains approximately 0.25 to 0.50 grams of cannabis, with indoor-grown herbal preparations typically comprising 15-19% of THC [38]. Although the daily dose could be distributed throughout the day, a study of 37 pregnant cannabis users calculated the average daily quantity of THC consumed as 198.0 (0.6–745.6) mg/day, based on the specific concentration and potency of the cannabis products used [39].

1.2.4 Maternal and fetal outcomes

Among women who use cannabis during pregnancy, >92% of them use it to alleviate pregnancy-related symptoms such as nausea, vomiting, and pain [40]. Other reasons to use cannabis during pregnancy include but not limited to stress or anxiety relief, management of pre-existing chronic insomnia, and mental health [41]. However, the use of cannabis during pregnancy poses significant risks to the health of the mother and the fetus. In a cohort study of 316,722 pregnancies, cannabis use during pregnancy was associated with an increased risk of gestational hypertension, preeclampsia, and placental abruption (adjusted risk ratio 1.17, 1.08, and 1.19, respectively) [42].

Besides these adverse maternal outcomes, prenatal cannabis exposure is also related to adverse long-term neurodevelopmental outcomes in the fetus/offspring. In a retrospective study of more than half a million births in Canada, the incidence of autism spectrum disorder (ASD) diagnosis was 51% higher in those that were exposed to cannabis prenatally (0.8% of total) compared to those that were not [43]. A meta-analysis of 14 studies, with a combined total of 203,783 participants, found that maternal prenatal cannabis use is associated with a 13% higher risk of attention deficit hyperactivity (ADHD) symptoms and a 30% higher risk of ASD in the

offspring [44]. In a cross-section analysis of 11,489 children, 655 who were exposed to cannabis in utero, showed greater psychopathology (psychosis, internalizing, and externalizing) during middle childhood [45]. In prospective studies, both the Ottawa Prenatal Prospective Study and the Maternal Health Practices and Child Development Study found that children ages 3 to 4 years, exposed to cannabis prenatally, had deficits in verbal and memory domains [46]. Given these deleterious effects associated with prenatal cannabis exposure, it is critical to understand the pharmacological properties of THC and its major metabolites, along with the mechanisms and extent of fetal exposure.

1.3 Pharmacodynamics of cannabinoids

1.3.1 Cannabinoid receptors

In humans, THC and 11-OH-THC primarily interact with the receptors of the endocannabinoid system to exert their pharmacological effects. Endocannabinoids are naturally occurring lipid-based neurotransmitters produced by the body with anandamide and 2-arachidonoylglycerol as the two most abundant representatives. Throughout the body, two main types of cannabinoid receptors (G protein-coupled receptors, GPCR) are CB_1 and CB_2, primarily expressed in the central nervous system (*e.g.*, brain) and peripheral tissues (*e.g.*, immune cells), respectively. CB_1 is involved in pain modulation, hypothermic effect, appetite regulation, and memory processing [47,48]. Upon binding to CB_1, THC activates GPCR pathways, primarily inhibiting adenylate cyclase activity, which leads to a decrease in cAMP levels, which modulates neurotransmitter release and affects synaptic plasticity [49].

Although both THC and 11-OH-THC bind with CB_1, the occupied binding site of THC and 11-OH-THC appears to differ based on the following observation. In displacement of [^{3}H]-CP55940 (a prototypic substrate of CB_1), THC had a lower *in vitro* binding affinity (K_i = 35 nM) for CB_1 than 11-OH-THC (K_i = 0.37 nM), but displaced all [^{3}H]-CP55940 while the maximum displacement by 11-OH-THC was only 30% [50]. Similar to CB_1, endocannabinoids and THC also bind to CB_2 which is associated with anti-inflammatory response and neuroprotection without producing any intoxicating effects [51].

1.3.2 Intoxicating and physiological effects

THC can cause various aspects of intoxicating and physiological effects within seconds to minutes when inhaled and 0.5-1.5 hours when ingested orally [52]. Key intoxicating effects of THC include euphoria ("marijuana high"), relaxation, time distortion, and other cognitive effects [53–55], while other physiological effects include tachycardia, bronchodilation, conjunctival suffusion, sedation, and immunosuppression [27,56–59]. Despite the discrepancies observed in the *in vitro* assays [50], 11-OH-THC displays equal, lower, or higher activity than THC. For instance, in a study involving 12 men aged between 21 to 24 years old, THC and 11-OH-THC were found to take effect almost simultaneously when given the same dose [0.2 mg/min intravenous infusion until the subject decided that he had achieved his desired level, with no statistical difference between the total dose received for THC (9.86 ± 2.86 μmol) and 11-OH-THC (6.87 ± 2.45 μmol)]. Both THC and 11-OH-THC induced similar tachycardia effects, but 11-OH-THC produced smaller-magnitude and shorter-duration of self-reported physiological effects [60]. However, in another clinical trial of 9 male volunteers aged between 22 to 24 years old, given the same dose of THC (1 mg, 3.18 μmol) and 11-OH-THC (1 mg, 3.03 μmol), a marked tachycardia and psychologic "high" occurred within 3-5 min after the intravenous administration of 11-OH-THC but was delayed 10-20 min after the intravenous administration of THC [61]. Moreover, greater psychological "high", symptom sign score, and tachycardia effects were observed after intravenous administration of 11-OH-THC compared to THC [61].

Unlike THC or 11-OH-THC, THC-COOH does not produce any intoxicating effects, and is primarily used as a biomarker of past cannabis consumption due to its slow release from adipose tissues to the bloodstream [27]. Although CBD is not intoxicating, it has been shown to enhance various pharmacodynamic effects of THC (20 mg) when orally co-administered with 640 mg CBD, likely due to inhibition of THC metabolism [62].

Besides these short-term effects, the partitioning of THC in tissues or organs with abundant adipose (acting as a depot) could have longer effects including but not limited to impairment of various cognitive domains, diminished attention and executive function, respiratory and cardiovascular risks, and exacerbated mental health symptoms [63,64].

1.4 Pharmacokinetics of cannabinoids

Given the deleterious effects of cannabinoids and cannabis use during pregnancy, understanding the extent and mechanisms of fetal exposure to THC and 11-OH-THC is critical. Since such exposure will be driven by maternal exposure, understanding the pharmacokinetics of THC and 11-OH-THC in the adult population is important.

1.4.1 Absorption

Cannabis is used recreationally primarily by inhalation (smoking, vaping) or orally (edibles) [65]. Different routes of administration and dose lead to different pharmacokinetic parameters including peak plasma concentration (C_{max}), time to reach peak plasma concentration (T_{max}), and bioavailability, as summarized by Cox *et al.* [66]. For instance, in one study with 11 healthy men aged between 18 and 35 years old, after 5-7 minutes of smoking THC (11.6-15.6 mg), THC was rapidly absorbed and reached C_{max} (33-118 μg/L) in 3 minutes with 8-24% bioavailability [67]. In contrast, oral administration of 20 mg THC in chocolate cookies resulted in slow absorption with a lower C_{max} (4.4-11 μg/L) at around 1-2 hours with low absolute bioavailability of 4-12% [31,67]. For the metabolites of THC, after smoking cannabis containing 1.75% THC, the intoxicating metabolite 11-OH-THC reached a C_{max} of 6.7 μg/L approximately 13.5 minutes after inhalation. In contrast, the nonintoxicating metabolite THC-COOH attained a higher C_{max} of 24.5 μg/L, but did so over a broader and delayed time frame, typically between 32 and 240 minutes [3].

Although THC and its major metabolites exhibit long plasma concentrations half-lives (see **Section 1.5.4**), THC does not significantly accumulate with repeated dosing. In contrast, both 11-OH-THC and THC-COOH show significant accumulation. In a clinical trial involving 6 men who received oral THC capsules (20 mg) every 4 to 8 hours, with escalating total daily doses (40-120 mg) over 7 days, the plasma unbound concentrations of 11-OH-THC and THC-COOH showed a 2.3-fold and 5.8-fold increase, respectively, whereas THC concentrations did not. This difference is likely due to the THC AUC under the long terminal half-life profile being a small fraction of the total AUC [68].

Overall, as summarized by Cox *et al.* [66], the highest total reported plasma concentrations of THC, 11-OH-THC, and THC-COOH after THC administration are 1392 nM (437.7 μg/L) (intravenous, 5 mg THC), 69.2 nM (22.9 μg/L) (oral, 45.7 mg THC), and 519 nM (179 μg/L)

(oral, 45.7 mg THC), respectively. Based on these concentrations and the physiochemical properties of THC and its major metabolites, we chose 5 μM, 0.3 μM, and 2.5 μM as the concentrations for THC, 11-OH-THC, THC-COOH, respectively, to test in our studies in **Chapter 2** and **Chapter 4**. Although these concentrations are higher than the highest reported plasma concentrations summarized by Cox *et al.* [66], they were chosen for several reasons: 1) doses consumed for recreational purposes could be higher than those reported by Cox *et al.* [66]; 2) to allow detection of transport in our experiments using liquid chromatography-tandem mass spectrometry (LC-MS/MS); 3) to quantify the inhibitory potency at these higher concentrations to determine if it is worthwhile exploring lower cannabinoid concentrations.

The high lipophilicity of THC (**Table 1.1**) also renders its absorption susceptible to food effects, particularly with high-fat meals. In a clinical trial involving 15 men and 12 women aged between 20 and 54 years old, high-fat meal significantly delayed the T_{max}, for the 5 and 10 mg doses, with studies reporting a 3.5-fold increase in T_{max}, while the area under the concentration-time curve ($AUC_{0–24\,h}$) was increased by about 2.7- and 2-fold compared to the fasted state, respectively [69].

1.4.2 Distribution

After absorption, THC is rapidly distributed into adipose and highly-vascularized organs such as the brain, lung, and liver [19], with the volume of distribution of 32 L/kg (calculated following intravenous administration) in humans [55]. In the human liver, THC, 11-OH-THC, and CBD may form ternary complexes with endocannabinoids or other fatty acids. Binding to fatty acid binding protein 1 (FABP1) may impact endocannabinoid signaling and metabolism [70]. Specifically, FABP1 facilitates the intracellular transport of THC to hepatic cytochrome P450s (CYPs) [71]. In human brain, THC binds with FABP3/5/7 with a low micromolar affinity (1.04-3.14 μM) [72]. Although direct evidence of THC interacting with FABPs in the human placenta remains limited, research highlights several membrane and intracellular transport systems as candidates. Plasma membrane FABP (FABPpm), fatty acid transporter proteins (FATPs), fatty acid translocase (FAT/CD36), and intracellular FABPs (notably FABP1 and FABP3) play significant roles in placental fatty acid uptake and transport processes [73–75].

In humans, the blood to plasma ratios of THC and its major metabolites are 0.71 (0.13-1.50) for THC (n = 684), 0.73 (0.42-1.40) for 11-OH-THC (n = 409), 0.65 (0.39-1.50) for THC-

COOH (n = 1112) [33], (**Table 1.1**) while the unbound fraction of THC is as low as 0.011 in nonpregnant plasma, 0.013 in maternal plasma (T3), and 0.0071 in fetal plasma [76]. Based on the postmortem data, the human tissue-to-plasma partition coefficient (K_p) of THC are 23.1, 1.50, and 51.0 in adipose, brain, and liver, respectively [76–80]. During pregnancy, the fetal THC exposure is lower than maternal exposure (see **Section 1.5**). In mice, the K_p of THC in white adipose tissue and brain are 200.9 and 1.9, respectively [81]. After repeated exposure, THC concentration is enriched in adipose tissue and demonstrates delayed release and redistribution [82,83].

1.4.3 Metabolism

In humans, after oral administration, THC undergoes metabolism predominantly via intestinal CYP2C9 [fraction of metabolism (f_m) = 0.89], with a minor contribution from intestinal CYP3A4 (f_m = 0.11) [84]. After absorption, THC undergoes extensive first-pass metabolism predominantly by hepatic CYP2C9 (f_m = 0.91) and 3A4 (f_m = 0.11), and is primarily metabolized to its intoxicating metabolite 11-OH-THC which is subsequently metabolized to its non-intoxicating metabolite THC-COOH primarily by CYP2C9 [3,34,61,68], and partially by cytosolic aldehyde dehydrogenases (ALDH) and aldehyde oxidase (AOX) [85]. THC-COOH is further glucuronidated before fecal and urinal excretion [86,87] (**Figure 1.2**).

During pregnancy, the abundance and activity of several drug-metabolizing enzymes undergo significant alterations. For instance, during T3, hepatic CYP2C9 activity increases by 16% while intestinal and/or hepatic CYP3A4 exhibits a 1.99-fold induction, compared to the postpartum period [88,89]. These enzymatic alterations could result in enhanced maternal clearance of THC and therefore influence absolute fetal exposure, but not fetal-to-maternal exposure ratios, at steady-state.

Besides the human liver, extrahepatic tissues also exhibit distinct roles in THC metabolism. Except for the intestine, no significant metabolic activity toward THC is observed in human lung or placental microsomes [84]. In contrast, human fetal liver microsomes metabolize THC primarily through CYP3A7 (f_m = 0.99), a fetal-specific CYP isoform [84]. No such quantification of extrahepatic metabolism has been done in rodents.

Despite THC's low unbound Michaelis-Menten constant ($K_{m,u}$ = 3 nM) for CYP2C9-mediated metabolism, no saturation of THC pharmacokinetics is observed in humans due to

rapid systemic distribution and blood flow-limited clearance after intravenous (or inhalational) administration [34].

1.4.4 Elimination and excretion

THC is predominantly excreted as glucuronide-conjugated THC-COOH in the feces (> 65%), and as 11-OH-THC in the urine (~20%) within 5 days [90–93]. 11-OH-THC can be glucuronidated by uridine diphosphate-glucuronosyltransferase (UGT) enzymes, primarily UGT1A9, UGT1A10, and UGT2B7 [94,95]. The clearance of THC is hepatic blood flow limited after intravenous administration [10,69,96]. The plasma half-life of THC is approximately 1 to 3 days in occasional users and 5 to 13 days in chronic users [3]. Plasma 11-OH-THC elimination half-life in infrequent cannabis users was 19 to 24 hours [97], while THC-COOH elimination half-lives were 5.2 and 6.2 days in frequent and infrequent users [98], respectively. These differences are not due to nonlinear pharmacokinetics but likely due to the more experienced users inhaling greater amount of THC and therefore the assay being able to detect the longer THC half-life.

1.5 THC fetal exposure is reduced relative to its maternal exposure

Fetal exposure to any drug is determined by several factors, namely maternal exposure, placental transport (efflux or influx), placental metabolism, and fetal metabolism. Maternal exposure drives the absolute fetal exposure but not the relative fetal-to-maternal exposure ratio. If passive diffusion were the only mechanism determining fetal drug exposure to THC, the ratio of fetal and maternal unbound steady-state plasma concentration (or AUC, i.e. $K_{p,uu}$) should be 1. However, the ratio of their respective total steady-state plasma concentrations (K_p) can deviate from 1 due to differences in THC fraction unbound in the maternal plasma (0.013) and fetal plasma (0.0071), resulting in a K_p value of 1.83 (**Section 1.4.2**) [76]. In catheterized pregnant macaques, fetal exposure to THC, as measured by the plasma AUC, was only ~30% of maternal exposure [4]. Similarly, in a human study of daily cannabis smokers during T3, the average THC umbilical vein-to-maternal serum concentration ratio at delivery was 0.26 ± 0.10 (n = 3) [5]. These results suggest that the blood-placental barrier plays a significant role in limiting fetal exposure to THC, but the mechanisms involved remain to be elucidated.

Human placenta microsomes generated from T1, T2, and term placentas, showed no significant depletion of THC or 11-OH-THC via CYPs or UGTs [84]. Although THC and 11-OH-THC are predominantly metabolized by CYP3A7 in human pooled T2 fetal liver microsomes (f_m = 0.99 and 0.80, respectively) [84], the limited fetal liver size is unlikely to reduce fetal THC exposure to ~30% of maternal exposure [4,99]. Therefore, placental efflux is the most likely contributor to the reduced fetal exposure to THC observed in human and non-human primates. Placental efflux transporters safeguard fetal development by actively preventing passage of potentially toxic xenobiotics into the fetal circulation. As detailed below, this is achieved by transporters expressed on the apical (maternal-facing) and/or basal (fetal-facing) side of the syncytiotrophoblast in the blood-placenta barrier.

1.6 Physiological barriers and transporters

1.6.1 Blood-placenta barrier and placental transporters

The blood-placenta barrier is a crucial physiological structure responsible for placental efflux and influx of nutrients, gases, and waste products, while also protecting the fetus from harmful substances [100]. The placenta is primarily composed of three unique functional units: fetal capillary endothelium, syncytiotrophoblast, and cytotrophoblast (**Figure 1.3**). Syncytiotrophoblast is a multinucleated layer that faces maternal blood, facilitating nutrient transfer and preventing entry of xenobiotics by efflux and influx transporters as well as acting as a barrier to pathogens. Cytotrophoblasts, are progenitor cells located beneath the syncytiotrophoblast and contribute to placental growth and development [101]. In human placenta, syncytiotrophoblast and cytotrophoblast start to differentiate from trophoblast approximately 6-10 days after fertilization. During pregnancy, the placenta continues to grow alongside the developing fetus [102].

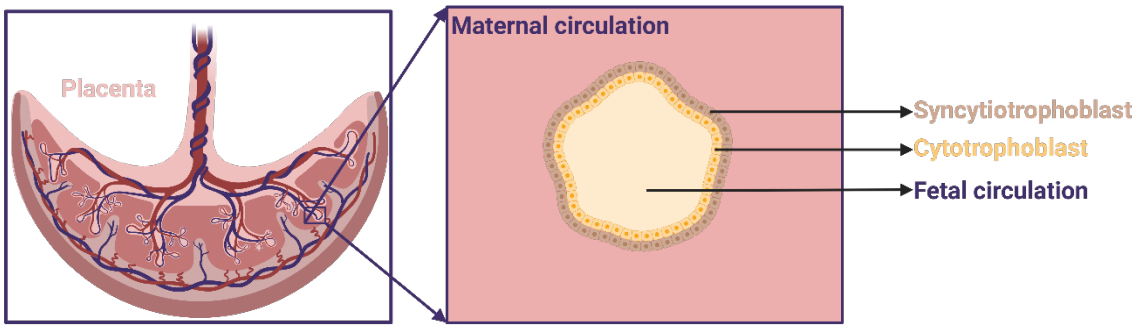

Figure 1.3 Schematic illustration of human placenta (This figure was created in biorender.com)

Apart from physiological functions, the blood placenta barrier also plays a significant role in fetal drug exposure due to the presence of various efflux and influx transporters on the maternal and/or fetal side of the syncytiotrophoblast (**Figure 1.1**). In humans, these transporters are generally categorized into two superfamilies: ATP-binding cassette (ABC) transporters, and solute carrier (SLC) transporters. In human placenta, most ABC transporters are expressed on the maternal (apical) side of the syncytiotrophoblast, such as P-gp (ABCB1), BCRP (ABCG2), and multidrug resistance-associated proteins 2/3/4 (MRP2/3/4, ABCC2/3/4), while most SLC transporters are expressed on the fetal (basal) side of the syncytiotrophoblast, such as OATP2B1, OCT3, and OAT4 [6,103,104] **(Figure 1.1).**

Rodent placenta exhibit both similarities and differences from those in humans. For instance, the rodent placenta is characterized by two distinct syncytiotrophoblast layers [105], where there is no direct contact between the maternal circulation and transporters such as P-gp and Bcrp [106]. In contrast, the human placenta comprises a single syncytiotrophoblast layer [107], which is directly exposed to maternal blood, placing P-gp and BCRP at the interface between maternal and fetal circulations [11,108]. As to localization, like human placenta, P-gp, Bcrp, and Mrp2 localize to the apical side of murine syncytiotrophoblast, with P-gp expression in mice involving two distinct genes (*Mdr1a* and *Mdr1b*) [109,110]. Similarly, murine Oct3 is also expressed on the basal side as is the case for human OCT3 [111]. However, key divergences emerge in other basal transporter localization: murine Mrp4/5/6 reside on the basal syncytiotrophoblast membrane rather than the apical side [110]. While multiple Oatp transporters demonstrate measurable expression levels in rodent placenta [110], conclusive evidence defining their precise

subcellular localization is lacking, hindering direct functional comparisons to the corresponding human placental transporters.

Despite these differences, the pregnant mouse serves as a good model to study the mechanisms of transport of xenobiotics by P-gp and/or Bcrp. This is due to the conserved localization of these transporters in the syncytiotrophoblast where they exhibit substantial substrate overlap and functional homology with their human orthologs [109] (see **Chapter 3)**. In addition, knockout mice of each and both transporters are commercially available. With these models, we can investigate not only the potential mechanisms underlying reduced fetal exposure to THC, but also quantify the extent of fetal exposure, providing clues as to the mechanism and extent of fetal exposure in humans. For example, the fetus/maternal plasma concentration ratios of digoxin, saquinavir, and paclitaxel are significantly increased in *P-gp*$^{-/-}$ mice compared to the wild-type mice [112], indicating the crucial role of this transporter in modulating fetal drug exposure.

Given the important roles of P-gp and BCRP as human placental efflux transporters, we hypothesized that they are the most likely candidates responsible for the placental efflux of THC in humans, explaining its lower fetal-to-maternal exposure ratio in humans and nonhuman primates. Indeed, studies in rodents, where P-gp and/or Bcrp, are highly expressed in the intestine and the blood-brain barrier (as detailed below) [113,114], provide evidence to support our hypothesis. Bonhomme-Faivre *et al.* reported that the plasma AUC of THC (administered orally, 25 mg/kg THC) in P-gp-deficient CF1 mice was 2.17-fold higher than that in wild-type CF1 mice, suggesting that the mouse intestinal P-gp limits THC oral absorption [8]. Another study using *P-gp* and *Bcrp* knock-out mice showed that the brain/blood THC ratios are higher than those in wild-type mice at certain time points after intraperitoneal administration of 3 mg/kg THC. In addition, *P-gp* and *Bcrp* knock-out mice are more sensitive to THC-induced hypothermia after intraperitoneal administration of 10 mg/kg THC [7]. These data suggest that THC is a substrate of mouse P-gp and Bcrp. Therefore, in **Chapter 2** and **Chapter 3,** we investigated if P-gp and BCRP are the primary human transporters effluxing THC in the fetal-to-maternal direction, resulting in a reduction in THC fetal exposure relative to maternal exposure.

Besides P-gp and BCRP, we cannot exclude the possibility of contribution from basal transporters to placental efflux of THC. Active influx of THC by the basal SLC transporters (OAT2B1, OCT3, OAT4) with or without efflux by P-gp/BCRP would also result in reduced

fetal THC exposure. THC could be transported (and passively diffuse) from the fetal compartment into the placenta and then it could be transported (and/or diffuse) out of the placenta into the maternal compartment, resulting in net fetal-to-maternal transport. Therefore, in **Chapter 4**, we investigated whether basal placental influx transporters could also contribute to reduced fetal exposure to THC and its major metabolites.

Cannabinoid-drug interactions may occur if the cannabinoid, at its pharmacologically relevant plasma concentrations, is a significant inhibitor of the transporter involved in the drug's tissue distribution or clearance. Therefore, in **Chapters 2** and **4**, we investigated whether THC and its major metabolites are also inhibitors of key placental efflux and uptake transporters at their pharmacologically relevant concentrations.

1.6.2 Gestational-dependent changes in placental transporter abundance

The reduced fetal-to-maternal plasma exposure ratio of THC in macaques was observed in late gestation macaques and at term in humans [4]. Placental transporter expression abundance and activity can be significantly influenced by gestational age [13,115]. In humans, placental transporters, quantified by quantitative targeted proteomics, showed a significant decrease in the expression of the ABC transporters P-gp and BCRP from T1 to term (measured as pmol/mg total membrane protein). At term, P-gp and BCRP expression was reduced to 31% and 45% of T1 levels, respectively. In contrast, SLC transporters exhibited differential regulation. The abundance of OATP2B1 at T2 was 68% of T1 levels, while the expression of OCT3 and OAT4 at term was 202% and 162% compared to the T1 and T2 levels, respectively [13]. This gestational-age dependent expression and activities of these transporters could lead to differential cannabinoid-drug interactions, provided the drug or the cannabinoid is significantly transported by these transporters.

1.6.3 Other physiological barriers and transporters

Besides the blood-placenta barrier, other physiological barriers also exhibit abundant expression of transporters. For example, the efflux transporters, P-gp and BCRP, are highly expressed in the brain capillary endothelial cells [113]. They function to limit entry of drug substrates into the brain thus protecting the brain from potentially harmful substances [116–119].

In the liver, a variety of transporters are responsible for drug and bile acid entry into the liver and their subsequent metabolism and biliary excretion of the drug or its metabolites. Key xenobiotic transporters include the OATPs, NTCP, MRPs, P-gp, and BCRP [120]. If THC and its metabolites are inhibitors or substrates of these transporters, there is potential for cannabinoid-drug interactions. Therefore, in **Chapter 4,** we investigated if THC and its major metabolites are substrates or inhibitors of the hepatic uptake transporters (OATP1B1, OATP1B3, OCT1, OAT2, and NTCP) resulting in cannabinoid-drug interactions.

1.7 Systems to investigate placental drug transport

Although placental efflux transporters are crucial for limiting fetal exposure to xenobiotics and are likely to cause reduced fetal exposure to THC [4], measurement of the extent and mechanism of fetal exposure to cannabinoids and their drug interaction in pregnant women is challenging. Instead, several *in vitro*, *in vivo*, *ex vivo* models, detailed below, can be used.

1.7.1 In vitro systems

In vitro systems include malignant human choriocarcinoma-derived cell lines (BeWo, JAR, JEG-3), and plasma membrane vesicles isolated from primary tissues [6]. Modern microengineered "organ-on-a-chip", for instance, "placenta-on-a-chip" with human trophoblast cells and endothelial cells cultured in two channels separated by a semipermeable membrane has also been developed to simulate physiological conditions of drug transport between the maternal and fetal circulation [121]. Though these models could be used to study the mechanism of transport, these *in vitro* assays may not fully recapitulate the actual physiological transporter expression due to altered transporter expression. For instance, P-gp is absent or minimally expressed in BeWo and JEG-3 cell lines [122]. Moreover, human choriocarcinoma-derived cell lines express multiple transporters, which could be confounding when investigating the role of specific transporters.

Cell lines overexpressing individual transporters are better models to investigate whether THC and its major metabolites are substrates or inhibitors of a transporter. Madin-Darby canine kidney II (MDCKII) cells and human embryonic kidney 293 (HEK) cells overexpressing a transporter are commonly used for *in vitro* transporter kinetics analysis. MDCKII can polarize

and form a monolayer with tight junctions, enabling the measurement of transepithelial transport and mimicking the placental barrier when grown in Transwells[123] . We have used MDCKII overexpressing human P-gp or BCRP to study if they are responsible for the placental efflux of THC and its metabolites (**Chapter 2)**. In contrast, although HEK cells are not polarized and do not form tight junctions (therefore cannot be used in Transwells), they are frequently transfected with individual transporters, which makes them valuable models for assessing substrate specificity, inhibition, and transporter kinetics [124]. In **Chapter 4,** we have used these overexpressing cells to investigate if THC and its metabolites are substrates or inhibitors of placental and hepatic uptake transporters.

Inside-out membrane vesicles overexpressing specific transporters are also widely used to evaluate inhibitor potency and substrate-transporter interactions *in vitro*. These vesicles enable direct measurement of ATP-dependent substrate accumulation by exposing the transporter's binding site to the external medium, bypassing the need for passive membrane permeation prior to efflux [125]. However, the use of vesicles (and all the above systems) poses a challenge to study the transport of highly lipophilic compounds like THC (and its major metabolites) due to their high passive diffusion across membranes and extensive non-specific binding. The high background signal due to the latter can obscure transporter-mediated uptake and could lead to false conclusions regarding the role of transporters in their mechanism of placental transfer. With that being said, vesicle assays are effective in evaluating the transporter inhibitory potency of THC and its major metabolite at their pharmacologically relevant concentrations as we have done in **Chapter 2**.

1.7.2 In vivo systems

Although the above *in vitro* models are versatile in the investigation of the mechanisms of transporters, *in vivo* animal models such as nonhuman primates and rodents can be used to study both mechanisms and extent of placental transport. Nonhuman primates (macaque, baboon) can be catheterized (fetal as well as maternal) to continuously sample from the same animal and generate drug concentration-time curves from both the maternal and fetal circulation [4]. However, the high cost, and the special expertise needed are often hurdles for such investigation. Rodents express some transporters highly homologous to human orthologs and are easy to foster colonies with lower cost. Therefore, transporter-knockout mice are commonly used

to study specific roles of transporters at many physiological barriers. As elaborated in **Section 1.7**, differences in the syncytiotrophoblast structure and transporter localization exist between rodent and human placentas, which may limit the translation of rodent studies to humans. The rodent P-gp and Bcrp have the same localization and similar biological function as their human orthologs. This similarity renders P-gp- and/or Bcrp-deficient pregnant mice good models to evaluate the extent and mechanism of the role of these transporters in the fetal and maternal tissue distribution of THC and its major metabolites as described in **Chapter 3**.

1.7.3 Ex vivo systems

The perfused human term placenta can also serve as an *ex vivo* model to determine the mechanism and extent of placental transporter of drugs. This model is used with either recirculation of maternal and fetal perfusates as a closed system or without recirculation as an open system [126]. This model has been successfully applied to determine (or confirm) P-gp mediated efflux of several drugs [127]. This model has the advantage that it utilizes human tissue and can be used to predict human fetal exposure to drugs even if the mechanism of placental transfer of the drug has not been elucidated [76]. The disadvantages are: 1) this model is challenging to routinely implement in the laboratory and needs special expertise and personnel; 2) the model can be used only with term placentas (preferably from C-sections) and therefore does not allow investigation of placental transfer earlier in gestation; 3) the model lacks the fetal compartment and therefore cannot be used to predict fetal exposure when fetal metabolism is extensive relative to placental transfer. This deficiency can be overcome by combining the placental transfer data from this model with the metabolism of the drug by human fetal tissue such as fetal liver microsomes [76,99].

1.7.4 Extrapolation and simulation

Once the placental transporter(s) responsible for modulating fetal exposure to a drug has been identified, our laboratory has shown that the efflux ratio-relative expression factor (ER-REF) approach, combined with maternal-fetal physiologically based pharmacokinetic (m-f PBPK) modeling and simulation (M&S), can be successfully used to predict fetal exposure to drugs from gestational week 15 to term. This approach can predict fetal (and other tissue)

exposure to drugs, irrespective of whether they are actively or passively transferred across the placenta (or tissue-to-blood) barrier [13,128–130]. This approach overcomes the inability to sample umbilical venous plasma concentration earlier in gestation which can be challenging even at term. In addition, it bypasses the limitations associated with primary human placental cells [131]. With the mechanism of transport in various organs/tissues (including the placenta) generated in **Chapter 2-4**, they can be incorporated into such models to predict fetal (or tissue) exposure to drugs.

1.8 Specific aims

In summary, our hypotheses are: 1) THC and its major metabolites are substrates but not inhibitors of the major human placental apical efflux transporters (*i.e.*, P-gp, BCRP), and/or major human placental basal uptake transporters (*i.e.*, OATP2B1, OCT3, OAT4), resulting in the reduced fetal exposure to cannabinoids; 2) THC and its major metabolites are substrates of mice P-gp/Bcrp that will result in enhanced fetal-to-maternal plasma, placenta-to-maternal plasma, maternal brain-to-maternal plasma exposure ratios of THC and its major metabolites; 3) THC and its major metabolites are substrates but not inhibitors of the major hepatic uptake transporters not expressed in the placenta (*i.e.*, OATP1B1, OATP1B3, OCT1, OAT2, NTCP). These hypotheses will be addressed through the following Specific Aims:

Aim 1 (Chapter 2)

To determine whether THC and its major metabolites are substrates and/or inhibitors of P-gp and BCRP at pharmacologically relevant concentrations, using transporter-expressing cells and membrane vesicles.

Aim 2 (Chapter 3)

To determine if P-gp and Bcrp limit fetal, placental, and brain exposure to THC, 11-OH-THC, and THC-COOH, using pregnant FVB wild-type, *P-gp*- and/or *Bcrp*-knockout mice.

Aim 3 (Chapter 4)

To determine whether THC and its major metabolites are substrates and/or inhibitors of placental **(Aim 3a)** and hepatic **(Aim 3b)** solute/drug carrier transporters at pharmacologically relevant concentrations, using transporter-expressing cells.

Chapter 2
In Vitro Assessment of THC and Its Major Metabolites as P-gp/BCRP Substrates and Inhibitors

The work presented in this chapter was previously published in

Drug Metabolism and Disposition 2021 Oct;49(10):910–918.

doi: 10.1124/dmd.121.000505

2.1 Abstract

(-)-*trans*-Δ^9-tetrahydrocannabinol (THC) is the primary intoxicating constituent of cannabis. In humans, 11-hydroxy-THC (11-OH-THC) and 11-*nor*-9-carboxy-THC (THC-COOH) are intoxicating and non-intoxicating circulating metabolites of THC, respectively. Whether these cannabinoids are substrates or inhibitors of human P-glycoprotein (P-gp) or breast cancer resistance protein (BCRP) is unknown. Previous animal studies suggest that THC and its metabolites could be substrates of these transporters. Therefore, we performed Transwell, cellular accumulation, and vesicular transport assays, at pharmacologically relevant concentrations of these cannabinoids, using Madin-Darby canine kidney II (MDCKII) cells or plasma membrane vesicles overexpressing human P-gp or BCRP. Neither THC nor 11-OH-THC was found to be a substrate or inhibitor of P-gp or BCRP. The efflux ratio of THC-COOH in MDCKII-BCRP cells was 1.6, which was significantly decreased to 1.0 by the BCRP inhibitor Ko143. Likewise, cellular accumulation of THC-COOH was significantly increased 1.6-fold in the presence vs. absence of Ko143. THC-COOH also significantly inhibited BCRP-mediated transport of lucifer yellow, a BCRP substrate; however, THC-COOH was neither a substrate nor an inhibitor of P-gp. Collectively, these results indicate that THC and 11-OH-THC are not substrates or inhibitors (at pharmacologically relevant concentrations) of either P-gp or BCRP. THC-COOH is a weak substrate and inhibitor of BCRP, but not of P-gp. Accordingly, we predict that P-gp/BCRP will not modulate the disposition of these cannabinoids in humans. In addition, use of these cannabinoids will not result in P-gp- or BCRP-based drug interactions.

2.2 Introduction

Cannabinoids are chemicals found in cannabis with diterpene structure [132]. Among over 100 well-characterized cannabinoids, (-)-*trans*-Δ^9-tetrahydrocannabinol (THC) is the principal intoxicating constituent of cannabis, and can be sequentially metabolized primarily by the cytochrome P450 (CYP) enzyme CYP2C9 to the intoxicating 11-hydroxy-THC (11-OH-THC) and then to the nonactive 11-*nor*-9-carboxy-THC (THC-COOH) [34,133]. Cannabis use is increasing in the United States [134]. While cannabis is widely used, oral synthetic THC (Dronabinol) is an U.S. Food and Drug Administration -approved drug for the treatment of nausea, vomiting, and anorexia [68]. As such, it is necessary to understand the mechanisms by which the disposition of THC and its metabolites is mediated. While the disposition of THC and its major metabolites via

drug-metabolizing enzymes such as the CYP enzymes has been extensively studied [34,95,135,136], very little information is available about the roles of drug transporters in the disposition of these cannabinoids.

P-glycoprotein (P-gp) is a member of the ATP-binding cassette (ABC) efflux transporter family encoded by the gene *ABCB1* [137]. P-gp is expressed throughout the human body, with particularly high expression at the blood-brain barrier, the placental syncytiotrophoblast, the intestinal epithelium, the liver bile canaliculi, and kidney proximal tubular epithelium [138]. Many structurally and chemically unrelated compounds are found to be P-gp substrates [138]. Its broad substrate specificity and high expression in organs important for drug disposition renders P-gp a critical role in determining drug pharmacokinetics, efficacy or toxicity. Breast cancer resistance protein (BCRP) encoded by the gene *ABCG2* is another vital member of the ABC transporter family [139–141]. The pattern of tissue distribution and expression of BCRP highly resembles that of P-gp [11,142,143]. Like P-gp, BCRP has a very broad spectrum of substrates, ranging from hydrophobic anticancer drugs to hydrophilic conjugate organic anions [144]. Therefore, BCRP also plays a critical role in the disposition of many drugs and xenobiotics [145].

Regarding the roles of P-gp and BCRP in the disposition of cannabinoids, Bonhomme-Faivre *et al.* reported that the area under concentration-time curve (AUC) of THC (administered orally) in P-gp-deficient CF1 mice was 2.17-fold higher than that in wild-type CF1 mice, suggesting that the mouse P-gp could limit oral absorption [8]. Another study using *P-gp* and *Bcrp* knock-out mice showed that the brain/blood THC ratios are higher than those in wild-type mice at certain time points after intraperitoneal administration. In addition, *P-gp* and *Bcrp* knock-out mice are more sensitive to THC-induced hypothermia [7]. These data suggest that THC is a substrate of mouse P-gp and Bcrp. Furthermore, a study using pregnant macaque revealed that, after THC intravenous administration, fetal THC AUC is ~30% of maternal THC AUC and fetal exposure of THC-COOH is undetectable [4]. These data suggest that P-gp and/or BCRP, highly expressed on the apical membrane of the placental syncytiotrophoblasts of the macaques, may limit fetal exposure to THC and THC-COOH by transporting these cannabinoids back to the maternal circulation. THC has been shown to be a weak inhibitor of human P-gp via *in vitro* inhibition studies using a rather high, not pharmacologically relevant, concentration (50 μM) [146]. Prior to this study in **Chapter 2**, no *in vitro* transport studies had been reported to show that THC and any of its metabolites, at pharmacologically relevant concentrations, are substrates

and/or inhibitors of human P-gp and BCRP. In this study, we systematically investigated whether THC, 11-OH-THC, or THC-COOH, at pharmacologically relevant concentrations, are substrates and/or inhibitors of human P-gp and BCRP.

2.3 Materials and methods

2.3.1 Materials

(-)-*trans*-Δ^9-THC (50 mg/mL) and loperamide-D_8 was purchased from Cayman Chemicals (Ann Arbor, MI). (±)11-OH-THC (100 µg/mL), and (±)11-*nor*-9-carboxy-THC (THC-COOH) (1 mg/mL), (-)-Δ^9-THC-D_3, (±)-11-OH-THC-D_3 in methanol were purchased from Cerilliant (Round Rock, TX). Bovine serum albumin (BSA) Fraction V, N-methyl-quinidine (NMQ), Ko143, ATP, AMP, and prazosin were from Sigma-Aldrich (St. Louis, MO). Tris, HEPES, 0.25% trypsin-EDTA, G418 (Geneticin™), GlutaMAX™, Dulbecco's phosphate buffered saline (DPBS), Hank's balanced salt solution (HBSS) (with Ca^{2+}), fetal bovine serum (FBS), Dulbecco's modified eagle medium (DMEM) (4.5 g/L glucose and 1.0 g/L glucose), acetonitrile (ACN), dimethyl sulfoxide (DMSO), and formic acid (liquid chromatography-mass spectrometry grade) were from Thermo Fisher Scientific (Hampton, NH). Multiscreen™ HTS Vacuum Manifold, 96-well FC Filter Plates (1.2/0.65 µm, opaque, non-sterile [MSFCN6B10]) were purchased from EMD Millipore (Billerica, MA). Tariquidar was obtained from AzaTrius Pharmaceuticals Private Limited, India. Lucifer yellow (LY) was from MP Biomedicals (Irvine, CA). Hygromycin B, 24-well cell culture plate, and 12-well Transwell plate were from Corning (Corning, NY). The bicinchoninic acid assay (BCA) protein quantification kit was from Pierce Chemical (Rockford, IL). SB MDR1/P-gp HEK293 and SB BCRP HEK293 plasma membrane vesicles (5 mg/mL) overexpressing human P-gp and BCRP, respectively, were obtained from SOLVO Biotechnology (Szeged, Hungary). Low-binding microcentrifuge tubes were from Genesee Scientific (San Diego, CA). Milli-Q water was used in all preparations. All other chemicals and reagents were obtained at the highest quality available commercially.

2.3.2 Cell culture

MDCKII-hMDR1-cMDR1-KO (MDCKII-P-gp) cells were a kind gift from Dr. Per Artursson, Uppsala University, Sweden, and MDCKII-BCRP cells were developed in the

laboratory of Dr. Qingcheng Mao by stable transfection of the pcDNA-BCRP plasmid into MDCKII cells. In MDCKII-P-gp cells, the canine P-gp/ABCB1 gene has been knocked out [147], while in MDCKII-BCRP cells, the canine BCRP/ABCG2 gene is not knocked out. However, parent MDCKII cells do not express canine BCRP protein or possess transport activity of canine BCRP [146]. All cells were preserved in liquid nitrogen. The passages of MDCKII cells used in Transwell and cellular accumulation assays ranged from the 1st to 10th passages. We adopted culture conditions established in respective laboratories for both cell lines, namely, MDCKII-P-gp cells were cultured in high glucose (4.5 g/L) DMEM supplemented with 10% FBS, 1% GlutaMAX™, 1% penicillin-streptomycin, and 375 µg/mL hygromycin B, and MDCKII-BCRP cells were cultured in low glucose (1.0 g/L) DMEM with 10% FBS, 1% penicillin-streptomycin, and 500 µg/mL G418. All cells were maintained in a humidified incubator at 37°C in 5% CO_2 with 95% humidity. When reaching ~90% confluency, cells were passed into a new flask after washing with DPBS and trypsinization, and then seeded into Transwell inserts or 24-well plates for subsequent transport assays (see below).

2.3.3 Bidirectional Transwell transport assay

MDCKII cells expressing human P-gp or BCRP were seeded onto Collagen I-coated Transwell plates with a density of approximately 5×10^5 cells per well and cultured for four days to form tight junctions. On the day of the assay, the transepithelial/endothelial electrical resistance (TEER) was measured to be at least 180 Ω. Each apical chamber was washed three times with 0.5 mL of HBSS (with Ca^{2+} and supplemented with 10 mM HEPES for all experiments unless specified), and each basal chamber was washed three times with 1 mL HBSS. Then, the Transwell plate was pre-incubated in HBSS at 37°C for 15 min. After the pre-incubation, 5 µM THC, 0.3 µM 11-OH-THC or 2.5 µM THC-COOH with 50 µM LY in the presence or absence of 5 µM tariquidar for MDCKII-P-gp cells or 5 µM Ko143 for MDCKII-BCRP cells was added to the donor chamber (either the apical or the basal chamber) to final concentrations as shown above. The organic solvent concentration was kept no more than 0.2% (v/v) for all assays. At 0 and 120 min of the assay, samples of 5 µL each were collected from the donor chamber, and samples of 100 µL each from the receiver chamber were collected at 30, 60, 90, 120 min. The donor samples were diluted to a final volume of 100 µL with HBSS. After the last time point, cells were washed with ice-cold HBSS three times to terminate transporter

activity. Cells were then lysed with 10% ACN for 1 h at room temperature, and cell lysates were collected and vortexed, and 100 µL was used for analysis. Meanwhile, 2 µM quinidine (a P-gp prototypic substrate) or 3 µM prazosin (a BCRP prototypic substrate) was used as a positive control on a separate Transwell plate for MDCKII-P-gp or MDCKII-BCRP cells, respectively. For the positive control experiments, samples from the donor chamber were collected at 0 and 60 min, and samples from the receiver chamber were collected at 15, 30, 45, 60 min. THC, 11-OH-THC, THC-COOH, quinidine or prazosin in all samples were spiked with 100 µL of internal standards (250 nM THC-D_3 for THC and THC-COOH, 250 nM 11-OH-THC-D_3 for 11-OH-THC, and 10 nM loperamide-D_8 for quinidine and prazosin) and vortexed before centrifugation at 19,083 × g (maximal speed) for 10 min at 4°C. Finally, 100 µL of supernatant was collected and subject to quantification using a validated liquid chromatography tandem mass spectrometry (LC-MS/MS) assay as described below. For quinidine and prazosin samples, LY was determined as an indication of paracellular tight junction using a fluorescence microplate reader under 430 nm for excitation and 538 nm for emission. The apparent permeability for LY was no more than 2×10^{-6} cm/s in all Transwell transport assays estimated using the same equation below while dQ/dt refers to change in absorption.

The apparent permeability (P_{app}) was calculated using the equation $P_{app} = (dQ/dt)/(c_0*Area)$, with a unit of cm/s, when the steady-state assumption was met, where dQ/dt is the change in amount divided by incubation time, Area is the cell growth area on the Transwell insert (1.13 cm^2), and c_0 is the initial concentration of a compound added to the donor chamber. If the steady-state assumption was not met, the initial concentration in the donor chamber declined substantially over time, and then P_{app} was calculated using the equation $P_{app} = Q_{receiver,\ last}/(AUC_{0\rightarrow last,\ donor}*Area)$, where $Q_{receiver,\ last}$ is the amount of a compound appeared in the receiver chamber at the last time point, -and $AUC_{0\rightarrow last,\ donor}$ is the area under the concentration-time curve of the compound from time 0 to the last time point in the donor chamber. The efflux ratio (ER) was calculated as $P_{app,B\rightarrow A}/P_{app,A\rightarrow B}$, where $P_{app,\ A\rightarrow B}$ is the apparent permeability of a compound from the apical to the basal side, and $P_{app,\ B\rightarrow A}$ is the apparent permeability of the compound from the basal to the apical side. The mass balance of a compound in the Transwell system at the last time point was calculated as $(A_R + A_{IC} + A_D)/A_{D0}$, where A_R is the amount of the compound in the receiver at the last time point, A_{IC} is the intracellular amount of the compound at the last time point, A_D is the amount of the compound in the donor at the last time

point, and A_{D0} is the amount of the compound in the donor at time 0. The contribution of the compound in the donor (A_D), receiver (A_R) and intracellular compartment (A_{IC}) to mass balance was calculated as a percentage of the total amount ($A_R + A_{IC} + A_D$).

2.3.4 Cellular accumulation assay

MDCKII cells overexpressing human P-gp or BCRP were seeded onto Collagen I-coated 24-well plates with a density of approximately 5×10^5 cells per well and cultured for 24 h. On the day of the assay, each well was washed three times with 0.5 mL of HBSS and preincubated in HBSS in the presence or absence of an inhibitor (5 μM tariquidar for P-gp or 5 μM Ko143 for BCRP) at 37°C for 30 min. After the preincubation, 5 μM THC, 0.3 μM 11-OH-THC, or 2.5 μM THC-COOH was added to each well in the presence or absence of an inhibitor to final concentrations as shown above, and incubated for 15, 30, 45, and 60 min. The organic solvent concentration was kept no more than 0.2% (v/v) for all assays. Meanwhile, 2 μM quinidine or 3 μM prazosin in the presence or absence of an inhibitor was used as a positive control on a separate plate for MDCKII-P-gp or MDCKII-BCRP cells, respectively. At each time point, cells were washed three times with 1 mL ice-cold HBSS to quench transporter activity. Cells were then lysed with 0.5 mL of 10% ACN for 1 h at room temperature, and cell lysates were then collected. 100 μL of cell lysates were spiked with 100 μL of respective internal standards as described in the Transwell transport assay and subject to quantification of THC, 11-OH-THC, THC-COOH, quinidine or prazosin using a validated LC-MS/MS assay as described below. Protein concentrations of cell lysates were determined by the BCA protein assay kit with BSA as standard. The cellular accumulation of a test compound was calculated by normalizing the amount of the compound to the amount of protein in each well and expressed as pmol/μg protein. Then, the AUC of cellular accumulation of the compounds was calculated using trapezoidal rule.

2.3.5 Vesicular transport assay

We used inside-out plasma membrane vesicles to determine whether THC, 11-OH-THC and THC-COOH are inhibitors of P-gp and BCRP. A rapid filtration protocol modified from a previously reported method was used for vesicular transport assays of NMQ (a P-gp substrate) [109], and LY (a BCRP substrate) [148]. All test compounds, vesicles, and ATP/AMP were prepared

in an incubation buffer (pH 7.0) containing 10 mM Tris-HCl, 10 mM $MgCl_2$, and 250 mM sucrose. Prior to initiation of P-gp-mediated transport reactions, 25 µL of 3 µM NMQ containing the solvent DMSO alone, tariquidar, or a cannabinoid, were pre-incubated with 25 µL of 1 mg protein/mL vesicles at 37°C for 10 min. Reactions were then initiated by adding pre-warmed 25 µL of 15 mM Mg-ATP or AMP and continued to incubate at 37°C for 5 min. The final concentrations of NMQ, THC, 11-OH-THC, THC-COOH, and ATP or AMP in the vesicular transport reactions were 1 µM, 1667 nM, 100 nM, 833.3 nM, and 5 mM, respectively. The reactions were stopped by adding 200 µL of ice-cold washing buffer (10 mM Tris-HCl, 100 mM NaCl, and 250 mM sucrose) and transferred to a prewet 96-well rapid filtration plate. Each well was washed five times with 200 µL of ice-cold washing buffer under vacuum. The NMQ trapped in the vesicles was eluted by adding 200 µL of ACN containing 100 nM quinidine as an internal standard under vacuum. The eluents were centrifuged under 19,083 × g for 10 min at 4°C, and 50 µL of supernatant were subject to quantification using LC-MS/MS as described below. In the case of BCRP-mediated vesicular transport, a final concentration of 50 µM LY and 15 µg of vesicle protein per reaction were used and incubated for 10 min, and reactions were initiated and incubated as described above. The elution was performed using 100 µL of 0.1 M NaOH, and the eluent was neutralized with 100 µL of 0.1 M HCl. LY in eluents was quantified by measuring fluorescence with excitation at 430 nm and emission at 538 nm. In all vesicular transport assays, the organic solvent concentration was kept no more than 0.2% (v/v). ATP-dependent uptake of NMQ or LY into membrane vesicles was calculated by subtracting the uptake in the presence of AMP from that in the presence of ATP and normalized as a percentage of the positive control. ATP-dependent uptake of NMQ or LY with DMSO alone was used as a positive control and set to 100%.

2.3.6 LC-MS/MS analysis

All samples including cell lysates were analyzed using an AB Sciex Triple Quad 6500 (SCIEX, Framingham, MA) coupled with the Acquity ultra-performance liquid chromatography system (Waters, Milford, MA). Acquity ultra-performance liquid chromatography BEH C_{18} column (1.7 µM 2.1×50 mm) attached to the C_{18}*2-mm guard column was used for chromatography analysis. The organic and aqueous phases used were water and ACN containing 0.1% formic acid, respectively (as solvents A and B, respectively). The mass spectrometer was

operated in the positive electrospray ionization mode. The inter-day and intraday variance for quality control samples were no more than 15% and standard curves were established with $1/y^2$ weighting. Liquid chromatography flow gradient and multiple reaction monitoring parameters used for quantification of cannabinoids were the same as previously described [95]. For quantification of quinidine and prazosin, the flow rate was 0.3 mL/min and the gradient conditions were as follows: starting 95% A in the first 2 min, and changed to 5% A for the next 55 seconds, and then switched to 95% A again and maintained until 4 min. The temperature of column was maintained at 45°C and the autosampler at 4°C. The injection volume was 10 µL. Analytes were quantified by the following transitions: quinidine 31.000 > 32.000 m/z, prazosin 45.000 > 40.000 m/z, loperamide-D_8, 25.000 > 20.000 m/z. For the quantification of NMQ, the flow rate was 0.5 mL/min and the gradient conditions were as follows: starting 90% A in the first 1.2 min, changed to 5% A and maintained until 4 min, and switch back to 90% A for the following 30 seconds. The temperature of column was maintained at 45°C and the autosampler at 6°C. The injection volume was 10 µL. Analytes were quantified by the 339.30 > 339.30 with 11 V collision energy. Integration of the chromatographic peaks was performed using Analyst v1.6 (Framingham, MA). The relative concentrations of a test compound in a sample were expressed as the peak area ratios of the compound to internal standard for Transwell assays, and the ratios were converted to molar concentration according to the standard curve for cellular accumulation and vesicular transport assays.

2.3.7 Statistical analysis

At least three independent experiments were performed for the Transwell transport (except for THC) and cellular accumulation assays with triplicate in each experiment, or for the vesicular transport assay with duplicate in each experiment. Data were reported as means ± standard deviation (SD) of at least three independent experiments using mean values in each experiment. Differences in transport activity between with and without an inhibitor or between A → B and B → A transport were analyzed by the paired Student's *t*-test, two-way analysis of variance (ANOVA) followed by the Šidák's *post hoc* test, or paired two-way ANOVA followed by the Tukey's *post hoc* test for Transwell transport and cellular accumulation assays. For the vesicular transport assay, all comparisons were analyzed by paired one-way ANOVA followed

by the Dunnett's *post hoc* test. Differences with *P* values of <0.05 were considered statistically significant. All the analysis was performed using GraphPad Prism 8 (La Jolla, CA).

2.4 Results

2.4.1 Bidirectional Transwell transport of cannabinoids in MDCKII-P-gp cells

To investigate whether THC, 11-OH-THC and THC-COOH are substrate of human P-gp, we first performed the bidirectional Transwell transport assay on the MDCKII cell monolayers overexpressing human P-gp, with 2 μM quinidine as a prototypic substrate and 5 μM tariquidar as the P-gp inhibitor. The ER of quinidine, although variable, was much greater than 2 in the absence of tariquidar, and decreased to ~1 in the presence of tariquidar (**Table 2.1**), confirming good P-gp activity in MDCKII cells. For 11-OH-THC and THC-COOH, the ERs were around 1 in the presence and absence of tariquidar (**Table 2.1**), suggesting that these cannabinoids were not transported by P-gp. Because THC was not quantifiable in the receiver chamber, the ER of THC could not be determined. Therefore, we analyzed the mass balance of THC. We noted that, ~80% of THC was trapped intracellularly when THC was tested in the A → B direction regardless of whether tariquidar was present (**Table 2.2**). When THC was tested in the B → A direction, 100% and ~85% of THC were trapped in the cells in the absence and presence of tariquidar, respectively (**Table 2.2**). And generally, less than 5% of THC appeared in the receiver chamber (**Table 2.2**). We also observed intracellular trapping of 11-OH-THC and THC-COOH, but to a much less extent, and the metabolites were quantifiable in the receiver chamber (**Table 2.2**). These results suggested that due to high intracellular trapping of THC, the Transwell system is not suitable to determine ER for THC. Thus, cellular accumulation assay was used as an alternative to investigate whether THC is a P-gp substrate and verify the Transwell transport data for 11-OH-THC and THC-COOH (see below).

Table 2.1. Efflux ratios of 11-OH-THC and THC-COOH in MDCKII-P-gp cells in Transwell transport assays

Group	Compound	Treatment	ER	Level of significance
11-OH-THC		DMSO	0.98 ± 0.46	NS

(n = 3)	0.3 μM 11-OH-THC	5 μM tariquidar	0.90 ± 0.42	
	2 μM Quinidine	DMSO	10.69 ± 7.45	$P = 0.0473$
		5 μM tariquidar	1.01 ± 0.35	
THC-COOH (n = 3)	2.5 μM THC-COOH	DMSO	1.04 ± 0.40	NS
		5 μM tariquidar	0.74 ± 0.05	
	2 μM Quinidine	DMSO	6.01 ± 1.13	$P = 0.0050$
		5 μM tariquidar	1.26 ± 0.12	

Data shown are means ± S.D. of three independent experiments with triplicate in each experiment. ER was calculated as the ratio of individual $P_{app, B \rightarrow A}$ to its corresponding $P_{app, A \rightarrow B}$. Differences in ERs between DMSO and tariquidar in each treatment group were analyzed by the paired Student's *t* test. ER of THC is not shown here because THC could not be detected in the receiver compartment (see Results for details).

Table 2.2. Mass balance of cannabinoids in bidirectional Transwell transport assays

MDCKII-P-gp		A→B		B→A	
Mass balance (%)	5 μM tariquidar	-	+	-	+
THC (n=2)	Receiver	0	3.86	0	0.32
	Donor	19.82	18.86	0	14.11
	Intracellular	80.18	77.28	100	85.57
11-OH-THC (n=3)	Receiver	4.89 ± 1.23	4.21 ± 0.70	2.71 ± 0.39	2.68 ± 1.06
	Donor	24.06 ± 11.99	23.57 ± 11.40	73.25 ± 4.18	73.04 ± 9.53
	Intracellular	71.04 ± 10.87	72.22 ± 11.06	24.04 ± 4.04	24.28 ± 8.52
THC-COOH (n=3)	Receiver	16.46 ± 3.69	21.35 ± 7.75	10.66 ± 2.42	10.78 ± 2.90
	Donor	44.37 ± 15.30	38.43 ± 13.41	76.35 ± 6.21	75.76 ± 5.32
	Intracellular	39.18 ± 17.49	40.22 ± 21.12	12.99 ± 8.59	13.45 ± 8.20
MDCKII-BCRP		A→B		B→A	
Mass balance (%)	5 μM Ko143	-	+	-	+
THC (n=2)	Receiver	0	0	0	0.22
	Donor	11.17	15.07	40.10	0
	Intracellular	88.83	84.93	59.90	99.78
11-OH-THC (n=4)	Receiver	6.07 ± 1.49	6.85 ± 2.52	3.06 ± 1.65	3.55 ± 1.29
	Donor	24.04 ± 5.48	24.93 ± 5.01	72.89 ± 7.61	70.83 ± 6.67
	Intracellular	69.89 ± 4.17	68.22 ± 2.92	24.05 ± 6.04	25.63 ± 5.42
THC-COOH (n=3)	Receiver	23.04 ± 7.07	25.62 ± 4.38	15.78 ± 3.02	12.59 ± 1.19
	Donor	47.98 ± 16.68	43.51 ± 7.57	75.23 ± 8.07	76.09 ± 1.19
	Intracellular	28.98 ± 10.15	30.86 ± 6.04	8.99 ± 5.09	11.32 ± 2.03

Data shown for THC are means of duplicate experiments, each conducted in triplicate, and for 11-OH-THC and THC-COOH are means ± S.D. of at least three independent experiments, each conducted in triplicate, in the absence (-) and presence (+) of an inhibitor. Mass balance data were expressed as percentage of the total mass quantified for the three compartments.

2.4.2 Cellular accumulation of cannabinoids in MDCKII-P-gp cells

To verify the observations in the Transwell transport assays that the cannabinoids were not transported by P-gp and, to resolve the issues mentioned above in the Transwell transport

assay for THC, we performed unidirectional cellular accumulation assay using MDCKII-P-gp cells. The cellular accumulation of quinidine, THC, 11-OH-THC, and THC-COOH in a representative experiment is shown in **Figure 2.1**. The AUCs of cellular accumulation were then calculated from at least three independent experiments and compared between the presence and absence of 5 μM tariquidar (**Table 2.3**). Although the activity of P-gp varied among different passages of cells (2.47-fold change in the ratio of AUC with tariquidar to the AUC without tariquidar for quinidine from 1.50 to 3.71), the AUC of cellular accumulation for quinidine in the presence of tariquidar was significantly greater than that in the absence of tariquidar, and the average AUC ratios in the presence and absence of tariquidar for quinidine were greater than 2 (**Table 2.3**), confirming P-gp activity in MDCKII-P-gp cells. In contrast, the cellular accumulation of THC, 11-OH-THC and THC-COOH were not significantly different between the presence and absence of tariquidar as shown in the representative experiment (**Figure 2.1**). Likewise, the AUCs of cellular accumulation for THC, 11-OH-THC, and THC-COOH in the presence of tariquidar were not significantly different from those in the absence of tariquidar, with the AUC ratios of around 1 for all the cannabinoids (**Table 2.3**). These results further supported that THC, 11-OH-THC, and THC-COOH are not P-gp substrates.

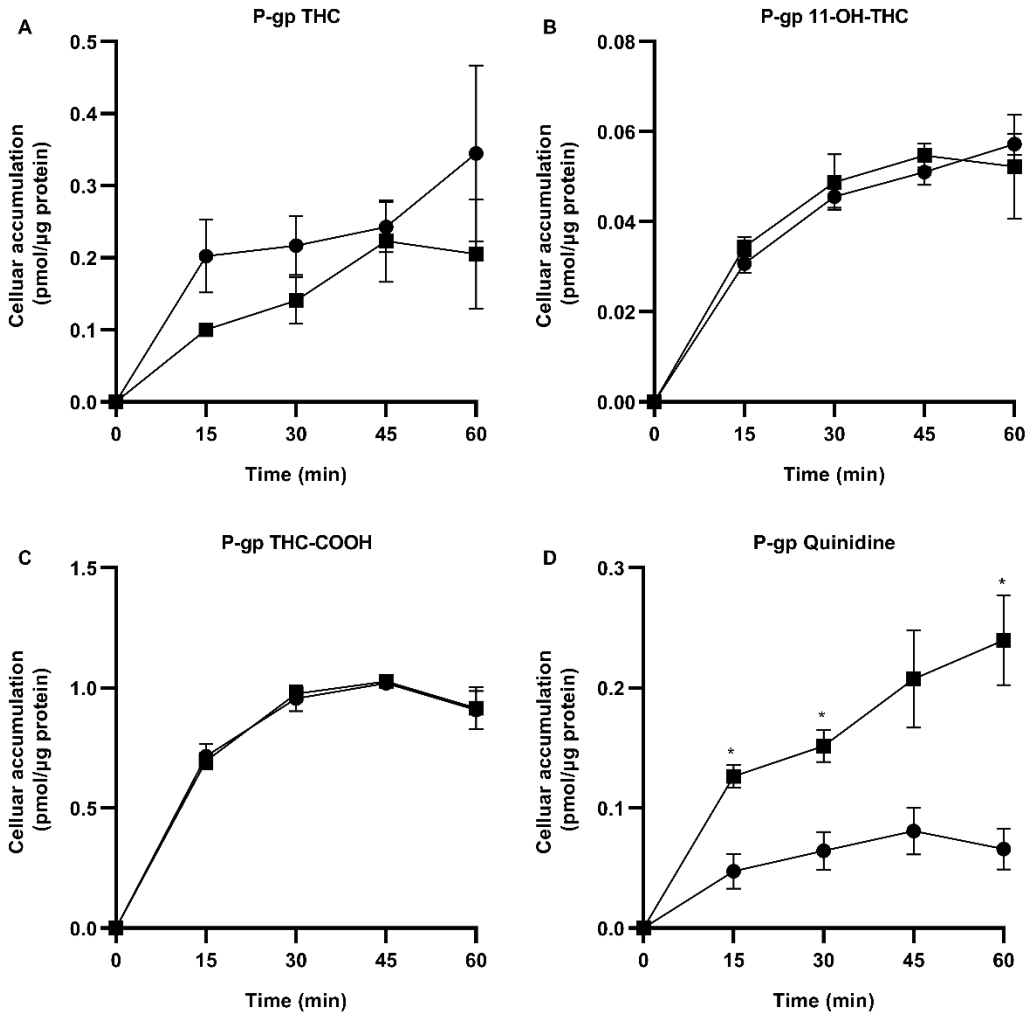

Figure 2.1. Cellular accumulation of THC, 11-OH-THC, or THC-COOH in MDCKII-P-gp cells in a representative experiment.

Cellular accumulation of 5 µM THC (**A**), 0.3 µM 11-OH-THC (**B**), 2.5 µM THC-COOH (**C**), and 2 µM quinidine (**D**), in MDCKII-P-gp cells in the absence (solid circles) or presence (solid squares) of 5 µM tariquidar in a representative experiment. Data shown are means ± S.D. of triplicates. Differences in cellular accumulation in the absence and presence of tariquidar were analyzed using two-way ANOVA followed by the Šidák's *post hoc* test. * $P < 0.05$.

Table 2.3. Cellular accumulation of cannabinoids in MDCKII-P-gp cells

Group	Treatment	AUC Ratio	Level of significance
THC	5 μM THC	1.16 ± 0.59	NS
(n = 4)	2 μM quinidine	2.30 ± 0.99	$P = 0.03$
11-OH-THC	0.3 μM 11-OH-THC	1.09 ± 0.08	NS
(n = 5)	2 μM quinidine	2.32 ± 0.54	$P = 0.002$
THC-COOH	2.5 μM THC-COOH	0.96 ± 0.06	NS
(n = 3)	2 μM quinidine	2.50 ± 0.40	$P = 0.0113$

Shown are the AUC ratios of cellular accumulation for 5 μM THC, 0.3 μM 11-OH-THC, and 2.5 μM THC-COOH in MDCKII-P-gp cells in the absence or presence of 5 μM tariquidar. Quinidine (2 μM) was used as a P-gp positive control prototypic substrate. The AUCs were calculated using the trapezoidal rule with 0, 15, 30, 45, and 60 min as the time points. Data shown are means ± S.D. from at least three independent experiments (n = 4 for THC; n = 5 for 11-OH-THC; and n = 3 for THC-COOH), each conducted in triplicate. Differences in AUC ratio between the absence and presence of tariquidar were analyzed using the paired Student's *t*-test. NS stands for "Not Significant".

2.4.3 Bidirectional Transwell transport of cannabinoids in MDCKII-BCRP cells

Next, we performed the Transwell transport assay for the cannabinoids using MDCKII-BCRP cells, with prazosin (3 μM) as a prototypic substrate and Ko143 (5 μM) as the BCRP inhibitor. The ERs of prazosin in the absence of Ko143 were much greater than 2, and were decreased to approximately 1 in the presence of Ko143 (**Table 2.4**), confirming BCRP activity in the MDCKII cells. Similar to what we observed in MDCKII-P-gp cells, 60-100% of THC was trapped in MDCKII-BCRP cells and THC in the receiver chamber was not quantifiable, while 11-OH-THC and THC-COOH were trapped in cells to a lesser (**Table 2.2**). For 11-OH-THC, its ERs in the presence and absence of Ko143 were around 1 (**Table 2.4**), indicating that 11-OH-THC was not transported by BCRP. Interestingly, the ERs of THC-COOH in the absence of Ko143 were ~1.6, and were significantly decreased to ~1.0 in the presence of Ko143 (**Table**

2.4), suggesting that THC-COOH is a weak substrate of BCRP. Transwell transport of THC-COOH and the BCRP prototypic substrate prazosin is shown in **Figure 2.2**.

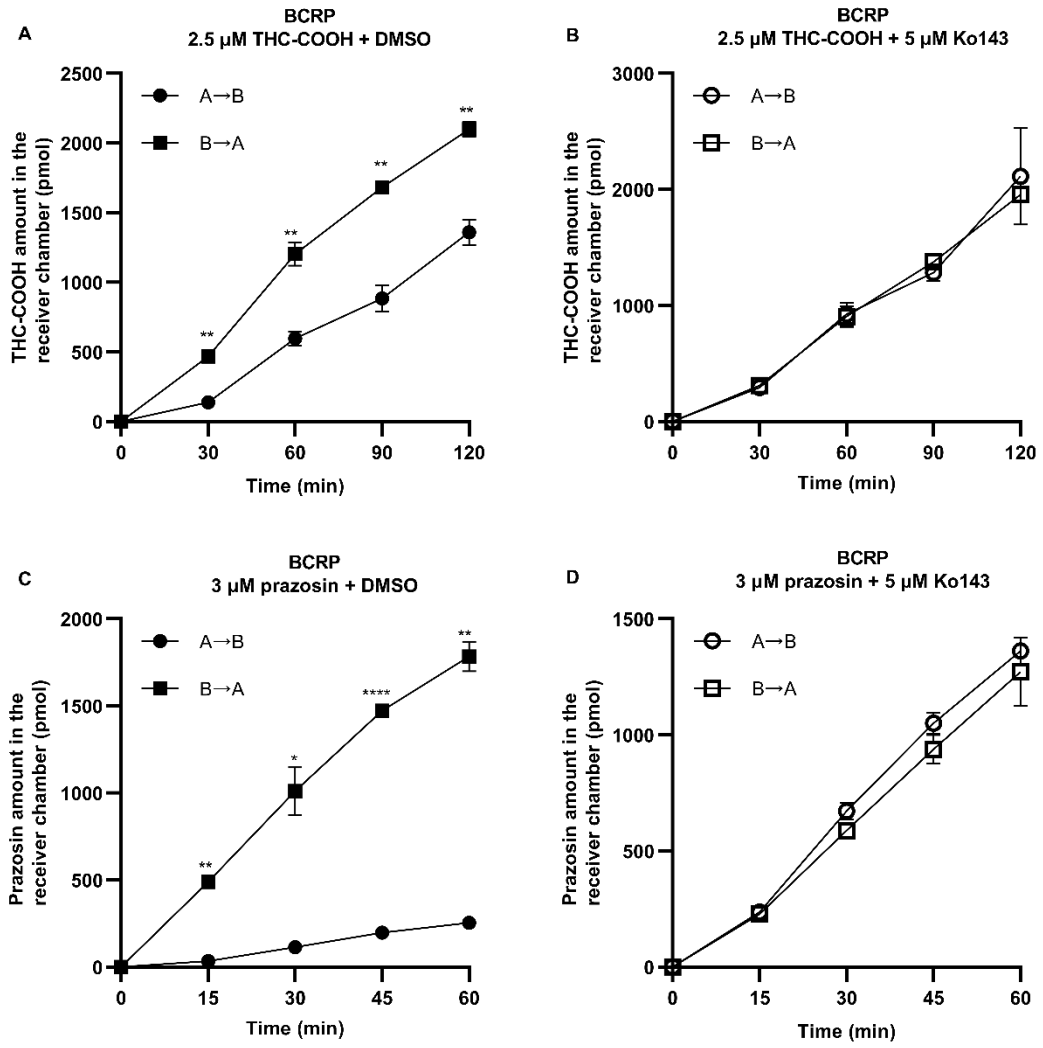

Figure 2.2. Transwell transport of THC-COOH by BCRP in MDCKII-BCRP cells. Shown are the Transwell transport data of 2.5 μM THC-COOH (**A** and **B**) and 3 μM prazosin (**C** and **D**) in MDCKII-BCRP cells in the absence (solid circles for A→B, and solid squares for B→A) or presence (open circles for A→B, and open squares for B→A) of 5 μM Ko143. Data shown are means ± S.D. of triplicates. Differences in transport between the A→B and B→A directions at each time point were analyzed using paired two-way ANOVA followed by the Tukey's *post hoc* test. * $P < 0.05$; ** $P < 0.01$; *** $P < 0.0001$.

Table 2.4. Efflux ratios of 11-OH-THC or THC-COOH in MDCKII-BCRP cells in Transwell assays.

Group	Compound	Treatment	ER	Level of significance
0.3 μM 11-OH-THC (n = 4)	0.3 μM 11-OH-THC	DMSO	0.78 ± 0.09	NS
		5 μM Ko143	0.96 ± 0.30	
	3 μM Prazosin	DMSO	5.48 ± 0.61	$P = 0.0004$
		5 μM Ko143	0.97 ± 0.13	
2.5 μM THC-COOH (n = 3)	2.5 μM THC-COOH	DMSO	1.61 ± 0.12	$P = 0.0101$
		5 μM Ko143	1.01 ± 0.13	
	3 μM Prazosin	DMSO	7.75 ± 4.19	$P = 0.0248$
		5 μM Ko143	0.77 ± 0.08	

Data shown are means ± S.D. of at least three independent experiments with triplicate in each experiment (n = 4 for the 11-OH-THC group; n = 3 for the THC-COOH group). Efflux ratio was calculated as the ratio of individual $P_{app, B \rightarrow A}$ to its corresponding $P_{app, A \rightarrow B}$. Differences in ERs between DMSO and Ko143 in each treatment group were analyzed by the paired Student's *t*-test. NS stands for "Not Significant". Efflux ratio of THC is not shown here because THC could not be detected in the received compartment (see Results for details).

2.4.4 Cellular accumulation of cannabinoids in MDCKII-BCRP cells

We also performed the monodirectional cellular accumulation assay for these cannabinoids using MDCKII-BCRP cells, and the cellular accumulation data for prazosin, THC, 11-OH-THC, and THC-COOH from a representative experiment are shown in **Figure 2.3**. Although the activity of BCRP varied with different cell passages (6.13-fold change in the ratio of AUC with Ko143 to the AUC without Ko143 for prazosin from 7.86 to 48.2), the AUCs of cellular accumulation for prazosin in the presence of Ko143 were significantly greater than those in the absence of Ko143, with the average AUC ratios in the presence over the absence of Ko143 of >20 (**Table 2.5**), confirming BCRP activity in MDCKII-BCRP cells. The AUCs for THC or 11-OH-THC in the presence and absence of Ko143 were not significantly different, with the

AUC ratios of around 1; however, the AUC for THC-COOH in the presence of Ko143 was significantly greater than that in the absence of Ko143with the AUC ratio of ~1.6 (**Table 2.5**). These results confirmed that THC-COOH is a weak substrate of BCRP, but THC and 11-OH-THC are not.

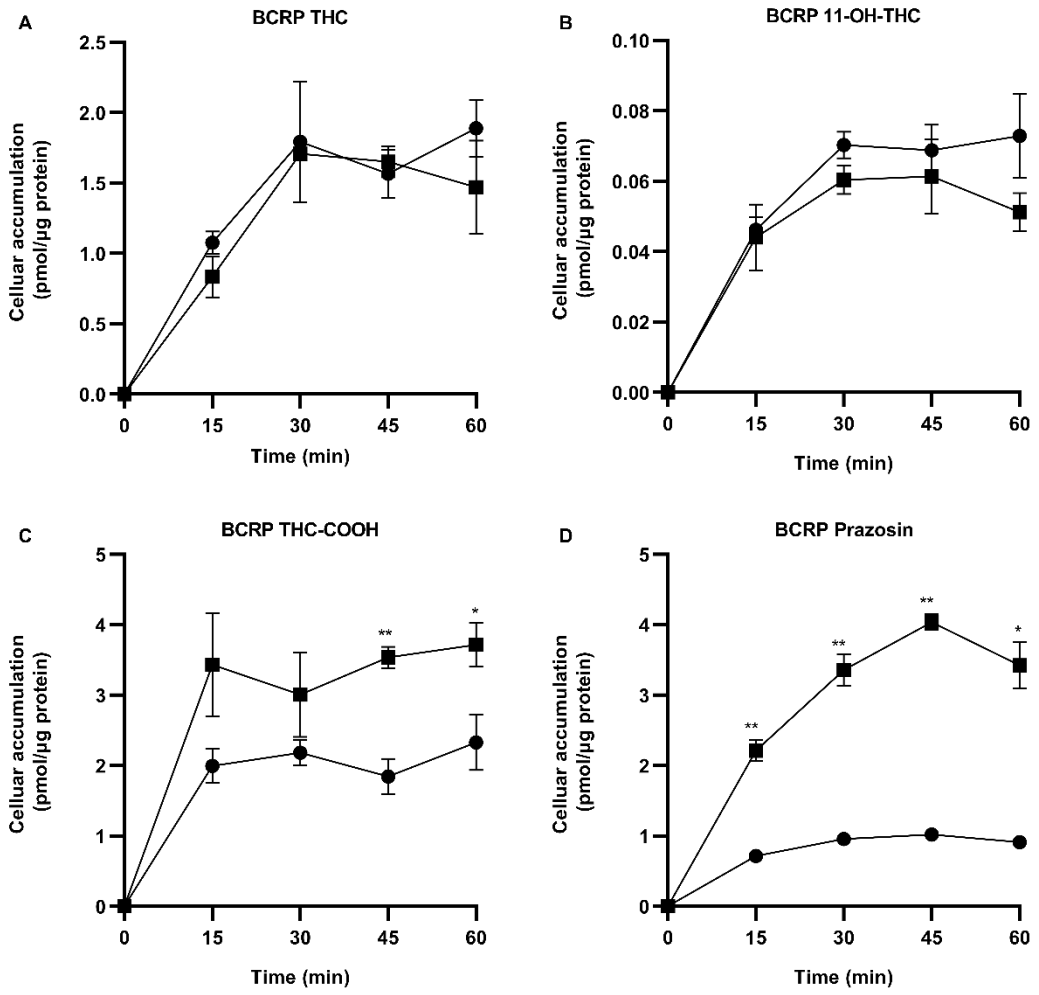

Figure 2.3. **Cellular accumulation of THC, 11-OH-THC, and THC-COOH in MDCKII-BCRP cells in a representative experiment**.

Shown are cellular accumulation data for 5 µM THC (**A**), 0.3 µM 11-OH-THC (**B**), 2.5 µM THC-COOH(**C**), and 3 µM prazosin (**D**), in MDCKII-BCRP cells in the absence (solid circles) or presence (solid squares) of 5 µM Ko143 in a representative experiment with triplicates. Data shown are means ± S.D. from triplicates in the experiment. Differences in cellular accumulation

between the absence and presence of Ko143 were analyzed using two-way ANOVA followed by the Šidák's *post hoc* test. * $P < 0.05$; ** $P < 0.01$.

Table 2.5 Cellular accumulation of cannabinoids in MDCKII-BCRP cells.

Group	Treatment	AUC Ratio	Level of significance
THC	5 μM THC	0.83 ± 0.06	NS
(n = 4)	3 μM prazosin	20.04 ± 11.77	$P = 0.0034$
11-OH-THC	0.3 μM 11-OH-THC	1.25 ± 0.32	NS
(n = 4)	3 μM prazosin	29.01 ± 16.61	$P = 0.0039$
THC-COOH	2.5 μM THC-COOH	1.61 ± 0.09	$P = 0.0005$
(n = 4)	3 μM prazosin	28.42 ± 7.07	$P = 0.0002$

Shown are the AUC ratios of cellular accumulation for 5 μM THC, 0.3 μM 11-OH-THC, and 2.5 μM THC-COOH in MDCKII-BCRP cells in the absence or presence of 5 μM Ko143. Prazosin (3 μM) was used as a BCRP prototypic substrate in positive controls. The AUCs were calculated using the trapezoidal rule with 0, 15, 30, 45, and 60 min as the time points. Data shown are means ± S.D. of quadruplicate with triplicate in each experiment. Differences in AUC ratio between the absence and presence of Ko143 were analyzed using the paired Student's *t*-test. NS stands for "Not Significant".

2.4.5 Inhibition of P-gp or BCRP-mediated vesicular transport by cannabinoids

Finally, we investigated whether these cannabinoids are inhibitors of human P-gp and BCRP at pharmacologically relevant concentrations. We performed vesicular transport assay using NMQ and LY as the prototypic substrates for P-gp and BCRP, respectively. We used THC at 1667 nM, 11-OH-THC at 100 nM, and THC-COOH at 833.3 nM to represent their respective pharmacologically relevant total plasma concentrations observed in humans [66,149]. As expected, tariquidar at 166.7 nM and 500 nM significantly inhibited P-gp-mediated ATP-dependent vesicular uptake of NMQ (**Figure 2.4A**). Likewise, Ko143 at 33.33 nM and 100 nM significantly inhibited BCRP-mediated ATP-dependent vesicular uptake of LY (**Figure 2.4B**). These results indicated that P-gp and BCRP in the plasma membrane vesicles were functional. We did not

observe significant inhibition of ATP-dependent vesicular uptake of NMQ by any of the cannabinoids at pharmacologically relevant concentration (**Figure 2.4A**). Likewise, we did not observe significant inhibition of ATP-dependent vesicular uptake of LY by THC or 11-OH-THC (**Figure 2.4B**). However, THC-COOH at 833.3 nM inhibited ATP-dependent vesicular uptake of LY by 48.7% (**Figure 2.4B**), suggesting that THC-COOH is a BCRP inhibitor at a pharmacologically relevant concentration. Collectively, these results indicated that THC-COOH is an inhibitor of BCRP, but not of P-gp, and neither THC nor 11-OH-THC is an inhibitor of both P-gp and BCRP, at pharmacologically relevant total plasma concentrations.

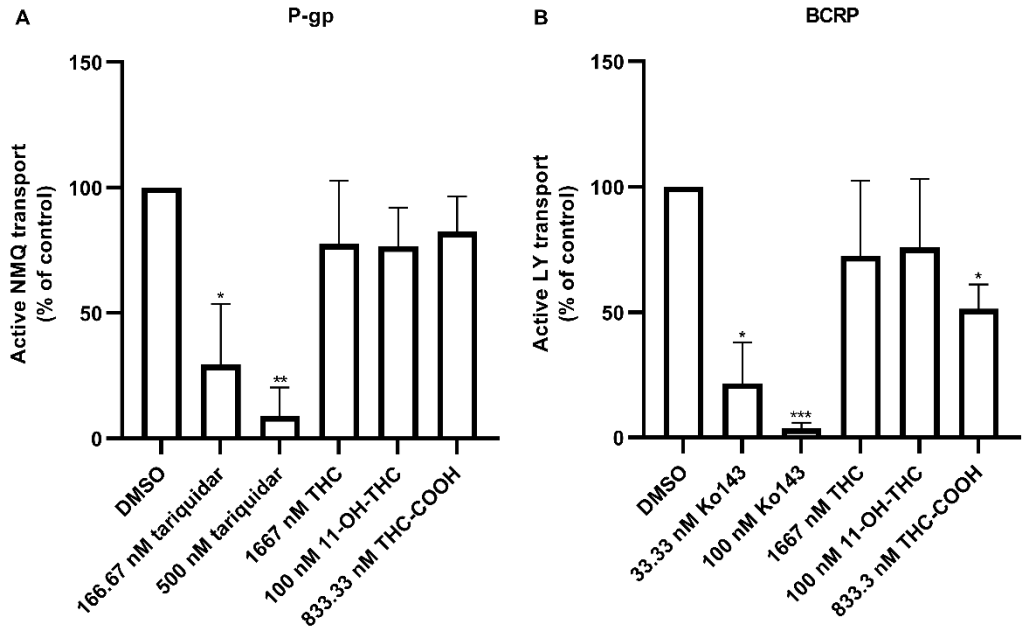

Figure 2.4. **Inhibition of P-gp- or BCRP-mediated vesicular transport by THC, 11-OH-THC or THC-COOH.**

Inhibition of P-gp- or BCRP-mediated vesicular transport by THC, 11-OH-THC or THC-COOH at pharmacologically relevant concentrations was assessed using inside-out plasma membrane vesicles overexpressing human P-gp (**A**) or BCRP (**B**). Data shown are means ± S.D. of triplicates with duplicate in each experiment. The final concentrations of NMQ (P-gp prototypic substrate) and LY (BCRP prototypic substrate) were 1 μM and 50 μM, respectively. Statistically significant differences between all treatment groups were evaluated using paired one-way

ANOVA followed by the Dunnett's *post hoc* test for multiple comparisons. * $P < 0.05$; ** $P < 0.01$; *** $P < 0.001$.

2.5 Discussion

In this study in **Chapter 2**, we systematically performed Transwell, cellular accumulation, vesicular transport studies for THC, 11-OH-THC, and THC-COOH using MDCKII cells or plasma membrane vesicles overexpressing human P-gp or BCRP to investigate whether these cannabinoids are substrates or inhibitors at pharmacologically relevant concentrations.

Three aforementioned assays were used as each has advantages and disadvantages in detecting whether a compound of interest is a substrate or an inhibitor of an efflux transporter. The Transwell assay is considered to be Optima™l, and superior to the cellular accumulation assay, in detecting efflux transport of lipophilic compounds such as the cannabinoids. This is because in the cellular accumulation assay, the transport signal may be overwhelmed by passive diffusion or partitioning of the compound into the cells or cell membrane. In contrast, in the Transwell assay, though a lipophilic compound will also extensively partition into the cells/cell membrane, its appearance in the receiver compartment (if detectable) can detect passive transfer or efflux transport of the compound with high sensitivity. Therefore, to determine if the cannabinoids are transported by P-gp or BCRP, our first choice was to use the Transwell assay with cells overexpressing P-gp or BCRP. However, due to extensive intracellular binding and accumulation, we were unable to detect the appearance of THC in the receiver compartment, making this assay unusable. Since THC seems to extensively partition into the cells and presumably into the cell membrane, we speculated that the cellular accumulation assay may be able to detect P-gp-mediated efflux of THC since this transporter acts as a vacuum cleaner to remove substrates from the lipid bilayer of cell membrane. Finally, the vesicular transport assay, using hydrophilic substrates and the cannabinoids as inhibitors, is a simple and rapid method to determine if a compound is an inhibitor of an efflux transporter.

Cannabinoids are highly lipophilic molecules with low aqueous solubility. THC solubility in pure water is estimated to be 8.9 μM and will decrease when ionic strength of solution increases [30]. The presence of organic solvent significantly increases THC solubility [30]. However, excess organic solvent can alter protein expression profiles of cells and/or disrupt cell

membrane [150]; therefore, we kept organic solvent concentration at 0.2% (v/v) to minimize the impact of organic solvent on cells and membrane vesicles. This low organic solvent concentration and salts in transport buffers limit the solubility of cannabinoids in the final transport buffers. These solubility issues of cannabinoids have been well recognized in previous cannabinoid metabolism studies [34,151]. Although higher THC solubility may be achieved in fasted-state and fed-state simulated intestinal fluids to be approximately 28 μM and 36 μM, respectively [151], bile acids [148] and surfactants in the intestinal fluids may interfere with both cell-based and vesicular transport assays.

Therefore, largely due to solubility issues, we used 5 μM THC, 0.3 μM 11-OH-THC, and 2.5 μM THC-COOH in the Transwell and cellular accumulation assays, which are the highest possible concentrations we could achieve due to low organic solvent concentration in transport buffers and the cannabinoid concentrations in stock solutions available to us. We chose these concentrations also because they are comparable to the total human plasma concentrations of these cannabinoids [66]. Cox *et al.* summarized that the highest total reported plasma concentrations of THC, 11-OH-THC, and THC-COOH after THC administration are 1392 nM (437.7 μg/L) (intravenous, 5 mg THC), 69.2 nM (22.9 μg/L) (oral, 45.7 mg THC), and 519 nM (179 μg/L) (oral, 45.7 mg THC), respectively [66]. Given high plasma protein binding of THC (98.9%), 11-OH-THC (98.8%) *[34]* and THC-COOH (assumed to be 98.8%) [151], the cannabinoid concentrations used in this study are much greater than the unbound human plasma concentrations of these cannabinoids. The Transwell and cellular accumulation assays revealed that THC and 11-OH-THC are not substrates of P-gp or BCRP, and THC-COOH is not a substrate of P-gp. The exception was that THC-COOH was weakly transported by BCRP, with an ER of less than 2. Based on United States Food and Drug Administration guideline *[152]*, THC-COOH is classified as a poor BCRP substrate.

In the Transwell studies, we showed that 80-100% of THC was trapped intracellularly. Given its extremely high plasma protein binding *[30]*, THC could tightly bind to intracellular proteins, such as fatty acid-binding proteins which are known to be intracellular carriers for THC in HeLa cells [72]. These findings provide novel insights into our understanding and interpretation of *in vivo* animal and human data. For example, due to its high lipophilic nature, THC could readily get into the placental syncytiotrophoblasts from the maternal circulation by passive diffusion. Once in the cells, THC may remain in the placenta via tight intracellular protein

binding. Thus, the lower fetal exposure to THC versus its maternal exposure observed in the pregnant macaque study could be due to sequestration of THC in the placental tissue [4]. Hence, the observation of fetal/maternal plasma AUC ratio of <1 may not be due to P-gp- and/or BCRP-medicated efflux of THC by the placenta. Human placenta perfusion studies are currently underway in our laboratory to confirm that THC and 11-OH-THC are not substrates of P-gp and/or BCRP. This confirmation is important for understanding and prediction of fetal and placental exposure to cannabinoids as well as their consequent fetal and placental toxicity. Interestingly, studies in *P-gp/Bcrp* knock-out mice show that THC is a weak substrate of intestinal P-gp (after oral THC administration) [8], while the data on brain distribution of THC are less convincing since they show an effect on brain concentrations of THC at only some sampling times, rather than an effect on brain/plasma AUC ratios [7]. Therefore, animal data regarding whether THC is a substrate of mouse P-gp and/or Bcrp remain inconclusive. We are currently conducting animal studies to further investigate whether P-gp and/or Bcrp plays a role in the fetal distribution of these cannabinoids.

Previous studies reported that THC and THC-COOH stimulate the ATPase activity of P-gp [153], suggesting that these cannabinoids do interact with P-gp. P-gp substrates can either stimulate or inhibit its ATPase activity [154]. Moreover, a substance that can stimulate ATPase activity of P-gp may not be a substrate of the transporter [155]. Therefore, stimulation of ATPase activity does not necessarily mean THC and THC-COOH are P-gp substrates. Our data suggest that the interaction of P-gp with cannabinoids (if any) did not result in P-gp transport of THC or THC-COOH. Another possibility is that these cannabinoids are inhibitors of P-gp or BCRP. Tournier *et al.* reported that THC inhibits P-gp at 50 μM, and the inhibitory potency of 50 μM THC is ~10-fold less than 5 μM valspodar [146]. Tournier *et al.* also mentioned that THC at 50 μM weakly inhibits BCRP [146]. Holland *et al.* also reported that THC inhibits BCRP [156]. However, organic solvent concentrations (*e.g.*, 2% ethanol) used to dissolve 10 or 50 μM THC in their assays were excessive and may be a complicating factor. THC concentrations used in these studies are not pharmacologically relevant and are greater than the water solubility of THC. The actual THC concentrations in their buffer solutions may be lower than the reported nominal concentrations.

To confirm whether the cannabinoids are inhibitors of human P-gp and BCRP at pharmacologically relevant concentrations, we performed the vesicular transport assay to

determine their inhibitory potency for P-gp or BCRP. The concentrations of THC, 11-OH-THC and THC-COOH used in the vesicular inhibition studies were 1667 nM, 100 nM, and 833.3 nM, respectively, which were higher than their highest total plasma concentrations reported to date [66]. We found that THC-COOH at 833.3 nM can moderately inhibit BCRP-mediated transport of LY, indicating that THC-COOH is a weak or moderate BCRP inhibitor, consistent with our finding that THC-COOH is a weak substrate of BCRP. In contrast, THC-COOH does not inhibit P-gp, and neither THC nor 11-OH-THC is an inhibitor of P-gp or BCRP. Due to the limited cannabinoid solubility, we were not able to determine the IC_{50} value of the inhibition of P-gp or BCRP by the cannabinoids.

In summary, in **Chapter 2**, we have demonstrated that, at pharmacologically relevant concentrations, THC-COOH is a weak substrate and inhibitor of BCRP, but not of P-gp, and that THC and 11-OH-THC are neither substrates nor inhibitors of P-gp and BCRP. These results suggest that P-gp or BCRP will not modulate the brain and fetal distribution or intestinal absorption of these cannabinoids in humans. In addition, significant *in vivo* drug interactions between these cannabinoids and P-gp or BCRP inhibitors and inducers are unlikely. Studies are needed to determine if cannabinoids are substrates and inhibitors of other placental drug transporters. These studies are shown in **Chapter 4**.

Chapter 3
In Vivo Role of P-gp/Bcrp in the distribution of THC and Its Major Metabolite Across Maternal-Fetal Barriers

The work presented in this chapter was previously published in

Drug Metabolism and Disposition 2023 Mar;51(3):269-275.

doi: 10.1124/dmd.122.001110.

3.1 Abstract

(-)-*trans*-Δ^9-tetrahydrocannabinol (THC) is the primary pharmacological active constituent of cannabis. 11-hydroxy-THC (11-OH-THC) and 11-*nor*-9-carboxy-THC (THC-COOH) are respectively the active and nonactive circulating metabolites of THC in humans. While previous animal studies reported that THC could be a substrate of mouse P-glycoprotein (P-gp) and breast cancer resistance protein (Bcrp), we have shown, *in vitro*, that only THC-COOH is a weak substrate of human BCRP, but not of P-gp. To confirm these findings and to investigate the role of P-gp and/or Bcrp in the maternal-fetal disposition of THC and its metabolites, we administrated 3 mg/kg THC retro-orbitally to FVB wild-type (WT), *P-gp*$^{-/-}$, *Bcrp*$^{-/-}$ or *P-gp*$^{-/-}$/*Bcrp*$^{-/-}$ pregnant mice on gestation-day 18 and estimated the area under the concentration-time curve (AUC) of the cannabinoids in the maternal plasma, maternal brain, placenta, and fetus, as well as the tissue/maternal plasma AUC geometric mean ratios (GMRs) using a pooled data bootstrap approach. We found that the dose-normalized maternal plasma AUCs of THC in *P-gp*$^{-/-}$ and *P-gp*$^{-/-}$/*Bcrp*$^{-/-}$ mice, and the placenta-to-maternal plasma AUC GMR of THC in *Bcrp*$^{-/-}$ mice were 279%, 271%, and 167% of those in WT mice, respectively. Surprisingly, the tissue-to-maternal plasma AUC GMRs of THC and its major metabolites in the maternal brain, placenta, or fetus in *P-gp*$^{-/-}$, *Bcrp*$^{-/-}$ or *P-gp*$^{-/-}$/*Bcrp*$^{-/-}$ mice were 28-78% of those in WT mice. This study revealed that P-gp and Bcrp do not play a role in limiting maternal brain and fetal exposure to THC and its major metabolites in pregnant mice.

3.2 Introduction

Cannabis usage is escalating in the United States [134,157]. Based on the self-reported prevalence of cannabis use in pregnant women in the United States from 2002-2003 to 2016-2017, past-month use doubled and past-month daily/nearly daily use quadrupled across the entire gestational period [1]. (-)-*trans*-Δ^9-tetrahydrocannabinol (THC) is the major intoxicating constituent in cannabis. In humans, THC is primarily metabolized by the cytochrome P450 (CYP) enzyme CYP2C9 to the intoxicating metabolite 11-hydroxy-THC (11-OH-THC) and sequentially to the non-intoxicating metabolite 11-*nor*-9-carboxy-THC (THC-COOH) [95,133]. Notwithstanding the increasing understanding of cannabinoid metabolism by CYP enzymes, little is known about the roles of transporters in cannabinoid disposition, including maternal and fetal exposure during pregnancy.

P-glycoprotein (P-gp), encoded by *ABCB1* in humans [137], is a member of ATP-binding cassette (ABC) efflux transporter superfamily. The rodent P-gp orthologs are encoded by two genes with high homology to human *ABCB1*, namely *Abcb1a* and *Abcb1b* [158]. Breast Cancer Resistance Protein (BCRP), encoded by *ABCG2* in humans, is another pivotal member of ABC efflux transporters [139–141]. In rodents, Bcrp is encoded by *Abcg2* with 80-90% homology to human *ABCG2* [159]. Both P-gp and BCRP are highly expressed in the brain capillary endothelial cells and placental syncytiotrophoblasts, exerting important roles in tissue distribution with a broad spectrum of substrates [109,160]. Both humans and rodents express P-gp and BCRP on the luminal membrane of brain capillary endothelial cells, directly facing the systemic circulation [161]. On the other hand, human placental P-gp and BCRP are localized on the apical membrane of the syncytiotrophoblast monolayer, directly facing the maternal systemic circulation [162,163]; however, rodent placental P-gp and BCRP are expressed on the apical membrane of the second layer of the syncytiotrophoblasts without direct contact with the maternal systemic circulation [106]. In rodents, connexin26 serves as the intracellular channel to connect the basal membrane of the first layer and the apical membrane of the second layer of the syncytiotrophoblasts [164].

A previous study using a catharized pregnant macaque model demonstrated that fetal plasma the area under concentration-time curve (AUC) of THC is ~30% of maternal plasma AUC of THC while fetal exposure to THC-COOH is almost unquantifiable, indicating that the placental barrier where P-gp and BCRP are highly expressed might limit fetal exposure to THC and THC-COOH [4]. Afterwards, animal studies revealed that the AUC of THC in plasma of *P-gp*-deficient CF1 mice was 2.17-fold higher than that in wild-type (WT) CF1 mice after oral administration of THC, suggesting the potential role of P-gp in limiting oral absorption of THC [8]. Subsequently, Spiro *et al.* showed higher brain/blood THC concentration ratios in *P-gp*$^{-/-}$ or *Bcrp*$^{-/-}$ FVB mice compared to that in FVB WT mice at certain time points after intraperitoneal administration of THC [7]. These animal data suggest that THC is a P-gp and Bcrp substrate [7,8]. However, in the study by Spiro *et al.*, the brain/blood THC concentration ratios in *P-gp*$^{-/-}$ or *Bcrp*$^{-/-}$ mice were not consistently higher than those in WT mice across all time points, making the conclusion that THC is a substrate of P-gp or Bcrp questionable. In **Chapter 2**, our *in vitro* transport study using Madin-Darby canine kidney II cells and plasma membrane vesicles overexpressing human P-gp or human BCRP revealed that at pharmacologically relevant concentrations, only THC-COOH is a weak substrate and inhibitor of BCRP, but not of P-gp,

while THC and 11-OH-THC are neither substrates nor inhibitors of P-gp or BCRP [165]. Given these conflicting data, it is worthwhile to investigate whether P-gp and Bcrp play a role in determining the *in vivo* disposition of THC and its major metabolites including exposure to the fetus. Due to logistical reasons, such studies in pregnant women are not possible, and thus studies in animal models are the only feasible alternatives to human *in vivo* studies. Prior to this study in **Chapter 3**, no such *in vivo* animal studies had been reported. Therefore, in this study in **Chapter 3**, we administered THC (3 mg/kg) retro-orbitally to FVB WT, *P-gp*$^{-/-}$, *Bcrp*$^{-/-}$, and *P-gp*$^{-/-}$/*Bcrp*$^{-/-}$ pregnant mice to determine if mouse P-gp and/or Bcrp limit brain, placental, and fetal exposure to THC, 11-OH-THC, and THC-COOH.

3.3 Materials and methods

3.3.1 Materials

THC (10 mg/mL in ethanol, >95% pure) stock solution was provided by the National Institute on Drug Abuse (Bethesda, MD). THC, 11-OH-THC, THC-COOH and their deuterated internal standards (THC-D_3, 11-OH-THC-D_3, THC-COOH-D_3) (100 μg/mL in methanol for each) were from Cerilliant (Round Rock, TX). Optima™ grade acetonitrile, water, and formic acid were from Thermo Fisher Scientific (Waltham, MA). Isoflurane was from Piramal Healthcare (Bethlehem, PA) through the University of Washington Medical Center Pharmacy (Seattle, WA). Hank's Balanced Salt Solution (1 ×) was purchased from Mediatech (Manassas, VA). Normal saline was from Quality Biological (Gaithersburg, MD). Tween-80 and dimethyl sulfoxide (DMSO) were from Sigma-Aldrich (St. Louis, MO). Dulbecco's phosphate-buffered saline was from Gibco Life Technologies (Carlsbad, CA). Ethanol was from Decon Labs (King of Prussia, PA). Homogenization tubes, beads, and bead ruptor homogenizer were obtained from Omni International (Kennesaw, GA). Heparinized microcentrifuge tubes, 1 mL syringes, and PrecisionGlide™ 26G½ needles were from BD Bioscience (San Jose, CA). Low-binding tubes were from Genesee Scientific (San Diego, CA). Polycarbonate ultracentrifuge tubes were from Beckman Coulter (Brea, CA). Kimwipe™ was from Kimberly-Clark Professional (Irving, TX).

3.3.2 Animals

FVB wild-type (WT), *P-gp*$^{-/-}$ (FVB.129P2-*Abcb1a*^{tm1Bor}*Abcb1b*^{tm1Bor} N12), *Bcrp*$^{-/-}$ (FVB.129P2-*Abcg2*^{tm1Ahs} N7), *P-gp*$^{-/-}$/*Bcrp*$^{-/-}$ (FVB.129P2-*Abcb1a*^{tm1Bor}*Abcb1b*^{tm1Bor}*Abcg2*^{tm1Ahs} N7) mice, aged 4-6 weeks upon delivery, were purchased from Taconic Biosciences (Germantown, NY) and cared for in accordance with the Guide for the Care and Use of Laboratory Animals published by the National Research Council. The animal protocol for this study was approved by the Institutional Animal Care and Use Committee at the University of Washington (Seattle, WA). Mice were maintained under 14/10 light/dark cycles while food and water were provided *ad libitum*. Female mice, 6-8 weeks of age, were mated with male mice of the same genotype overnight. The presence of a sperm plug after overnight housing was defined as gestational day (GD) 1. Progress of pregnancy was monitored by body weight increase and visual inspection.

3.3.3 Animal studies

THC was dissolved in a solution containing 5.6% ethanol (v/v), 5.6% Tween-80 (v/v), and 88.8% normal saline (v/v) at a concentration of 1 mg/mL in a low-binding tube. Under anesthesia (2-5% isoflurane), pregnant mice on GD18 were administered 3 mg/kg body weight of THC by retro-orbital injection. Depth of anesthesia was evaluated using the front-toe pinch method. The 3 mg/kg dose was selected according to Spiro *et al*. [7]. At various time points (2, 5, 10, 30, 60, 120, 180, and 240 min) after administration, mice (n = 3 per time point) were euthanized by cardiac puncture followed by organ collection under anesthesia. Maternal blood was collected in heparinized microcentrifuge tubes and centrifuged at 2,000 × *g* for 10 min at 4°C to harvest plasma. Maternal brain as well as individual placentas and fetuses were collected from pregnant mice immediately following maternal blood collection. Half of the fetuses collected were subject to separation of fetal brains from the remainder of the fetus (henceforth referred to as fetal remains) under a microscope. All tissues were immediately rinsed with Hank's Balanced Salt Solution. Maternal plasma and miscellaneous tissue samples were snap-frozen on dry ice and stored at -80°C until analysis.

3.3.4 Determination of protein binding in maternal plasma

Maternal plasma samples from pregnant mice of each genotype were diluted 10-fold by adding Dulbecco's phosphate-buffered saline (DPBS) in low-binding tubes. Maternal plasma from three randomly chosen pregnant mice per genotype was used. For each genotype, 0.8 mL diluted plasma was spiked (1:100, v/v) with a cocktail of THC/11-OH-THC/THC-COOH (final concentration 333.3 ng/mL for each cannabinoid). After spiking, samples were mixed by placing them on a shaker (500 rpm) at 37°C for 20 min. For each sample, each 180 µL sample was aliquoted into 4 ultracentrifuge tubes. Half of the ultracentrifuge tubes was incubated at 37°C on a shaker (120 rpm) for 90 min, while the other half were centrifuged at 37°C at 435,000 ×*g* for 90 min. Then, 50 µL of the centrifuged (middle layer) or uncentrifuged sample was mixed with 100 µL acetonitrile containing THC-D_3/11-OH-THC-D_3/THC-COOH-D_3 (100 nM each) and centrifuged at 4°C at 25,314 ×*g* (maximal speed) for 20 min. For the ultracentrifuged samples, the outer surface of the pipette tip was gently wiped with Kimwipes to remove adhered lipids before mixing with the internal standards. Finally, the supernatant was transferred to disposable clean glass inserts and 10 µL of the sample were analyzed using liquid chromatography in tandem with mass spectrometry (LC-MS/MS) as described before [95]. The unbound percentage in the diluted plasma ($f_{u,d}$, calculated by peak-area ratio of the ultracentrifuged sample by the peak-area ratio of the corresponding non-centrifuged sample) was extrapolated back to the unbound percentage in plasma ($f_{u,p}$) [166]: $f_{u,p} = (\text{dilution factor} \cdot f_{u,d})/[1- f_{u,d} \cdot (1- \text{dilution factor})]$.

3.3.5 Determination of protein binding in mouse maternal brain homogenate

Maternal brain homogenates from 6 female mice (time points of samples and animals were chosen randomly) of each genotype were diluted 10-fold by adding DPBS in low-binding tubes. For each sample, 1 mL diluted maternal brain homogenate was spiked (1:100, v/v) with a cocktail of THC/11-OH-THC/THC-COOH (final concentration: 333.3 ng/mL for each cannabinoid). After spiking, samples were placed on a shaker (500 rpm) at 37°C for 20 min. For each sample, each 180 µL was aliquoted into 4 ultracentrifuge tubes. Then the unbound percentage was determined using the same procedure as described above for the plasma.

3.3.6 LC-MS/MS quantification of THC, 11-OH-THC, THC-COOH in maternal plasma and tissues

For maternal brains, individual whole fetuses, and fetal remains, 200 µL normal saline were added to100 mg of tissue and homogenized at 4°C using Omni Bead Ruptor Homogenizer at 5.8 m/s, 45 sec/cycle, 2 cycles, 30 sec dwell time. For placenta and fetal brain, 400 µL normal saline was used due to the small quantity of these tissues. Then, all tissue homogenates were transferred to low-binding tubes. To every 50 or 100 µL of maternal plasma or tissue homogenate, 150 or 300 µL acetonitrile containing THC-D_3/11-OH-THC-D_3/THC-COOH-D_3 (100 nM each) were added to precipitate proteins, respectively. All samples were vigorously vortexed for 30 s and centrifuged at 25,314 ×*g* for 20 min at 4°C. Supernatants were transferred to disposable clean glass inserts and, except for maternal brain samples, 10 µL per sample were injected for LC-MS/MS analysis as described previously [95]. For analysis of the maternal brain concentration, the LC gradient was modified to separate interference peaks from the analytes but the MS/MS method remained unchanged. Specifically, the gradient (0.3 mL/min) was: from 0 to 0.5 min, 90% A (water + 0.1% formic acid) and 10% B (acetonitrile + 0.1 % formic acid); from 0.5 to 5 min, linearly decreased A from 90% to 5%, and maintained up to 6 min; from 6 to 6.1 min, linearly increased A from 5% to 90%, and then maintained up to 8 min. No obvious matrix effects were seen between mouse plasma or tissue of any genotype and human plasma (data not shown). Therefore, human plasma spiked with serially-diluted cannabinoid stocks (in DMSO) was used to prepare the calibrators (2.06 nM to 2000 nM) and the quality control samples. The lower quantification limits for THC/11-OH-THC/THC-COOH were 1 nM. The intraday and inter-day variation was below 15%. All plasma or tissue quantification concentrations were converted back to ng/mL for maternal plasma and ng/g tissue for tissue (assuming 1 g/cm^3 tissue density) based on the molecular weight, dilution of the tissue homogenate. Cannabinoid concentration in the placenta, fetal brain, fetal remains, and the whole fetus was determined and averaged for each dam.

3.3.7 Data analyses

The placental concentrations of cannabinoids were corrected for blood in the placenta prior to further analysis using the equation proposed by Barker *et al.* [167,168]. To fit the equation, cannabinoid concentrations in maternal blood were estimated from the maternal plasma

concentrations and the previously published blood/plasma concentration ratios [169], and cannabinoid concentrations in fetal blood were assumed to be the same as fetal concentrations. The maternal concentrations of cannabinoids were expressed in ng/mL/μg THC dose (3 mg/kg × body weight) when computing and comparing the dose-normalized AUCs among the genotypes. Using a bootstrapping method with 10,000 iterations, the AUCs over 0 to 240 min for each analyte in maternal plasma (normalized or not normalized) or tissues from each genotype were estimated and extrapolated back to time 0 using noncompartmental approach using the linear trapezoidal rule (https://github.com/shirewoman2/LaurasHelpers). All AUCs were extrapolated to time infinity and the percentage of extrapolation was calculated. A small number of not available (NA) values due to the algorithm in the bootstrapped AUCs were excluded for further processing. The geometric means (GMs) of dose-normalized maternal plasma AUCs, and tissue-to-maternal plasma AUC geometric mean ratios (GMRs), and 95% confidence intervals (95% CI) were calculated for each genotype-analyte-tissue group. The statistically significant differences in maternal plasma or tissue exposure of each cannabinoid between WT and each genotype mice were analyzed using two-way analysis of variance (ANOVA) followed by Dunnett's *post hoc* test assuming a significance level of 0.05. Differences with adjusted *P values* of < 0.05 were considered statistically significant. The differences in unbound percentage of cannabinoids in plasma or maternal brain for all genotypes were analyzed using the ANOVA. All analyses were performed using R (version 4.0.5) or GraphPad Prism 9 (La Jolla, CA).

3.4 Results

3.4.1 Maternal plasma exposure to THC, 11-OH-THC, and THC-COOH in WT, P-gp$^{-/-}$, Bcrp$^{-/-}$ or P-gp$^{-/-}$/Bcrp$^{-/-}$ pregnant mice

The bootstrapped dose-normalized maternal plasma geometric mean $AUC_{0\text{-}240}$ of THC in *P-gp*$^{-/-}$ or *P-gp*$^{-/-}$/*Bcrp*$^{-/-}$ pregnant mice was significantly increased 2.79-fold or 2.71-fold, respectively, as compared to that in WT pregnant mice (**Table 3.1**). However, such significant differences in $AUC_{0\text{-}\infty}$ of THC disappeared after extrapolation to infinity (**Table 3.1**). We did not calculate $AUC_{0\text{-}\infty}$ of 11-OH-THC in *P-gp*$^{-/-}$ or *P-gp*$^{-/-}$/*Bcrp*$^{-/-}$ pregnant mice due to lack of discernible terminal phase (**Figure 3.1**), even though the terminal phase could be observed in unnormalized maternal plasma concentration-time profiles for 11-OH-THC (**Figure S3.1**). No significant differences were observed in dose-normalized geometric mean AUC ($AUC_{0\text{-}240}$ or $AUC_{0\text{-}\infty}$) of THC between WT and *Bcrp*$^{-/-}$ pregnant mice, or in dose-normalized geometric mean AUCs of 11-OH-THC and THC-COOH between WT and any of the transporter knockout genotype (**Table 3.1**). While the percentages of extrapolation of AUCs for THC were below 6%, the percentages of extrapolation of AUCs for THC-COOH exceeded 20% in *P-gp*$^{-/-}$ or *P-gp*$^{-/-}$/*Bcrp*$^{-/-}$ pregnant mice (**Table 3.1**).

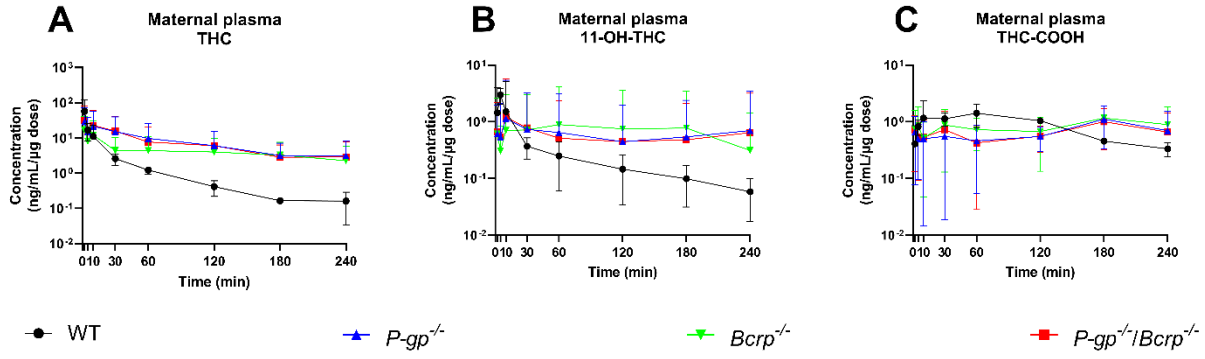

Figure 3.1. Dose-normalized maternal plasma concentration-time profiles of THC, 11-OH-THC and THC-COOH. Compared with the WT mice (●), the mean dose-normalized maternal plasma concentration-time profiles of THC (**A**), were significantly higher in *P-gp*$^{-/-}$ (▲) and *P-gp*$^{-/-}$/ *Bcrp*$^{-/-}$ (■), but not in *Bcrp*$^{-/-}$ (▼) mice. However, the mean dose-normalized maternal plasma concentration-time profiles of 11-OH-THC (**B**), and THC-COOH (**C**) were not different across the genotypes. Mice were administered 3 mg/kg of THC by retro-orbital injection on gestational day 18. Data are mean ± S.D. (n = 3 at each time point).

Table 3.1. Dose-normalized maternal plasma geometric mean AUCs of THC, 11-OH-THC, and THC-COOH in WT and knockout mice

Dose-normalized geometric mean $AUC_{0\text{-}240}$ (95% CI) (µg/mL/µg dose · min)	WT	*P-gp*$^{-/-}$	Adjusted *P* value	*Bcrp*$^{-/-}$	Adjusted *P* value	*P-gp*$^{-/-}$/*Bcrp*$^{-/-}$	Adjusted *P* value
THC	0.56 (0.39, 0.80)	**1.56 (0.94, 2.57)**	**0.0030**	0.88 (0.56, 1.38)	0.26	**1.52 (0.93, 2.48)**	**0.0037**
11-OH-THC	0.07 (0.06, 0.08)	0.12 (0.08, 0.19)	0.23	0.14 (0.08, 0.24)	0.068	0.11 (0.07, 0.17)	0.28
THC-COOH	0.21 (0.19, 0.23)	0.13 (0.10, 0.17)	0.23	0.18 (0.14, 0.23)	0.91	0.14 (0.11, 0.18)	0.36

Dose-normalized geometric mean $AUC_{0\text{-}\infty}$ (95% CI) (µg/mL/µg dose · min)	WT	*P-gp*$^{-/-}$	Adjusted *P* value	*Bcrp*$^{-/-}$	Adjusted *P* value	*P-gp*$^{-/-}$/*Bcrp*$^{-/-}$	Adjusted *P* value
THC	0.59 (0.36, 0.99)	1.56 (0.65, 3.74)	0.50	0.89 (0.30, 2.69)	0.92	1.56 (0.63, 3.86)	0.49
11-OH-THC	0.08 (0.07, 0.09)	NA[a]	NA[a]	0.15 (0.05, 0.45)	0.37[b]	NA[a]	NA[a]
THC-COOH	0.24 (0.22, 0.26)	0.21 (0.05, 0.89)	1.0	0.21 (0.04, 1.05)	1.0	0.21 (0.05, 0.79)	1.0

Extrapolation%	WT	*P-gp*$^{-/-}$	*Bcrp*$^{-/-}$	*P-gp*$^{-/-}$/*Bcrp*$^{-/-}$
THC	5.54	0.03	1.55	2.40
11-OH-THC	11.24	NA[a]	4.39	NA[a]
THC-COOH	13.34	37.85	16.03	32.41

[a] NA stands for not available. [b] Statistical analysis performed using unpaired *t*-test. As shown in Figure 1, the dose-normalized plasma concentrations of 11-OH-THC in *P-gp*$^{-/-}$ and *P-gp*$^{-/-}$/*Bcrp*$^{-/-}$ pregnant mice the terminal phase could not be discerned and therefore could not be extrapolated to infinity. Data shown are the bootstrapped geometric means (GM) (95% confidence interval) (n = 3) of

dose-normalized maternal plasma $AUC_{0\text{-}240}$ and $AUC_{0\text{-}\infty}$ of THC, 11-OH-THC, THC-COOH after retro-orbital injection of THC (3 mg/kg) to pregnant mice on gestational day 18. Percentages of extrapolation were also calculated for each cannabinoid in each genotype. Differences between WT and *P-gp*$^{-/-}$, *Bcrp*$^{-/-}$, or *P-gp*$^{-/-}$/*Bcrp*$^{-/-}$ pregnant mice were analyzed by two-way ANOVA followed by the Dunnett's *post hoc* test. Differences indicated in underline were statistically significant with *P values* of < 0.05 that were adjusted for multiple comparison.

3.4.2 Maternal brain exposure to THC, 11-OH-THC, and THC-COOH in WT, P-gp$^{-/-}$, Bcrp$^{-/-}$ or P-gp$^{-/-}$/Bcrp$^{-/-}$ pregnant mice

Next, we examined maternal brain exposure to THC and its major metabolites in WT, *P-gp*$^{-/-}$, *Bcrp*$^{-/-}$, and *P-gp*$^{-/-}$/*Bcrp*$^{-/-}$ pregnant mice. Since the absolute tissue exposure is driven by the absolute maternal plasma exposure, we determined the maternal brain-to-maternal plasma AUC geometric mean ratios (GMRs). We found that the maternal brain/maternal plasma $AUC_{0\text{-}240}$ GMR of THC in *P-gp*$^{-/-}$ pregnant mice was significantly decreased by 72% compared to that in WT pregnant mice (**Table 3.2**). While the maternal brain/maternal plasma $AUC_{0\text{-}240}$ GMRs of 11-OH-THC in *P-gp*$^{-/-}$ and *P-gp*$^{-/-}$/*Bcrp*$^{-/-}$ pregnant mice were significantly, but modestly, decreased by 35% and 39%, respectively, versus WT pregnant mice, the difference between *Bcrp*$^{-/-}$ and WT pregnant mice was not statistically significant (**Table 3.2**). The maternal brain/maternal plasma $AUC_{0\text{-}240}$ GMR of THC-COOH in *P-gp*$^{-/-}$/*Bcrp*$^{-/-}$ pregnant mice was significantly, but modestly, lower by 24% compared to that in WT pregnant mice; whereas no significant differences were observed between WT and *P-gp*$^{-/-}$ *or Bcrp*$^{-/-}$ pregnant mice (**Table 3.2**). Compared to WT pregnant mice, we found similar observations for the maternal brain/maternal plasma $AUC_{0\text{-}\infty}$ GMR of THC in *P-gp*$^{-/-}$ pregnant mice and the maternal brain/maternal plasma $AUC_{0\text{-}\infty}$ GMR of 11-OH-THC in *P-gp*$^{-/-}$/*Bcrp*$^{-/-}$ pregnant mice, but not of any other cannabinoids in any other genotypes (**Table S3.1**). The percentages of extrapolations of AUCs of cannabinoids were generally not greater than 20% except for AUC of THC-COOH in WT pregnant mice and AUCs of 11-OH-THC and THC-COOH in *P-gp*$^{-/-}$ pregnant mice (**Table S3.2**).

Table 3.2. The maternal brain, placental, and fetal-to-maternal plasma AUC_{0-240} GMRs of THC, 11-OH-THC, and THC-COOH

	AUC_{0-240} GMR (95% CI)	AUC_{0-240} GMR (95% CI)	Adjusted *P* value	AUC_{0-240} GMR (95% CI)	Adjusted *P* value	AUC_{0-240} GMR (95% CI)	Adjusted *P* value
THC	WT	*P-gp*$^{-/-}$		*Bcrp*$^{-/-}$		*P-gp*$^{-/-}$/*Bcrp*$^{-/-}$	
Maternal brain	0.55 (0.37, 0.80)	**0.15 (0.09, 0.26)**	**<0.0001**	0.64 (0.55, 0.74)	0.77	0.35 (0.24, 0.51)	0.065
Placenta	0.36 (0.24, 0.55)	0.28 (0.23, 0.34)	0.40	**0.61 (0.52, 0.71)**	**0.029**	0.53 (0.40, 0.69)	0.14
Fetal remains	0.20 (0.14, 0.30)	0.14 (0.12, 0.16)	0.12	0.27 (0.23, 0.32)	0.31	0.20 (0.15, 0.26)	1.0
Fetus	0.17 (0.11, 0.25)	0.16 (0.14, 0.19)	1.0	0.22 (0.18, 0.27)	0.39	0.16 (0.12, 0.21)	0.97
11-OH-THC	WT	*P-gp*$^{-/-}$		*Bcrp*$^{-/-}$		*P-gp*$^{-/-}$/*Bcrp*$^{-/-}$	
Maternal brain	1.26 (1.07, 1.49)	**0.82 (0.72, 0.93)**	**0.0011**	1.45 (1.26, 1.67)	0.48	**0.77 (0.61, 0.96)**	**0.0002**
Placenta	1.38 (1.18, 1.62)	**1.02 (0.88, 1.18)**	**0.026**	1.51 (1.31, 1.75)	0.77	1.25 (1.08, 1.45)	0.71
Fetal remains	1.17 (1.00, 1.36)	**0.76 (0.67, 0.86)**	**0.0013**	1.01 (0.88, 1.17)	0.47	**0.78 (0.70, 0.88)**	**0.0026**
Fetus	1.15 (0.98, 1.35)	**0.57 (0.50, 0.64)**	**<0.0001**	1.02 (0.87, 1.21)	0.60	**0.59 (0.51, 0.68)**	**<0.0001**
THC-COOH	WT	*P-gp*$^{-/-}$		*Bcrp*$^{-/-}$		*P-gp*$^{-/-}$/*Bcrp*$^{-/-}$	
Maternal brain	0.25 (0.22, 0.28)	0.23 (0.19, 0.26)	0.48	0.22 (0.20, 0.26)	0.43	**0.19 (0.15, 0.24)**	**0.0064**
Placenta	0.87 (0.76, 0.98)	0.75 (0.68, 0.83)	0.25	1.02 (0.92, 1.13)	0.14	**0.67 (0.61, 0.74)**	**0.012**
Fetal remains	0.54 (0.47, 0.61)	**0.40 (0.36, 0.44)**	**0.0020**	0.46 (0.40, 0.52)	0.16	**0.33 (0.29, 0.36)**	**<0.0001**
Fetus	0.50 (0.43, 0.58)	**0.27 (0.23, 0.31)**	**<0.0001**	**0.39 (0.33, 0.46)**	**0.013**	**0.29 (0.26, 0.31)**	**<0.0001**

Data shown are the bootstrapped tissue/maternal plasma AUC GMRs of THC, 11-OH-THC, THC-COOH after retro-orbital injection of THC (3 mg/kg) to pregnant mice on gestational day 18 over 240 min. Data are reported as geometric mean ratio (GMR) (95% confidence interval) (n = 3). Differences in AUC GMRs between WT and *P-gp*$^{-/-}$, *Bcrp*$^{-/-}$, or *P-gp*$^{-/-}$/*Bcrp*$^{-/-}$ pregnant mice were analyzed by two-way ANOVA followed by the Dunnett's *post hoc* test. Differences indicated in underline were statistically significant with *P values* of < 0.05 that were adjusted for multiple comparisons.

3.4.3 Placental exposure to THC, 11-OH-THC, and THC-COOH in WT, P-gp$^{-/-}$, Bcrp$^{-/-}$ or P-gp$^{-/-}$/Bcrp$^{-/-}$ pregnant mice

The placenta/maternal plasma $AUC_{0\text{-}240}$ GMRs of THC in *Bcrp*$^{-/-}$ pregnant mice was increased 1.67-fold as compared to that in WT pregnant mice (**Table 3.2**). The placenta/maternal plasma $AUC_{0\text{-}240}$ GMR of 11-OH-THC in *P-gp*$^{-/-}$ pregnant mice was significantly, but modestly, decreased by 26% compared to that in WT pregnant mice (**Table 3.2**). The placenta/maternal plasma $AUC_{0\text{-}240}$ GMR of THC-COOH in *P-gp*$^{-/-}$/*Bcrp*$^{-/-}$ pregnant mice was significantly, but modestly, decreased by 22% versus that in WT pregnant mice (**Table 3.2**). None of other placenta/maternal plasma $AUC_{0\text{-}240}$ GMRs in transporter knockout mice significantly differed from those in WT pregnant mice (**Table 3.2**). None of the $AUC_{0\text{-}\infty}$ GMRs of the cannabinoids in transporter knockout mice significantly differed from those in WT pregnant mice (**Table S3.1**). About half of the percentages of extrapolations of the placental AUCs exceeded 20% (**Table S3.2**).

3.4.4 Fetal exposure to THC, 11-OH-THC, and THC-COOH in WT, P-gp$^{-/-}$, Bcrp$^{-/-}$, or P-gp$^{-/-}$/Bcrp$^{-/-}$ pregnant mice

We found no statistically significant differences in fetal (both fetus and fetal remains) $AUC_{0\text{-}240}$ GMRs of THC among all four mouse groups (**Table 3.2**). The fetal (fetus and fetal remains) $AUC_{0\text{-}240}$ GMRs of 11-OH-THC in *P-gp*$^{-/-}$ and *P-gp*$^{-/-}$/*Bcrp*$^{-/-}$ pregnant mice were significantly, but modestly, decreased by 33-51% compared to that in WT pregnant mice (**Table 3.2**). The fetal (fetus and fetal remains) $AUC_{0\text{-}240}$ GMRs of THC-COOH in *P-gp*$^{-/-}$ and *P-gp*$^{-/-}$/*Bcrp*$^{-/-}$ pregnant mice were significantly, but modestly, decreased by 26-46% versus WT pregnant mice (**Table 3.2**). While the fetus $AUC_{0\text{-}240}$ GMR of THC-COOH in *Bcrp*$^{-/-}$ pregnant mice was moderately decreased by 22% versus WT pregnant mice, its fetal remains $AUC_{0\text{-}240}$ GMR in *Bcrp*$^{-/-}$ pregnant mice was not significantly different from that in WT mice despite with the same trend (**Table 3.2**). Compared to WT pregnant mice, we did not observe significant differences in $AUC_{0\text{-}\infty}$ GMRs of 11-OH-THC/THC-COOH in fetal remains of *P-gp*$^{-/-}$ pregnant mice, or in $AUC_{0\text{-}\infty}$ GMR of THC-COOH in fetus of *Bcrp*$^{-/-}$ pregnant mice (**Table S3.1**). The majority of the percentages of extrapolation of the fetal AUCs exceeded 20% (**Table S3.2**).

3.4.5 Fetal brain exposure to THC, 11-OH-THC, and THC-COOH

THC and its major metabolites in fetal brain tissues were not quantifiable by LC-MS/MS in any of the mouse groups investigated in this study. The peaks for THC, 11-OH-THC, and THC-COOH in their corresponding channel were either not greater than the lower limit of detection or the lower limit of quantification except for only a few individual samples (data not shown).

3.4.6 Protein binding of cannabinoids in maternal plasma

To investigate whether the differential tissue distributions of the cannabinoids described above were due to differential plasma protein binding of THC and its major metabolites amongst different genotypes, we determined the unbound percentages of THC, 11-OH-THC, and THC-COOH in maternal plasma samples from WT, *P-gp$^{-/-}$, Bcrp$^{-/-}$, and P-gp$^{-/-}$/Bcrp$^{-/-}$* mice using ultracentrifugation. The unbound percentages of THC, 11-OH-THC, and THC-COOH in maternal ~~mouse~~ plasma were within the range 2.84-5.87%, 2.38-5.45%, and 2.31-6.92%, respectively, and did not differ significantly among the four mouse genotypes (**Table 3.3**).

Table 3.3. Unbound percentages of THC, 11-OH-THC, and THC-COOH in maternal plasma

f_u (%)	THC	11-OH-THC	THC-COOH
WT	3.09 ± 1.54	5.87 ± 5.47	3.65 ± 0.34
P-gp$^{-/-}$	2.38 ± 2.04	5.45 ± 3.70	4.20 ± 0.94
Bcrp$^{-/-}$	2.31 ± 2.01	6.92 ± 4.76	4.56 ± 0.47
P-gp$^{-/-}$/Bcrp$^{-/-}$	3.09 ± 1.54	5.87 ± 5.47	3.65 ± 0.34

Data shown are the unbound percentages of THC, 11-OH-THC, THC-COOH in maternal plasma of WT, *P-gp$^{-/-}$, Bcrp$^{-/-}$*, and *P-gp$^{-/-}$/Bcrp$^{-/-}$* male mice after spiking 1:10 diluted blank male mouse plasma with 0.33 μg/mL (final concentration 333.3 ng/mL) of each cannabinoid. Data are reported as mean ± S.D. plasma samples from three pregnant mice per genotype with duplicate determinations for each plasma sample. Differences among the four mouse groups were analyzed

by ANOVA and considered statistically significant with *P values* of < 0.05. No statistically significant differences were found.

3.4.7 Protein binding of cannabinoids in maternal brain homogenates

To investigate whether the differential tissue distributions of the cannabinoids described above were due to differential tissue binding of THC and its major metabolites, we determined the unbound percentages of THC, 11-OH-THC, and THC-COOH in maternal brain homogenates from WT, *P-gp*$^{-/-}$*, Bcrp*$^{-/-}$*, and P-gp*$^{-/-}$*/Bcrp*$^{-/-}$ pregnant mice using ultracentrifugation. We chose maternal brain homogenates in these analyses because the greatest statistically significant difference we observed was in maternal brain exposure to THC between WT and *P-gp*$^{-/-}$ pregnant mice (**Table 3.2**). The unbound percentages of THC, 11-OH-THC, and THC-COOH fell within the ranges of 0.009-0.010%, 0.098-0.115%, and 1.08-1.23%, respectively, and did not significantly differ among the four mouse genotypes (**Table 3.4**).

Table 3.4. Unbound percentages of THC, 11-OH-THC, and THC-COOH in maternal brain homogenates

f_u (%)	THC	11-OH-THC	THC-COOH
WT	0.009 ± 0.001	0.098 ± 0.019	1.08 ± 0.16
***P-gp*$^{-/-}$**	0.009 ± 0.001	0.101 ± 0.013	1.12 ± 0.08
***Bcrp*$^{-/-}$**	0.010 ± 0.002	0.110 ± 0.027	1.15 ± 0.07
***P-gp*$^{-/-}$/*Bcrp*$^{-/-}$**	0.010 ± 0.003	0.115 ± 0.031	1.23 ± 0.12

Data shown are unbound percentages of THC, 11-OH-THC, THC-COOH in maternal brain homogenates of WT, *P-gp*$^{-/-}$*, Bcrp*$^{-/-}$, and *P-gp*$^{-/-}$*/Bcrp*$^{-/-}$ pregnant mice after spiking 1:10 diluted pregnant mouse maternal brain homogenates with 0.33 μg/mL (final concentration 333.3 ng/mL) of each cannabinoid. Data are reported as mean ± S.D. (n = 6). Differences among the four mouse groups were analyzed by ANOVA, but none were found. Differences were considered statistically significant with *P values* of < 0.05.

3.5 Discussion

In **Chapter 3**, our primary goal was to compare the maternal brain, placental, and fetal exposure to THC and its metabolites between WT and *P-gp*$^{-/-}$, *Bcrp*$^{-/-}$ or *P-gp*$^{-/-}$/*Bcrp*$^{-/-}$ pregnant mice. Tissue exposure is driven by maternal plasma exposure. Since maternal plasma exposure could be influenced by cofounding factors, such as variation in body weight of pregnant mice due to variation in litter size and potential impact of transporter knockout on systemic clearance of the cannabinoids, we focused our analyses on tissue-to-maternal plasma AUC ratios as the primary endpoint, which should not be affected by systemic clearance of the cannabinoids provided the maternal plasma and tissue AUCs are sufficiently captured over the duration of sampling. We used 240 min as the last time point of plasma sampling based on a previous study [8] which well captured maternal plasma AUC. However, the high percentages of extrapolation for calculating $AUC_{0-\infty}$ values of the cannabinoids, especially in fetal tissues, made the interpretation of $AUC_{0-\infty}$ GMR of concern. Therefore, we primarily interpretated AUC_{0-240} GMR in this study.

We found ~3-fold higher maternal plasma exposure to THC in *P-gp*$^{-/-}$ or *P-gp*$^{-/-}$/*Bcrp*$^{-/-}$ pregnant mice, suggesting that the systemic clearance of THC in *P-gp*$^{-/-}$ or *P-gp*$^{-/-}$/*Bcrp*$^{-/-}$ pregnant mice is decreased given that retro-orbital injection mimics intravenous administration. Since the metabolite to parent molar AUC ratios did not significantly differ among all the genotypes (**Table S3.3**), changes in cannabinoid-metabolizing enzymes by P-gp knockout seem unlikely. Given that the blood clearance of THC in the WT pregnant mice is ~2.7 mL/min, it appears to be blood flow-limited (mouse hepatic blood flow is ~1.8 mL/min) [170]. Therefore, if hepatic blood flow is affected by the P-gp knockout, this could partially explain our findings. Nevertheless, we cannot rule out the contribution of other transporters to the systemic disposition of THC. Such transporters remain to be determined in future studies.

Surprisingly, we found that the maternal brain/maternal plasma AUC GMR of THC in *P-gp*$^{-/-}$ mice was decreased by 72% (**Table 3.2**). We also observed a general trend of decrease in maternal brain/maternal plasma or fetal/maternal plasma AUC GMRs of 11-OH-THC or THC-COOH in *P-gp*$^{-/-}$ and *P-gp*$^{-/-}$/*Bcrp*$^{-/-}$ mice or no change (mostly in *Bcrp*$^{-/-}$ mice) compared to WT mice (**Table 3.2**). Likewise, the fetal/maternal plasma AUC GMR of THC were not affected by P-gp and/or Bcrp knockout (**Table 3.2**). These data strongly indicate that THC and its metabolites are not substrates of P-gp or Bcrp because, if they were, knocking out these efflux transporters at the blood-brain or blood-placental barrier should result in an increase (not a

decrease) in their AUC GMR in the knockout mice. In addition, when drugs are substrates of these transporters, knocking them out results in a larger increase in maternal brain/maternal plasma AUC GMR versus the fetus/maternal plasma AUC GMR [171,172]. Here we observed a reverse trend in *P-gp*$^{-/-}$ mice for THC-COOH where the fetal/maternal plasma AUC GMR was significantly reduced while the maternal brain/maternal plasma AUC GMR was unchanged (**Table 3.2**). Moreover, the direction of transport by P-gp cannot be inverted unless artificial mutations are introduced in P-gp [173], which is unlikely to occur *in vivo*. Collectively, these data are consistent with our *in vitro* findings that THC, 11-OH-THC or THC-COOH are not substrates of human P-gp and only THC-COOH is a weak substrate of human BCRP [165].

We attempted to interpret our surprising finding of reduced distribution of the cannabinoids into maternal brain or fetus in *P-gp*$^{-/-}$ or *P-gp*$^{-/-}$/*Bcrp*$^{-/-}$ mice. The cannabinoid concentrations we quantified in this study were total concentrations. Theoretically, only the unbound cannabinoids can cross the tissue membrane barriers by passive diffusion. Therefore, one possibility could be that the differences in protein binding of the cannabinoids in tissues between WT and *P-gp*$^{-/-}$ or *P-gp*$^{-/-}$/*Bcrp*$^{-/-}$ mice led to greater asymmetric distributions of the cannabinoids across the tissue barriers in transporter knockout mice. For instance, lower brain tissue binding in knockout mice versus WT, while maintaining equal degree of binding to maternal plasma, could result in lower total THC tissue/maternal plasma AUC ratio in knockout mice versus WT mice, as observed in *P-gp*$^{-/-}$ mice (72% decrease). Indeed, previous investigations using *in vitro* autoradiography by incubating ^{11}C-tariquidar (a P-gp and BCRP substrate and inhibitor) with isolated brain sections showed that the binding of ^{11}C-tariquidar (a highly lipophilic compound as are the cannabinoids) to isolated brain sections from *P-gp*$^{-/-}$ and/or *Bcrp*$^{-/-}$ mice is ~50% of that in WT mice [174]. Therefore, we determined the unbound percentages of THC and its major metabolites in mouse plasma and paired maternal brain homogenate samples of 6 randomly selected mice. However, unlike Bauer *et. al.*, we found no significant difference in unbound percentages of the cannabinoids in maternal brain (or plasma) between WT and transporter-knockout mice (**Tables 3.3 and 3.4**) [174]. A limitation of this aspect of this study is that our plasma protein binding study was done with male and not pregnant female plasma (these studies were conducted after all the pregnant females had been sacrificed and the lack of sufficient blank pregnant female plasma).

Another possible explanation is the potential induction of other transporters at the blood-brain and blood-placental barrier in the transporter-knockout mice. However, previous studies have shown that the expressions of 12 ABC transporters and 10 solute carrier transporters in the brain capillary endothelial cells isolated from *P-gp*$^{-/-}$, *Bcrp*$^{-/-}$, and *P-gp*$^{-/-}$/*Bcrp*$^{-/-}$ FVB mice are not significantly altered compared to those isolated from WT mice [14]. Whether other transporters are induced in the placenta of *P-gp*$^{-/-}$ or *Bcrp*$^{-/-}$ mice is currently unknown. Moreover, to the best of our knowledge, whether THC and its metabolites are substrates of any other transporters has not been systemically investigated.

In WT mice, fetal exposure to THC was only about 17-20% of its maternal plasma exposure (**Table 3.2**), suggesting either extensive placental/fetal metabolism and/or efflux by transporters other than P-gp or Bcrp. This finding is consistent with the previous macaque study which showed that fetal exposure to THC was ~30% of its maternal plasma exposure [4]. In humans, THC is not metabolized by placental microsomes, but it is rapidly metabolized by fetal liver microsomes [84]. Thus, the fetal/maternal plasma AUC GMR of <1 for THC suggests that these processes may act to reduce fetal exposure to this potentially toxic cannabinoid.

Since THC is thought to produce long-term deleterious effect on the developing human brain [46], it is important to determine if THC and its metabolites distribute into the fetal brain. Both P-gp and Bcrp are known to be expressed in fetal brain [109]. However, THC and its metabolites were not detectable or quantifiable by LC-MS/MS in the fetal brain samples regardless of genotypes in our study.

In summary, in **Chapter 3**, we showed that *P-gp*$^{-/-}$, *Bcrp*$^{-/-}$, and/or *P-gp*$^{-/-}$/*Bcrp*$^{-/-}$ significantly decrease exposure to THC and/or its metabolites in maternal brain, placenta, or the fetus, except for Bcrp which limits placental (but not fetal) exposure to THC. The mechanistic basis for this decreased tissue exposure is puzzling, not clear and needs further investigation. Based on these findings, we conclude that mouse P-gp or Bcrp plays a minor or no role in limiting maternal brain and fetal exposure to the cannabinoids and, in fact, P-gp and Bcrp knockout appears to reduce such exposure. These data, together with our *in vitro* data that these cannabinoids are not substrates or weak substrates (THC-COOH) of human P-gp and BCRP [165], make it unlikely that P-gp or BCRP-mediated drug-cannabinoid interactions are of concern. In addition, it is unlikely that people with reduced function genotype variants of P-gp or BCRP will experience enhanced intoxicating effects or fetal toxicity to these cannabinoids. Interestingly, the

fetal/maternal plasma AUC GMR of <1 for THC suggests that the placental/fetal metabolism or placental efflux by transporters other than P-gp or Bcrp may act to reduce fetal exposure to this potentially toxic cannabinoid. The latter is the subject of investigation of **Chapter 4**. Also, studies with human tissues (*e.g.* perfused placenta) are needed to confirm these findings.

3.6 Supplementary materials

Table S3.1. The maternal brain, placental, and fetal to maternal plasma $AUC_{0-\infty}$ GMRs of THC, 11-OH-THC, and THC-COOH

	$AUC_{0-\infty}$ GMR (95% CI)	$AUC_{0-\infty}$ GMR (95% CI)	Adjusted *P* value	$AUC_{0-\infty}$ GMR (95% CI)	Adjusted *P* value	$AUC_{0-\infty}$ GMR (95% CI)	Adjusted *P* value
THC	WT	*P-gp*$^{-/-}$		*Bcrp*$^{-/-}$		*P-gp*$^{-/-}$/*Bcrp*$^{-/-}$	
Maternal brain	0.55 (0.37, 0.84)	**0.16 (0.10, 0.25)**	**0.0010**	0.65 (0.56, 0.75)	0.9348	0.39 (0.20, 0.76)	0.5718
Placenta	0.42 (0.27, 0.67)	0.37 (0.26, 0.53)	0.9644	0.64 (0.55, 0.75)	0.4616	0.82 (0.49, 1.39)	0.1199
Fetal remains	0.30 (0.12, 0.80)	0.17 (0.13, 0.22)	0.1939	0.36 (0.25, 0.51)	0.9246	0.29 (0.17, 0.49)	0.9952
Fetus	0.23 (0.09, 0.59)	0.21 (0.17, 0.25)	0.9658	0.26 (0.13, 0.52)	0.9731	0.22 (0.17, 0.29)	0.9965
11-OH-THC	WT	*P-gp*$^{-/-}$		*Bcrp*$^{-/-}$		*P-gp*$^{-/-}$/*Bcrp*$^{-/-}$	
Maternal brain	1.18 (1.00, 1.40)	0.94 (0.66, 1.34)	0.5721	1.44 (0.96, 2.17)	0.6695	**0.67 (0.48, 0.94)**	**0.0302**
Placenta	1.49 (1.28, 1.73)	1.34 (0.73, 2.48)	0.9327	1.54 (1.34, 1.77)	0.9967	1.08 (0.82, 1.43)	0.3175
Fetal remains	1.38 (1.16, 1.63)	0.91 (0.08, 10.11)	0.1441	1.19 (0.79, 1.80)	0.8318	**0.67 (0.51, 0.86)**	**0.0037**
Fetus	1.45 (1.03, 2.05)	**0.52 (0.44, 0.61)**	**<0.0001**	1.09 (0.65, 1.83)	0.3958	**0.48 (0.37, 0.63)**	**<0.0001**
THC-COOH	WT	*P-gp*$^{-/-}$		*Bcrp*$^{-/-}$		*P-gp*$^{-/-}$/*Bcrp*$^{-/-}$	
Maternal brain	0.32 (0.23, 0.43)	0.43 (0.18, 1.01)	0.6948	0.20 (0.14, 0.28)	0.3225	0.21 (0.14, 0.32)	0.4710
Placenta	1.34 (0.91, 1.99)	1.11 (0.85, 1.45)	0.8866	0.95 (0.65, 1.38)	0.5840	0.79 (0.71, 0.89)	0.2620
Fetal remains	1.04 (0.58, 1.85)	1.13 (0.45, 2.84)	0.9874	0.57 (0.36, 0.92)	0.1873	**0.42 (0.35, 0.50)**	**0.0223**
Fetus	1.00 (0.49, 2.05)	**0.38 (0.24, 0.59)**	**0.0136**	0.48 (0.18, 1.29)	0.0830	**0.37 (0.31, 0.44)**	**0.0106**

Data shown are the bootstrapped tissue/maternal plasma $AUC_{0-\infty}$ GMRs of THC, 11-OH-THC, THC-COOH after retro-orbital injection of THC (3 mg/kg) to pregnant mice on gestation day 18 over 240 min. Data are reported as geometric mean ratio (GMR) (95% confidence interval) (n = 3). Differences in $AUC_{0-\infty}$ GMRs between WT and *P-gp*$^{-/-}$, *Bcrp*$^{-/-}$, or *P-gp*$^{-/-}$/*Bcrp*$^{-/-}$ pregnant mice were analyzed by two-way ANOVA followed by the Dunnett's *post hoc* test. Differences indicated in underline were statistically significant with *P* values of < 0.05 that were adjusted for multiple comparisons.

Table S3.2. The percentages of extrapolation of tissue AUCs

THC Extrapolation%	**WT**	***P-gp*$^{-/-}$**	***Bcrp*$^{-/-}$**	***P-gp*$^{-/-}$/*Bcrp*$^{-/-}$**
Maternal brain	6.65	3.29	2.31	11.35
Placenta	19.05	26.66	5.88	36.70
Fetal remains	37.80	20.88	24.89	32.41
Fetus	31.81	22.12	17.67	29.64

11-OH-THC Extrapolation%	**WT**	***P-gp*$^{-/-}$**	***Bcrp*$^{-/-}$**	***P-gp*$^{-/-}$/*Bcrp*$^{-/-}$**
Maternal brain	5.47	27.26	8.96	11.49
Placenta	17.71	36.58	10.13	10.19
Fetal remains	25.00	30.26	22.03	8.71
Fetus	29.76	8.34	14.87	4.08

THC-COOH Extrapolation%	**WT**	***P-gp*$^{-/-}$**	***Bcrp*$^{-/-}$**	***P-gp*$^{-/-}$/*Bcrp*$^{-/-}$**
Maternal brain	31.86	57.40	14.38	17.40
Placenta	44.35	44.53	20.37	21.61
Fetal remains	55.46	71.39	40.85	28.53
Fetus	56.57	42.24	43.96	28.25

Data shown are the percentages of extrapolation of the tissue AUCs of THC, 11-OH-THC, THC-COOH in WT, *P-gp*$^{-/-}$*, Bcrp*$^{-/-}$*, and P-gp*$^{-/-}$*/Bcrp*$^{-/-}$ pregnant mice. Data are calculated by 1-(AUC_{0-240})/($AUC_{0-\infty}$), and reported as mean.

Table S3.3. Metabolite to parent maternal plasma AUC molar ratios

Molar ratio	WT	*P-gp*$^{-/-}$	*Bcrp*$^{-/-}$	*P-gp*$^{-/-}$ */Bcrp*$^{-/-}$
11-OH-THC/THC	0.14 ± 0.05	0.08 ± 0.01	0.14 ± 0.02	0.14 ± 0.03
THC-COOH/11-OH-THC	2.83 ± 0.40	2.89 ± 0.30	3.02 ± 0.32	2.91 ± 0.27

Data shown are metabolite to parent maternal plasma AUC molar ratios in WT, *P-gp*$^{-/-}$, *Bcrp*$^{-/-}$, and *P-gp*$^{-/-}$*/Bcrp*$^{-/-}$ pregnant mice. Data are reported as mean ± S.D. (n = 3). Differences among the four mouse groups were analyzed by ANOVA and were considered statistically significant with *P* values of < 0.05. No statistically significant differences were found.

Figure S3.1. Unnormalized maternal plasma concentration-time profiles of THC, 11-OH-THC and THC-COOH.

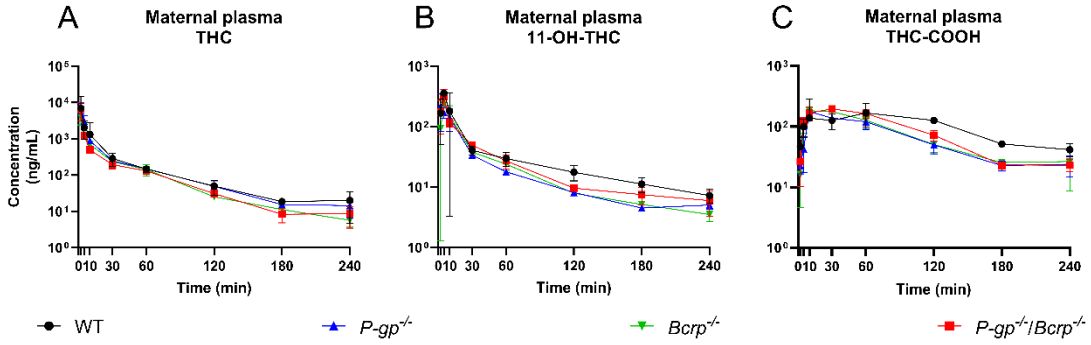

Maternal plasma concentration-time profiles of THC (**A**), 11-OH-THC (**B**), and THC-COOH (**C**) over 240 min after retro-orbital injection of 3 mg/kg THC to pregnant wild-type (●), *P-gp*$^{-/-}$ (▲), *Bcrp*$^{-/-}$ (▼), and *P-gp*$^{-/-}$/*Bcrp*$^{-/-}$ (■) mice on gestation day 18. Data shown are mean ± S.D. (n = 3 at each time point).

Chapter 4
Interaction of THC and Its Major Metabolites with Placental and Hepatic Solute Carrier Transporters

The work presented in this chapter was previously published in

International Journal of Molecular Sciences 2024 Nov 9;25(22):12036.

doi: 10.3390/ijms252212036

4.1 Abstract

(-)-*trans*-Δ^9-tetrahydrocannabinol (THC) is the primary intoxicating component of cannabis which is increasingly consumed by pregnant people. In humans, THC is sequentially metabolized in the liver to its circulating metabolites 11-hydroxy-THC (11-OH-THC, intoxicating) and 11-*nor*-9-carboxy-THC (THC-COOH, non-intoxicating). Human and macaque data show that fetal exposure to THC is considerably lower than its corresponding maternal exposure. Through perfused human placenta studies, we have shown that this is due to active efflux of THC (fetal-to-maternal) by a placental transporter(s) other than P-glycoprotein or breast cancer resistance protein. The identity of this placental transporter(s) as well as whether THC or its metabolites are substrates or inhibitors of hepatic solute carrier transporters is unknown. Therefore, we investigated whether 5 μM THC, 0.3 μM 11-OH-THC, and 2.5 μM THC-COOH are substrates and/or inhibitors of placental or hepatic solute carrier transporters at their pharmacological-relevant concentrations. Using HEK cells overexpressing human OATP1B1, OATP1B3, OATP2B1, OCT1, OCT3, OAT2, OAT4, or NTCP, and prototypic substrates/inhibitors of these transporters, we found that THC and THC-COOH were substrates but not inhibitors of OCT1. THC-COOH was a weak substrate of OCT3 and a weak inhibitor of OAT4. THC, 11-OH-THC, and THC-COOH were found not to be substrates/inhibitors of the remaining transporters investigated.

4.2 Introduction

The use of cannabis by pregnant people in the United States is increasing [1,15], raising concerns about potential fetal and neurodevelopmental toxicity [175,176] of (-)-*trans*-Δ^9-tetrahydrocannabinol (THC), the primary intoxicating constituent of cannabis. To inform such toxicity, it is important to determine the mechanism and extent of placental transfer of THC and its intoxicating circulating metabolite 11-OH-THC.

In both humans and non-human primates, THC is effluxed in the fetal-to-maternal direction, resulting in fetal circulatory concentrations that are less than the corresponding maternal concentrations [4,99]. These data suggest the involvement of efflux transporters at the blood-placenta barrier, particularly P-glycoprotein (P-gp) and/or breast cancer resistance protein (BCRP), which are highly expressed in the apical membrane of the syncytiotrophoblast [109]. This hypothesis is supported by some studies in the P-gp knockout mice [8], but not by those conducted

in our laboratory [165,177]. Using both, P-gp or BCRP overexpressing cells, vesicles in **Chapter 2**, or pregnant P-gp or BCRP knockout mice in **Chapter 3**, we found that THC is not a substrate or inhibitor of P-gp or BCRP at pharmacologically relevant concentrations [165,177]. Moreover, in our perfused human placenta studies, the THC unbound clearance in the fetal-to-maternal direction (normalized to the unbound clearance of the passive diffusion marker, antipyrine) was significantly greater than its corresponding maternal-to-fetal direction indicating active efflux of THC in the maternal-to-fetal direction. In addition, this active efflux was not inhibitable by a pan-P-gp/BCRP inhibitor, valspodar [99]. In these perfused placental studies, 11-OH-THC and THC-COOH were found to cross the placenta passively [99].

The above findings raise an interesting question: which transporter(s) is responsible for the fetal-to-maternal efflux of THC? Studies to predict and verify the observed fetal umbilical vein concentrations in our human studies through physiologically based pharmacokinetic (PBPK) modeling suggest that the transporter(s) is more likely to be localized in the basal membrane of the syncytiotrophoblast. We hypothesized that this transporter could be one of the solute carrier (SLC) uptake transporter, such as the organic anion transporting polypeptide (OATP2B1), the organic cation transporter (OCT3), or the organic anion transporter (OAT4) (**Figure 4.1A**) [13,103]. That is, THC could be actively transported from the fetal circulation into the syncytiotrophoblast by one of these transporters and then THC could reach the maternal circulation by diffusion across the apical membrane of the syncytiotrophoblast. Therefore, here we investigated if THC or its major circulatory metabolites are substrates or inhibitors of these basal placental transporters at their pharmacologically relevant concentrations.

In humans THC is primarily metabolized in the liver [via cytochrome P450 (CYP) 2C9] to its intoxicating circulatory metabolite, 11-OH-THC, which is further metabolized (via CYP2C9 and 3A) to the non-intoxicating circulatory metabolite,11-*nor*-9-carboxy-THC (THC-COOH) [95,178]. After intravenous dosing of THC (0.5 mg), 41-45% of the dose is excreted in the feces 72 hours after administration [90]. It is possible that hepatic transporters may be important in the hepatic uptake of THC or its metabolites and subsequent excretion in the bile or urine. If they are, this has potential implications for drug-drug interactions, either as object drugs or as perpetrators when present in the circulation at their upper range of their pharmacological concentrations (5 μM THC, 0.3 μM 11-OH-THC, or 2.5 μM THC-COOH, as justified by our previous publication [165]). Therefore, we also investigated if THC and its major circulatory

metabolites are substrates or inhibitors of hepatic SLC transporters such as OATP1B1/1B3/2B1, OCT1, and sodium taurocholate co-transporting polypeptide (NTCP) (**Figure 4.1B**) [179].

Figure 4.1. Localization and directionality of placental and hepatic transporters.

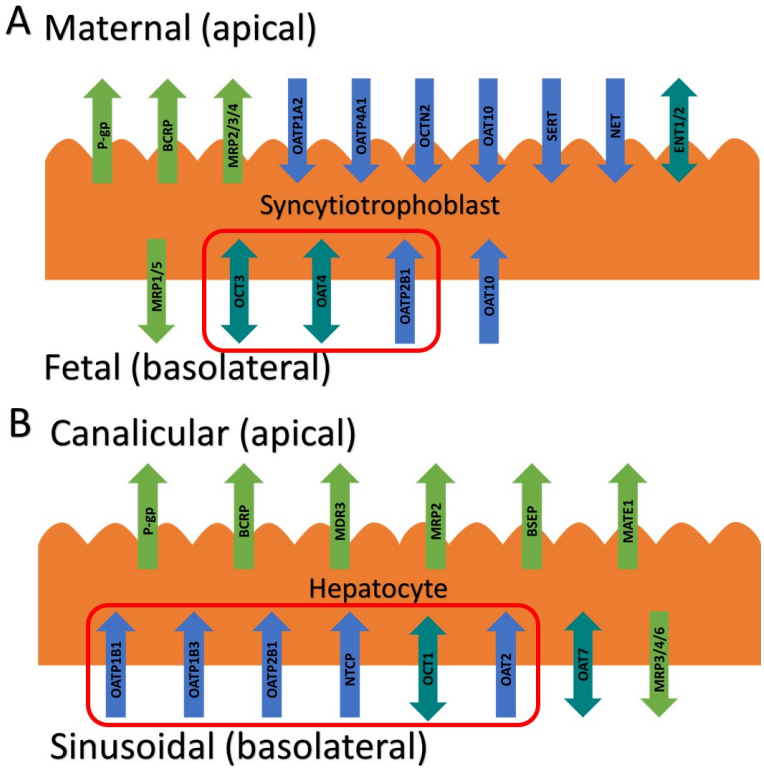

Placental (**A**) and hepatic (**B**) transporters with their localization and directionality of transport. Transporters in red boxes were those that were investigated. BCRP, breast cancer resistance protein; BSEP, bile salt export pump; ENT, equilibrative nucleoside transporter; MATE, multidrug and toxin extrusion protein; MDR, multidrug resistance protein; MRP, multidrug resistance associated protein; NET, norepinephrine transporter. NTCP, sodium taurocholate cotransporter protein; OAT, organic anion transporter; OATP, organic anion transporting peptide; OCT, organic cation transporter; OCTN, organic cation/carnitine transporter; P-gp, P-glycoprotein; SERT, serotonin transporter.

4.3 Materials and methods

4.3.1 Materials

THC (50 mg/mL) was purchased from Cayman Chemicals (Ann Arbor, MI). (±)11-OH-THC (1 mg/mL), (±)-11-nor-9-carboxy-THC (THC-COOH) (1 mg/mL), (-)-Δ^9-THC-D_3 (1 mg/mL), (±)11-OH-THC-D_3 (1 mg/mL), and (±)-11-*nor*-9-carboxy-Δ^9-THC-D_3 (1 mg/mL) in methanol were from Cerilliant Corporation (Round Rock, TX). Bromsulphthalein, bulevirtide trifluoroacetate, corticosterone, erlotinib, ketoprofen, quinidine, and rifampin were from Sigma-Aldrich (St. Louis, MO). For radiolabeled compounds, 1 mCi/mL (25 Ci/mmol) [^{3}H]-rosuvastatin, 1 mCi/mL (40 Ci/mmol) [^{3}H]-estrone-3-sulfate, 1 mCi/mL (25 Ci/mmol) [^{3}H]-cGMP, and 1 mCi/mL (20 Ci/mmol) [^{3}H]-taurocholic acid were from American Radiolabeled Chemicals (St. Louis, MO), while 0.1 mCi/mL (110 mCi/mmol) [^{14}C]-metformin was from Moravek Biochemicals, Inc (Brea, CA). Hank's balanced salt solution (HBSS), 0.25% trypsin-EDTA, GlutaMAX™, fetal bovine serum (FBS), Dulbecco's modified eagle medium (DMEM) (4.5 g/L glucose and 1.0 g/L glucose), dimethyl sulfoxide (DMSO), acetonitrile (liquid chromatography-mass spectrometry grade), acetic acid (liquid chromatography-mass spectrometry grade), SureSTART™ polypropylene insert (Catalog #6EME03CPPSP) were from ThermoFisher Scientific (Hampton, NH). Poly-D-lysine-coated 48-well cell culture plate were from Corning (Corning, NY). Low-binding microcentrifuge tubes were from Genesee Scientific (San Diego, CA). Milli-Q water was used in all preparations. High Density Polyethylene MiniVial (7 mL, catalog #125500) was from RPI Research Products International (Mount Prospect, IL). All other chemicals and reagents were obtained commercially at the highest quality available.

4.3.2 Cell culture

HEK-OATP2B1, HEK-OCT1, HEK-OCT3, HEK-OAT4, and HEK-NTCP cells were generously provided by SOLVO Biotechnology (Szeged, Hungary). HEK-OATP1B1 and HEK-OATP1B3 cells were generously provided by Gilead Sciences Inc (Foster City, CA). HEK-OAT2 cells were generously provided by Pfizer Inc (Cambridge, MA). All cells were preserved in liquid nitrogen. The passage number of all cells used was no greater than 10. Except for HEK-OATP1B1 and HEK-OATP1B3 cells, all cells were cultured in high glucose (4.5 g/L) DMEM

supplemented with 10% FBS, 1% GlutaMAX™, 1% penicillin-streptomycin. HEK-OATP1B1 and OATP1B3 cells were cultured in high glucose (4.5 g/L) DMEM supplemented with 10% FBS, 1% penicillin-streptomycin, 25 mM HEPES, 0.1 mM MEM non-essential amino acid solution, 600 µg/mL geneticin, and 10 µg/mL blasticidin. All cells were maintained in a humidified incubator at 37°C in 5% CO_2 with 95% humidity. When cells reached ~90% confluency, after washing with HBSS and trypsinization, they were passaged into a new flask, and then seeded into 48-well plates at a density of 20,000 cells per well for transport assays.

4.3.3 Cannabinoid uptake by SLC transporters

When confluent in the 48-well plate, cells were rinsed twice with 0.5 mL 37°C HBSS and preincubated with 0.5 mL HBSS at 37°C for 15 min. In order to ensure that the contents of the transport assays were at 37°C, pilot studies showed that the setting of the water bath or hot plate needed to be at 42°C. After aspiration of HBSS, cells were incubated with 5 µM THC, 0.3 µM 11-OH-THC, or 2.5 µM THC-COOH with or without the transporter inhibitor (or inhibitory condition) in HBSS (0.2 mL) containing DMSO (final concentration <0.2% v/v) at 37°C for 15 s (preliminary studies showed that this time was within the linear uptake range, data not shown). After aspirating HBSS, cells were immediately washed three times with 0.5 mL ice-cold HBSS. Then, cells were lysed with 200 µL 80% acetonitrile containing 100 nM THC-D_3, 100 nM 11-OH-THC-D_3, or 100 nM THC-COOH-D_3. All cell lysates were vortexed for 15 s and centrifuged at 19,083 × *g* for 15 min at 4°C. The supernatant (100 µL) was transferred to a disposable clean SureSTART™ polypropylene insert and stored at -20°C until analysis by liquid chromatography-tandem mass spectrometry (LC-MS/MS).

4.3.4 LC-MS/MS analysis

On the day of analysis, 10 µL sample was injected onto LC-MS/MS for analysis using a Xevo TQ-XS Triple Quadrupole Mass Spectrometer (Waters, Milford, MA) coupled with the Acquity ultra-performance liquid chromatography system (Waters, Milford, MA). The samples were eluted on an Acquity ultra-performance liquid chromatography BEH C_{18} column (130Å, 1.7 µm, 2.1 mm × 50 mm) attached to the AccQ Tag Ultra C_{18} VanGuard Pre-column (100Å, 1.7 µm, 2.1 mm × 5 mm). For other analytical conditions, please see **Tables S4.1 and S4.2**. All sample was

quantified and analyzed by MassLynx™ V4.2. Given that the corresponding deuterated cannabinoid was employed as an internal standard, a single-point calibration method was utilized to quantify the molar concentration of the analytes, assuming that the analyte and the internal standard produce equivalent signal intensity.

4.3.5 Inhibition of SLC transporters by the cannabinoids

When confluent in 48-well plate, cells were processed as described above. After aspirating HBSS, the cells were incubated with the radiolabeled transporter substrate, transport inhibitor (see **Table 4.1** for concentrations), 5 μM THC, 0.3 μM 11-OH-THC, or 2.5 μM THC-COOH in 0.2 mL of HBSS containing DMSO (final concentrations <0.2% v/v) at 37°C for 2 min for substrates labeled with [^{3}H] or for 10 min for substrates labeled with [^{14}C] (preliminary studies showed that these times were within the linear uptake range). Uptake was quenched by aspirating the buffer and immediately washing the cells three times with ice-cold HBSS. Then, cells were lysed with 80% acetonitrile and 100 μL of the cell lysate were added to 5 mL Ecoscint™ (National Diagnostics, Atlanta, GA) in High Density Polyethylene MiniVial and capped. After 15s of mixing on a vortex, the radioactivity (corrected for background radioactivity) was quantified using a scintillation counter (PerkinElmer Tri-Carb 3110TK).

Table 4.1 Substrates and inhibitors used

Transporter	Substrate	Inhibitor
OATP1B1	40 nM [^{3}H]-rosuvastatin	500 μM rifampin
OATP1B3	40 nM [^{3}H]-rosuvastatin	500 μM rifampin
OATP2B1	25 nM [^{3}H]-estrone-3-sulfate	10 μM erlotinib
OCT1	0.91 μM [^{14}C]- metformin	100 μM quinidine
OCT3	0.91 μM [^{14}C]- metformin	100 μM corticosterone
OAT2	40 nM [^{3}H]-cGMP	200 μM ketoprofen
OAT4	25 nM [^{3}H]-estrone-3-sulfate	200 μM bromsulphthalein
NTCP	100 nM [^{3}H]-taurocholic acid	1 μM bulevirtide

4.3.6 Statistical Analysis

Three independent experiments were performed, each in triplicate, for all the uptake and inhibition assays. Data are reported as means of each experiment and were analyzed using the paired *t*-test. *P* values of <0.05 were considered statistically significant. All analyses were performed using GraphPad Prism 10 (La Jolla, CA).

4.4 Results

4.4.1 Uptake of cannabinoids by the basal syncytiotrophoblast transporters

Although day-to-day variability was observed, uptake of THC or 11-OH-THC by HEK-OATP2B1, OCT3 or OAT4 cells was not significantly different in the presence of the respective transporter inhibitor compared with that in the absence of the inhibitor (DMSO only) (**Figure 4.2**). Likewise, cellular accumulation of THC-COOH in these cells was not affected the respective transporter inhibitor except in HEK-OCT3 cells where it was slightly but significantly decreased in the presence of 100 μM corticosterone (**Figure 4.2**). Interestingly, bromsulphthalein significantly, but modestly, stimulated (rather than inhibited) the uptake of THC-COOH into HEK cells expressing OAT4 (**Figure 4.2**).

Figure 4.2

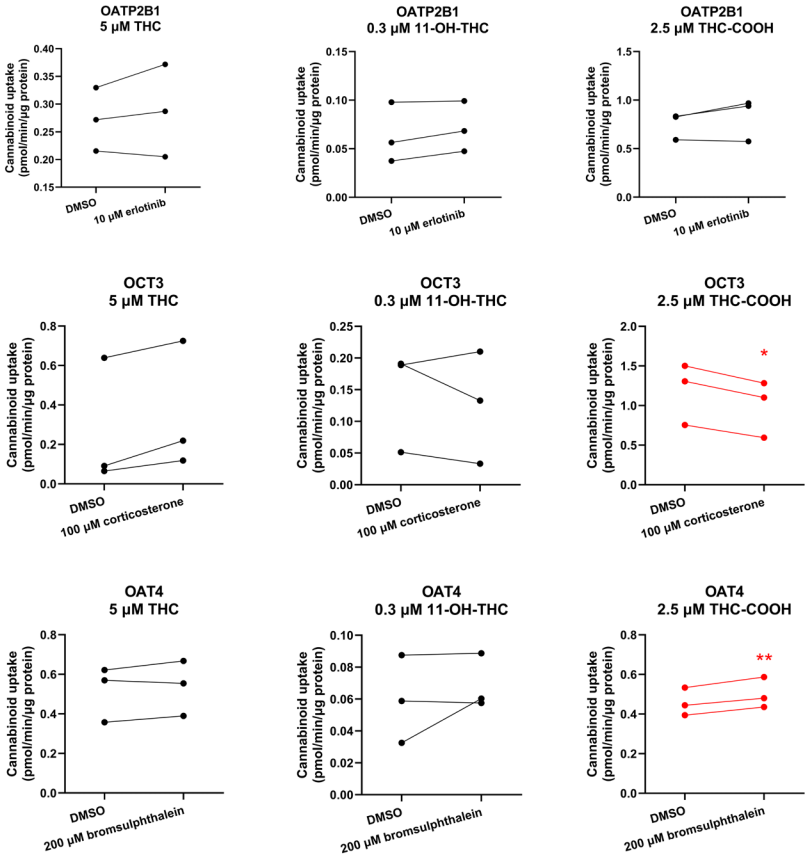

Cannabinoids as substrates of placental transporters: Uptake (over 15s) of 5 µM THC, 0.3 µM 11-OH-THC, and 2.5 µM THC-COOH by HEK cells overexpressing human placental transporters in the absence or presence of the prototypic inhibitors of the respective transporter (10 µM erlotinib for OATP2B1, 100 µM corticosterone for OCT3, 200 µM bromsulphthalein for OAT4). Data on the y-axis are uptake rate of the cannabinoid normalized to protein concentration. Data are from three independent experiments, each conducted in triplicate. Technical variability within each independent experiment is shown in **Table S4.3**. Statistically significant difference in cannabinoid uptake in the presence or absence of the prototypic inhibitor (marked in red) was determined using the paired *t*-test. *$P < 0.05$; **$P < 0.01$.

4.4.2 Inhibition of the basal syncytiotrophoblast transporters by the cannabinoids

To determine if THC and its major metabolites are inhibitors of these placental transporters at their pharmacologically relevant concentrations, the uptake of prototypic substrates of OATP2B1/OCT3/OAT4 (25 nM [^{3}H]-estrone-3-sulfate for OATP2B1 and OAT4, 1.67-2 μM [^{14}C]-metformin for OCT3) was determined in the presence or absence of the cannabinoids or known inhibitors of the respective transporter (positive control). Although THC did not inhibit the uptake of the prototypic substrates by the tested placental transporters, THC-COOH slightly, but significantly, inhibited OAT4-mediated uptake of estrone-3-sulfate, while 11-OH-THC and THC-COOH modestly increased (43% and 19%, respectively) OATP2B1-mediated uptake of estrone-3-sulfate (**Figure 4.3**).

Figure 4.3

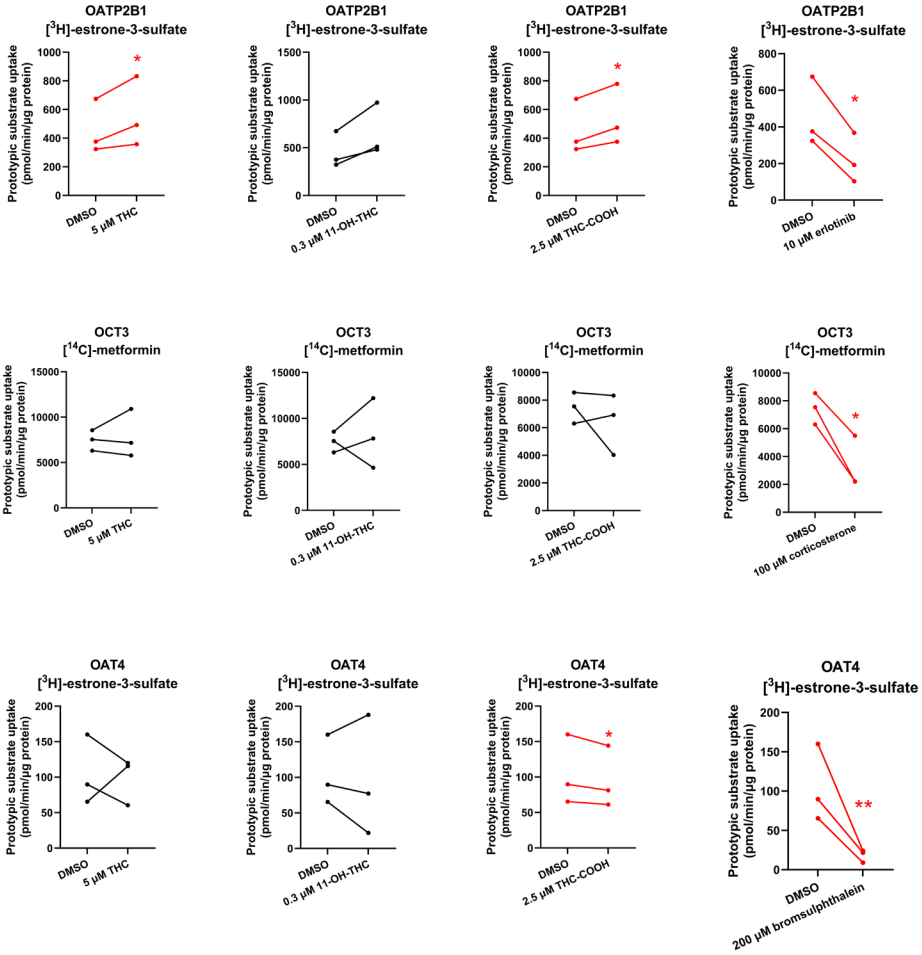

Cannabinoids as inhibitors of placental transporters: Rate of uptake (over 2 min for OATP2B1/OAT4 and 10 min for OCT3) of prototypic substrates of the placental transporters, OATP2B1/OAT4 ([^{3}H]-estrone-3-sulfate) or OCT3 ([^{14}C]-metformin), in the presence or absence of 5 µM THC, 0.3 µM 11-OH-THC, 2.5 µM THC-COOH or their prototypic selective inhibitors (10 µM erlotinib for OATP2B1, 100 µM corticosterone for OCT3, 200 µM bromsulphthalein for OAT4). Data on the y-axis are the rates of uptake of the prototypic substrate normalized to protein concentration. Data are from three independent experiments, each conducted in triplicate. Technical variability within each independent experiment is shown in **Table S4.3**. Statistically significant difference in the rate of uptake of the prototypic substrate in the presence and the absence of the inhibitor (marked in red) was determined using the paired *t*-test. *$P < 0.05$; **$P < 0.01$.

4.4.3 Uptake of cannabinoids by the sinusoidal hepatic transporters

OCT1-mediated uptake of THC and THC-COOH (but not of 11-OH-THC) was decreased 51% and 38%, respectively, in the presence of the OCT1 inhibitor, quinidine (100 μM). In contrast, the uptake of the cannabinoids by OATP1B1/OATP1B3/OAT2/NTCP was not affected by their respective inhibitors. 11-OH-THC was not found to be a substrate of OATP1B1, OATP1B3, OCT1, OAT2, or NTCP (**Figure 4.4**).

Figure 4.4

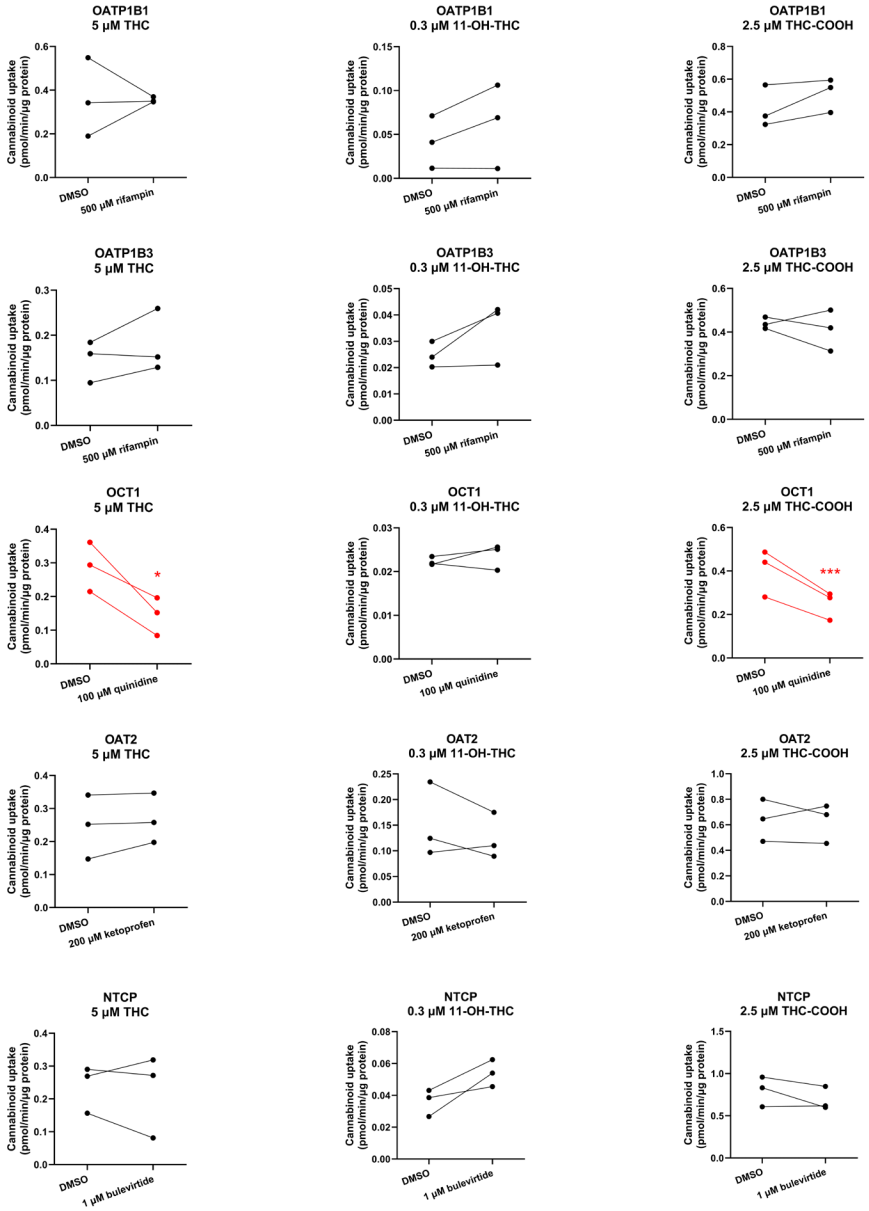

Cannabinoids as substrates of hepatic transporters: Uptake (over 15s) of 5 µM THC, 0.3 µM 11-OH-THC, or 2.5 µM THC-COOH by human sinusoidal hepatic transporters in the absence or presence of their respective inhibitors (500 µM rifampin for OATP1B1/1B3, 100 µM quinidine for OCT1, 200 µM ketoprofen for OAT2, 1 µM buleviritde for NTCP). Data on the y-axis are uptake rate of the cannabinoid normalized to protein. Data are from three independent experiments, each conducted in triplicate. Technical variability within each independent experiment is shown in **Table S4.4**. Statistically significant difference in cannabinoid uptake in

the presence or absence of the inhibitor (marked in red) was determined using the paired *t*-test. *$P < 0.05$; **$P < 0.01$.

4.4.4 Inhibition of the sinusoidal hepatic transporters by the cannabinoids

At their pharmacologically relevant concentrations, none of the cannabinoids were found to inhibit the uptake of substrates of OATP1B1, OATP1B3, OCT1, OAT2, or NTCP (**Figure 4.5**).

Figure 4.5

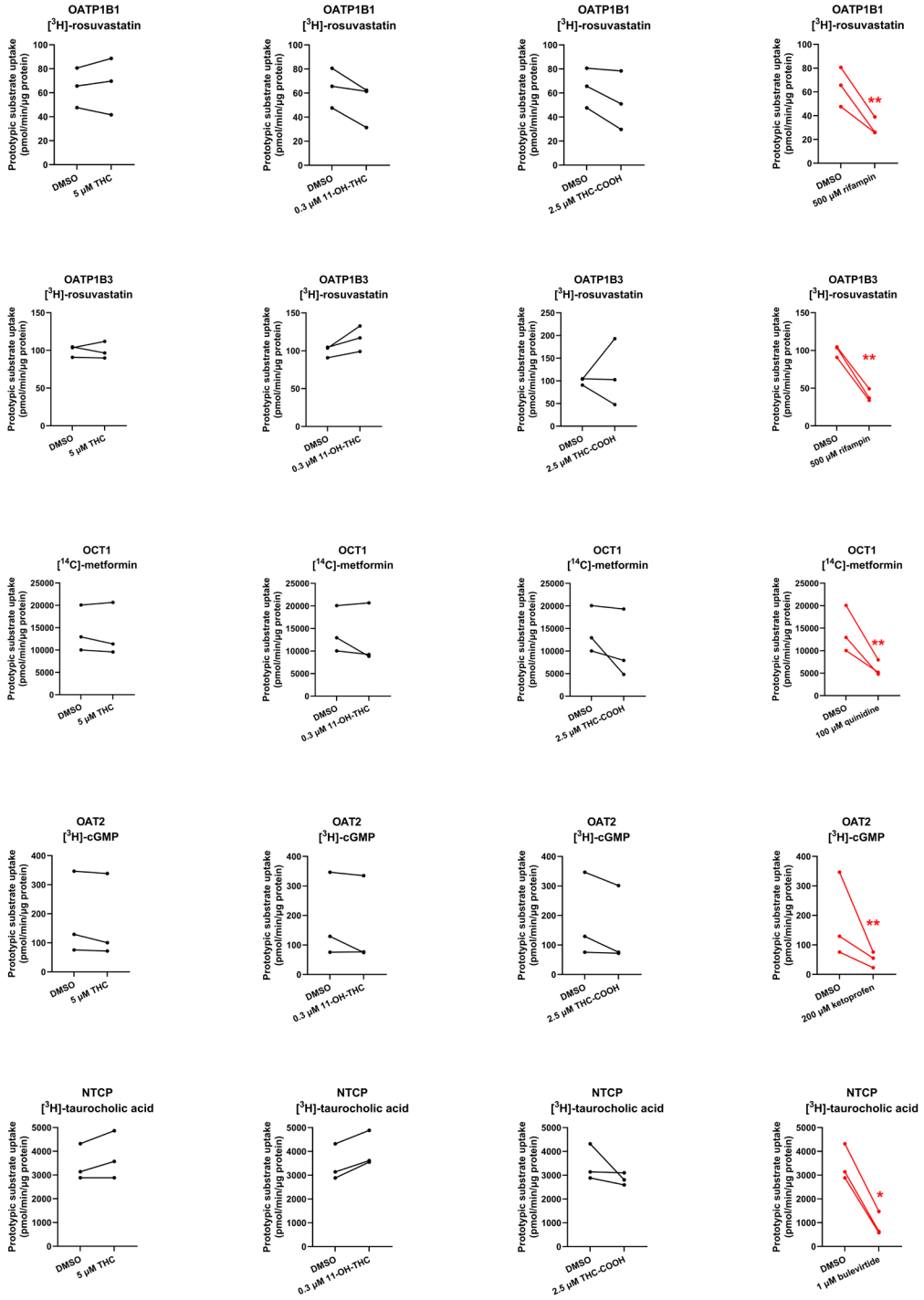

Cannabinoids as inhibitors of hepatic transporters: Uptake (over 2 min for OATP1B1/OATP1B3/OAT2/NTCP and 10 min for OCT1) of the prototypic substrates of the hepatic transporters, OATP1B1/1B3 ([^{3}H]-rosuvastatin), OCT1 ([^{14}C]-metformin), OAT2 ([^{3}H]-

cGMP), NTCP ([^{3}H]-taurocholic acid) in the presence or absence of 5 μM THC, 0.3 μM 11-OH-THC, 2.5 μM THC-COOH or their prototypic inhibitors (500 μM rifampin for OATP1B1/1B3, 100 μM quinidine for OCT1, 200 μM ketoprofen for OAT4, 1 μM buleviritde for NTCP), respectively. Data on the y-axis are the rates of the prototypic substrate uptake normalized to protein concentration. Data are from three independent experiments, each conducted in triplicate. Technical variability within each independent experiment is shown in **Table S4.4**. Statistically significant difference in the rate of uptake of the prototypic substrate in the presence or absence of the inhibitor or cannabinoids (marked in red) was determined using the paired *t*-test. *$P <$ 0.05; **$P < 0.01$.

4.5 Discussion

In **Chapter 4**, we systemically evaluated whether THC and its major metabolites, 11-OH-THC and THC-COOH, at their pharmacologically relevant concentrations, are substrates or inhibitors of numerous placental and hepatic SLC transporters. The impetus for this study arose from our previous findings that THC (but not 11-OH-THC or THC-COOH) is transported in the fetal-to-maternal direction in the term perfused human placenta [99]. An obvious explanation is that THC is transported by either P-gp and/or BCRP, two efflux transporters highly expressed in the apical membrane of the syncytiotrophoblast (**Figure 4.1**). However, in our perfused human placenta studies, the fetal-to-maternal THC transport was not inhibitable by valspodar, an inhibitor of P-gp, BCRP and multidrug resistance associated proteins 4 (MRP4). In addition, studies in cells overexpressing human P-gp or BCRP (**Chapter 2**) or in mice where P-gp and/or Bcrp was knocked-out (**Chapter 3**), THC was not transported by either P-gp or Bcrp [165,177]. An alternative explanation is that THC is effluxed in the perfused human placenta by MRP2/3 expressed in the apical membrane of the syncytiotrophoblast. However, through PBPK modeling and simulations together with observed THC concentrations in the fetal circulation and tissues, we concluded that THC is most likely effluxed in the fetal-to-maternal direction via an uptake transporter(s) in the basal membrane of the syncytiotrophoblast *[180]*. Thus, based on our previous quantitative targeted proteomics data, we chose to investigate OATP2B1, OCT3, and OAT4 as potential candidates as they are highly expressed in the basal membrane of the syncytiotrophoblast [13] (**Figure 4.1**). Though OAT10 is also expressed there (not quantified in our proteomics study) [181], we did not have access to a cell line overexpressing this transporter. We

deliberately utilized cells that overexpress human SLCs (such as HEK293 cells) to allow maximum sensitivity to identify the transporter(s) involved in the placental efflux of THC. Endogenous transporters in our HEK cell lines were not a confounding factor as uptake of cannabinoids or the transporter prototypic substrates in the presence and absence of selective inhibitors of the transporters in the non-transfected HEK cells was found not to be significantly different (data not shown).

We found that THC or 11-OH-THC are not substrates of OATP2B1, OCT3 or OAT4 (**Figure 4.2, Table S4.3**). Therefore, the identity of the transporter(s) mediating fetal-to-maternal efflux of THC remains unknown. At the same time, we cannot completely discount efflux transporters in the apical membrane of the syncytiotrophoblast other than P-gp, BCRP or MRP4. Possible candidates are MRP2 and MRP3 based on immunohistochemistry, colocalization, and proteomics data [13,103,182]. We were unable to investigate these transporters as cell lines expressing these transporters to conduct efflux studies in Transwells were not available to us. Experiments using Transwells (rather than using membrane vesicles) is best suited to identify transport of highly lipophilic compounds such as THC (pK_a = 10.6, Log P = 6.97) which binds avidly to labware. Moreover, the majority of the reported substrates of MRP2/3 are hydrophilic compounds [183].

Surprisingly, THC-COOH (an anion, pKa = 4.2, Log P = 5.24) was found to be a weak substrate of OCT3 and therefore OCT3 could potentially limit fetal exposure to THC-COOH provided OCT3 transports drugs in the fetal-to-maternal direction. There is evidence to suggest that OCT3 transport can be bidirectional [111]. In *Oct3*$^{-/-}$ pregnant mice, the fetal-to-maternal area under the curve ($AUC_{0-\infty}$) ratio exposure to metformin, an OCT3 substrate, is decreased by 44% [111]. Irrespective of the directionality of OCT3 transport, our perfused human placenta studies indicate that THC-COOH passively crosses the placenta [99]. These data indicate that any *in vivo* (or *ex vivo*) transport of THC-COOH by placental OCT3 is likely negligible. OCT3 is highly expressed in the human placenta but not in the human liver or kidneys where OCT1 and OCT2 are respectively highly expressed [184]. Thus, it is likely to play a lesser role than OCT1 in the distribution of THC-COOH into the liver (see below for further discussion). Prompted by our findings, it would be interesting to determine if THC-COOH is a substrate of OCT2.
None of the cannabinoids were found to be inhibitors of the investigated placental SLC transporters except for THC-COOH which weakly inhibited OAT4 (**Figure 4.3, Table S4.3**).

Given the high plasma protein binding of THC-COOH (96.35% in mice) [177] and its estimated *in vivo* maximal fetal plasma concentrations (~125 nM after maternal oral administration of 14.8 mg THC [31,185], assuming it crosses the placenta by passive diffusion, it is unlikely to result in any *in vivo* inhibition of placental OAT4. Interestingly, 11-OH-THC, and THC-COOH slightly stimulated OATP2B1-mediated uptake of estrone-3-sulfate, suggesting that they allosterically modulate OATP2B1 activity.

THC's blood clearance in humans after intravenous or inhalation administration is blood-flow limited [96] while its oral clearance is dependent on its intrinsic hepatic clearance. However, it is unknown whether THC utilizes transporters to gain entry into the hepatocytes. If it does, drug-drug interactions or genetic polymorphism of the transporters may affect its blood clearance (especially after oral administration). Therefore, we investigated whether THC and its major metabolites are substrates or inhibitors of sinusoidal transporters namely, OATP1B1, OATP1B3, OATP2B1, OCT1, OAT2, and NTCP.

Except for OCT1, none of the cannabinoids were substrates or inhibitors of the investigated transporters. We found THC and THC-COOH are OCT1 substrates (**Figure 4.4, Table S4.4**) but not OCT1 inhibitors at their pharmacologically relevant concentrations (**Figure 4.5, Table S4.4**). That OCT1 can transport THC was surprising because THC is an anion at physiological pH (pKa = 10.6 [30]). Anions transported by OCTs are usually zwitterions like creatinine, cimetidine [186,187]. Based on these data, THC and THC-COOH are unlikely to be perpetrators of OCT1 drug interactions but could be objects of OCT1-related cannabinoid-drug interactions provided their fraction transported *in vivo* by OCT1 is significant.

Our data has some limitations. First, there was a moderate degree of inter-day variability in transporter activity. However, this does not detract from the conclusions drawn. We were not able to evaluate all the major drug transporters expressed in the placenta (*e.g.* MRPs) due to lack of availability of cells that express these transporters and can form tight junctions (*e.g.* Madin-Darby canine kidney cells).

In summary, in **Chapter 4**, we found that THC is not a substrate of OATP2B1, OCT3 or OAT4. Therefore, the identity of the transporter(s) mediating fetal-to-maternal efflux of THC remains unknown. Perhaps THC is a substrate of one of the many transporters that transport endogenous compounds (*e.g.* nutrients) and are distinct from transporters investigated here. Further studies are needed to identify this transporter. Surprisingly, we found that THC and

THC-COOH are substates of the hepatic transporter, OCT1. Thus, they could be objects of OCT1-related cannabinoid-drug interactions provided their fraction transported *in vivo* by OCT1 is significant.

4.6 Supplementary materials

Table S4.1. Mass spectrometer conditions

Compound	Parent/Daughter (m/z)	Cone (V)	Collision (eV)
THC	315.2900/123.0800	30	22
THC-D_3	318.2900/123.3000	31	20
11-OH-THC	331.2872/193.1584	30	26
11-OH-THC-D_3	334.2872/196.2826	30	26
THC-COOH	345.2872/299.2664	30	20
THC-COOH-D_3	348.2872/302.2859	30	20

Table S4.2. LC-MS/MS gradient

Time (min)	Gradient A%
0.0	90
0.5	90
5.0	5
6.0	5
6.1	90
8.0	90

Table S4.3. Coefficient of variation (CV% of triplicate determinations) of the uptake of the cannabinoids by placental or hepatic transporters in the absence (DMSO) and presence of their respective inhibitor

OATP2B1	**CV%**	**DMSO**			**10 µM erlotinib**		
	THC	2.9	22.2	12.4	2.2	24.2	7.8
	11-OH-THC	30.4	11.5	11.4	10.0	11.3	4.7
	THC-COOH	13.3	9.7	6.5	8.9	8.1	6.3
OCT3	**CV%**	**DMSO**			**100 µM corticosterone**		
	THC	31.7	9.3	12.3	8.1	5.7	13.9
	11-OH-THC	11.8	17.8	28.1	22.9	11.5	9.5
	THC-COOH	13.1	8.6	18.7	5.5	6.1	8.4
OAT4	**CV%**	**DMSO**			**200 µM bromsulphthalein**		
	THC	29.0	15.2	5.6	23.0	2.2	2.3
	11-OH-THC	21.8	30.0	10.8	12.7	18.4	8.3
	THC-COOH	12.3	6.8	3.7	4.9	7.3	4.4
OATP1B1	**CV%**	**DMSO**			**500 µM rifampin**		
	THC	21.9	20.1	6.7	5.1	11.9	14.7
	11-OH-THC	76.9	57.8	57.1	23.3	45.5	100.0
	THC-COOH	7.9	7.3	17.8	4.9	7.6	4.4
OATP1B3	**CV%**	**DMSO**			**500 µM rifampin**		
	THC	7.8	8.5	79.8	4.3	2.5	80.0
	11-OH-THC	23.1	15.8	26.7	23.1	20.0	23.1
	THC-COOH	4.1	8.1	15.1	8.4	24.0	17.6
OCT1	**CV%**	**DMSO**			**100 µM quinidine**		
	THC	19.5	26.1	10.3	50.5	9.4	13.0
	11-OH-THC	20.0	28.6	14.3	18.8	30.8	18.8
	THC-COOH	13.8	10.9	6.6	37.0	14.7	16.9
OAT2	**CV%**	**DMSO**			**200 µM ketoprofen**		
	THC	7.5	17.1	7.6	41.9	29.2	9.7
	11-OH-THC	14.3	15.4	14.8	18.4	21.4	13.0
	THC-COOH	11.6	21.3	6.0	19.0	32.8	3.3
NTCP	**CV%**	**DMSO**			**1 µM bulevirtide**		
	THC	3.3	8.2	10.7	5.3	9.8	4.5
	11-OH-THC	23.5	14.8	33.3	20.6	12.8	21.4
	THC-COOH	5.6	18.0	10.3	5.3	6.2	23.8

Table S4.4. Coefficient of variation (CV% of triplicate determinations) of the uptake of the prototypic substrates of the placental or hepatic transporters in the absence and presence of their respective prototypic inhibitor (see Table 1) or cannabinoids

CV%	DMSO	Prototypic inhibitor	5 µM THC	0.3 µM 11-OH-THC	2.5 µM THC-COOH
OAPTP2B1	42.4	3.8	27.6	8.5	13.4
	2.7	7.1	20.2	6.2	30.6
	37.3	3.4	10.9	21.2	29.5
OCT3	13.4	47.4	61.8	2.1	4.5
	57.1	95.1	4.4	12.2	5.7
	6.0	13.8	12.5	13.5	15.5
OAT4	68.0	6.8	72.6	15.2	114.0
	15.7	12.7	35.5	13.8	11.9
	2.9	18.5	9.1	21.7	10.0
OATP1B1	3.2	90.5	18.2	9.2	11.4
	16.6	69.1	25.2	30.2	15.0
	3.3	15.3	4.7	12.9	9.3
OATP1B3	3.9	26.5	15.9	4.1	4.1
	3.2	33.1	13.2	4.2	23.5
	12.0	12.5	30.5	14.2	15.8
OCT1	7.9	1.2	12.4	1.6	3.8
	10.7	9.8	20.9	4.5	32.6
	8.9	1.1	43.1	43.9	35.7
OAT2	24.1	5.3	37.1	9.0	8.3
	20.2	8.3	6.3	15.4	3.6
	7.8	3.1	8.8	27.2	16.0
NTCP	7.0	17.6	8.1	12.7	14.4
	9.5	11.1	12.9	3.2	4.7
	10.2	4.9	34.1	42.3	7.6

Chapter 5
Conclusions and future directions

5.1 Future directions and limitations of our studies

In our study, we sought to identify the placental transporters responsible for the reduced fetal exposure to THC and to investigate the potential for cannabinoid-drug interactions, particularly in cases where a significant fraction of a compound is transported *in vivo* by the relevant transporter. However, our findings indicate that THC and its major metabolites are neither substrates nor inhibitors of the placental transporters we investigated. In **Chapters 2 and 3**, we ruled out THC as a substrate for P-gp and BCRP, a result that stands in contrast to previous studies conducted in rodents [7,8]. We acknowledge that the cell-based transport studies and conclusions could have been confounded by the high non-specific binding of THC. In **Chapter 4**, we also excluded several highly abundant basal placental transporters, specifically OATP2B1, OCT3, and OAT4 in the fetal to maternal transport of THC. However, several limitations exist in our research, which require further investigation.

One limitation is that we only focused on the placental transporters that can be quantified by proteomics from our group's previous research, P-gp, BCRP, OATP2B1, OCT3, and OAT4 [13]. However, it is important to note that high expression does not necessarily equate to significant functional role. Transporters with low abundance can still be crucial if they mediate significant extent of a substrate's transport. Consequently, our analysis left open the question of the potential roles of less abundant transporters, particularly those located on the basal side of the syncytiotrophoblast, as suggested by our m-f PBPK simulation [180]. Alternatively, it is also possible that our perfused placenta studies using valspodar (conducted by another graduate student) did not show inhibition of THC's fetal to maternal transport due to P-gp's multiple binding sites (see discussion in **Chapter 4**) [188]. Valspodar may have inhibited the P-gp binding site where saquinavir (the prototypic P-gp substrate used) binds but not where THC binds. For example, in the perfused human placenta, no significant inhibition was observed of digoxin transport (a well-established P-gp substrate) by the P-gp inhibitors quinidine or verapamil [189]. Thus, conducting perfused human placenta studies with THC and a cocktail of P-gp inhibitors could allow us to definitively discount the role of P-gp in the placental efflux of THC. This avenue is important to investigate as conclusions from our cellular THC transport studies may have been confounded by high non-specific THC binding to the cells.

Another limitation is our inability to assess the role of other efflux transporters, such as MRP2, MRP3, and MRP4. This was primarily due to the lack of access to the necessary cell

lines in our laboratory. While vesicles for these MRP transporters are commercially available, high non-specific binding and passive diffusion of highly lipophilic compounds like THC and its major metabolites (see **Section 1.7.1**) make it challenging to determine whether these compounds are substrates of MRPs. Thus, future studies are needed to clarify the involvement of MRPs in THC transport, with the similar approach (Transwell and animal studies) we used for the other placental transporter investigated in this dissertation.

While our study has several limitations in elucidating the precise mechanisms underlying reduced fetal THC exposure, **Chapter 3** produced some provocative findings when we quantified the extent of both fetal and maternal brain exposure ratios of THC. Notably, we observed a significant decrease in the maternal brain-to-maternal plasma exposure ratio of THC in P-gp deficient pregnant mice compared to wild-type controls. However, this was based on the total concentration not the unbound concentration. After excluding technical issues and differences in the unbound fraction between maternal plasma and brain homogenates, we have proposed a new hypothesis regarding the potential involvement of FABPs in the disposition of THC in the maternal brain, given their established roles in THC binding as described in **Section 1.4.2**. We hypothesize that knocking out P-gp results in decreased expression of Fabps in the mouse brain. As a result, THC binding to Fabp 3/5/7 in the maternal brain will be significantly lower in P-gp-deficient pregnant mice compared to wild-type pregnant mice. Consequently, at steady state, the total THC brain concentration will be significantly reduced in the P-gp-deficient pregnant mice assuming that passive diffusion is the only mechanism of THC transfer across the blood-brain barrier. Studies need to be performed to test this hypothesis. Addressing this knowledge gap would advance our understanding of not only cannabinoid-transporter interactions, but also of results obtained from utilizing these animal models to study P-gp transport of other drugs.

Although THC and its major metabolites are not substrates of the placental transporters we investigated, surprisingly, we found that THC and THC-COOH are substrates, but not inhibitors, of OCT1 at their pharmacologically relevant concentrations (**Chapter 4**). OCT1 is characterized as a cation-selective transporter, which makes our observation counterintuitive given that THC, at physiological pH, is predominantly uncharged (neutral) rather than a cation. However, OCT1 has also been shown to transport a spectrum of noncanonical substrates, including positively charged, uncharged, zwitterionic, and even negatively charged compounds

[190], which may at least partially explain our observation. Despite this, the fraction of THC and THC-COOH transported by OCT1 under physiological conditions remains unknown, representing another important area for future studies with primary human hepatocytes and selective inhibitors of OCT1. Moreover, no studies have reported that cannabis or THC consumption leads to *in vivo* cannabinoid-drug interactions involving OCT1 substrates such as metformin and imatinib [191]. Therefore, such future *in vivo* studies are necessary to address this knowledge gap. In **Chapters 2 and 4** we also investigated the inhibition potential of THC and its major metabolites towards several placental and hepatic transporters at their pharmacologically relevant concentrations. None of the examined cannabinoids demonstrated inhibitory activity against any of the investigated transporters. This indicates that, for the transporters studied, THC and its major metabolites are unlikely to produce *in vivo* transporter-mediated cannabinoid-drug interactions. Such studies need to be extended to a broader network of transporters such as MRPs. However, the localization of murine Mrp transporters differs from that of their human orthologs. Specifically, in both human and murine placenta, Mrp2 is found on the apical side of the syncytiotrophoblast [110]. In contrast, murine Mrp4, Mrp5, and Mrp6 are localized to the basal membrane of the syncytiotrophoblast, whereas their human counterparts are situated on the apical side [110]. Therefore, species differences in transporter localization must be carefully considered when investigating other potential transporters responsible for reduced fetal exposure to cannabinoids. In addition to MRPs, transporters such as OAT10—an understudied basal uptake transporter—could also be potential candidates. Further research is needed to clarify the physiological and pharmacological roles of these transporters in determining fetal exposure to various compounds.

In **Chapters 2 and 4**, we found that THC-COOH is a weak substrate of human BCRP and OCT3. Whether THC-COOH is a substrate of mouse Oct3 needs to be investigated. Nevertheless, in **Chapter 3**, we did not observe a significant increase in fetal-to-maternal plasma or placenta-to-maternal geometric mean THC-COOH AUC ratio in *Bcrp*$^{-/-}$ mice versus wild-type mice. Moreover, given the low unbound fraction of THC-COOH *in vivo*, whether these observations can be translated into *in vivo* cannabinoid-drug interactions remains to be determined.

In our studies, we assumed that THC, the primary intoxicating constituent of cannabis, and its major metabolite, 11-OH THC are the perpetrators of the neurodevelopmental deficits

caused by *in utero* exposure to cannabis constituents. We cannot discount the possibility that these deficits are caused by other constituents of cannabis. Animal studies comparing the effects of cannabis versus synthetic THC can help answer this question.

5.2 Other Future studies

While mechanistic characterization of reduced fetal THC exposure remains critical, the neurodevelopmental consequences of prenatal cannabis exposure are still not fully understood. To address this knowledge gap, we are conducting integrated transcriptomic and proteomic analyses of the human fetal brain tissues from women who consumed cannabis during pregnancy and terminated their pregnancy during the 1st (T1) or 2nd trimester (T2). Our preliminary data indicate that cannabis-associated dysregulation is more pronounced in T2 brain, with observed disruption of several key neurodevelopmental pathways such as Wnt signaling, cadherin-mediated cell adhesion, synaptic function, and retinoic acid metabolism, alongside upregulation of ribosomal functions and RNA processing pathways. Therefore, integrating multiomics signatures with fetal exposure data could facilitate evaluation of neurodevelopmental risks of *in utero* fetal exposure to THC.

References

1. Volkow, N. D., Han, B., Compton, W. M. & McCance-Katz, E. F. Self-reported Medical and Nonmedical Cannabis Use Among Pregnant Women in the United States. *JAMA* **322**, 167 (2019).

2. Morales, P., Reggio, P. H. & Jagerovic, N. An Overview on Medicinal Chemistry of Synthetic and Natural Derivatives of Cannabidiol. *Front Pharmacol* **8**, 422 (2017).

3. Huestis, M. A., Henningfield, J. E. & Cone, E. J. Blood cannabinoids. i. absorption of thc and formation of 11-oh-thc and thccooh during and after smoking marijuana. *J Anal Toxicol* **16**, 276–282 (1992).

4. Bailey, J. R., Cunny, H. C., Paule, M. G. & Slikker, W. J. Fetal disposition of delta 9-tetrahydrocannabinol (THC) during late pregnancy in the rhesus monkey. *Toxicol Appl Pharmacol* **90**, 315–321 (1987).

5. Human Placental Transfer of Cannabinoids. *New England Journal of Medicine* **311**, 797–797 (1984).

6. Mao, Q. & Chen, X. An update on placental drug transport and its relevance to fetal drug exposure. *Medical review* **2**, 501–511 (2022).

7. Spiro, A. S., Wong, A., Boucher, A. A. & Arnold, J. C. Enhanced brain disposition and effects of Δ 9-tetrahydrocannabinol in P-glycoprotein and breast cancer resistance protein knockout mice. *PLoS One* **7**, 3–8 (2012).

8. Bonhomme-Faivre, L., Benyamina, A., Reynaud, M., Farinotti, R. & Abbara, C. Disposition of Δ9 tetrahydrocannabinol in CF1 mice deficient in mdr1a P-glycoprotein. *Addiction Biology* **13**, 295–300 (2008).

9. Hillowe, A. *et al.* Fatty acid binding protein 5 regulates docetaxel sensitivity in taxane-resistant prostate cancer cells. *PLoS One* **18**, e0292483 (2023).

10. Lucas, C. J., Galettis, P. & Schneider, J. The pharmacokinetics and the pharmacodynamics of cannabinoids. *Br J Clin Pharmacol* **84**, 2477–2482 (2018).

11. Maliepaard, M. *et al.* Subcellular localization and distribution of the Breast Resistance Protein Transporter in normal human tissues. *Cancer Res* **61**, 3458–3464 (2001).

12. Macfarland, A., Abramovich, D. R., Ewen, S. W. B. & Pearson, C. K. Stage-specific distribution of P-glycoprotein in first-trimester and full-term human placenta. *Histochem J* **26**, 417–423 (1994).

13. Anoshchenko, O. *et al.* Gestational Age-Dependent Abundance of Human Placental Transporters as Determined by Quantitative Targeted Proteomics. *Drug Metabolism and Disposition* **48**, 735–741 (2020).

14. Agarwal, S. *et al.* Quantitative Proteomics of Transporter Expression in Brain Capillary Endothelial Cells Isolated from P-Glycoprotein (P-gp), Breast Cancer Resistance Protein (Bcrp), and P-gp/Bcrp Knockout Mice. *Drug Metabolism and Disposition* **40**, 1164 (2012).

15. Young-Wolff, K. C. *et al.* Rates of Prenatal Cannabis Use Among Pregnant Women Before and During the COVID-19 Pandemic. *JAMA* **326**, 1745–1747 (2021).

16. Badowski, S. & Smith, G. Cannabis use during pregnancy and postpartum. *Canadian Family Physician* **66**, 98 (2020).

17. Reece, A. S. & Hulse, G. K. Canadian Cannabis Consumption and Patterns of Congenital Anomalies: An Ecological Geospatial Analysis. *J Addict Med* **14**, E195–E210 (2020).

18. Crocq, M. A. History of cannabis and the endocannabinoid system. *Dialogues Clin Neurosci* **22**, 223–228 (2020).

19. Lucas, C. J., Galettis, P. & Schneider, J. Pharmacokinetics and the pharmacodynamics of cannabinoids. *Br J Clin Pharmacol* **84**, 2477–2482 (2003).

20. Bow, E. W. & Rimoldi, J. M. The Structure–Function Relationships of Classical Cannabinoids: CB1/CB2 Modulation. *Perspect Medicin Chem* **8**, 17 (2016).

21. Suárez-Jacobo, Á., Díaz Pacheco, A., Bonales-Alatorre, E., Castillo-Herrera, G. A. & García-Fajardo, J. A. Cannabis Extraction Technologies: Impact of Research and Value Addition in Latin America. *Molecules 2023, Vol. 28, Page 2895* **28**, 2895 (2023).

22. McPartland, J. M. Cannabis Systematics at the Levels of Family, Genus, and Species. *Cannabis Cannabinoid Res* **3**, 203 (2018).

23. Gloss, D. An Overview of Products and Bias in Research. *Neurotherapeutics* **12**, 731 (2015).

24. Bajtel, Á. *et al.* The Safety of Dronabinol and Nabilone: A Systematic Review and Meta-Analysis of Clinical Trials. *Pharmaceuticals* **15**, 100 (2022).

25. Ward, A. & Holmes, B. Nabilone: A Preliminary Review of its Pharmacological Properties and Therapeutic Use. *Drugs* **30**, 127–144 (1985).

26. Spanagel, R. & Bilbao, A. Approved cannabinoids for medical purposes – Comparative systematic review and meta-analysis for sleep and appetite. *Neuropharmacology* **196**, 108680 (2021).

27. Sharma, P., Murthy, P. & Bharath, M. M. S. Chemistry, Metabolism, and Toxicology of Cannabis: Clinical Implications. *Iran J Psychiatry* **7**, 149 (2012).

28. Mechoulam, R. Plant cannabinoids: a neglected pharmacological treasure trove. *Br J Pharmacol* **146**, 913 (2005).

29. Skopp, G. & Pötsch, L. An investigation of the stability of free and glucuronidated 11-nor-delta9-tetrahydrocannabinol-9-carboxylic acid in authentic urine samples. *J Anal Toxicol* **28**, 35–40 (2004).

30. Garrett, E. R. & Hunt, C. A. Physicochemical properties, solubility, and protein binding of Δ9 -tetrahydrocannabinol. *J Pharm Sci* **63**, 1056–1064 (1974).

31. Huestis, M. A. Human Cannabinoid Pharmacokinetics. *Chem Biodivers* **4**, 1770–1804 (2007).

32. Thomas, B., Compton, D. & Martin, B. Characterization of the lipophilicity of natural and synthetic analogs of delta 9-tetrahydrocannabinol and its relationship to pharmacological potency. *J Pharmacol Exp Ther.* **255**, 624–630 (1990).

33. Hartman, R. L. *et al.* Controlled vaporized cannabis, with and without alcohol: subjective effects and oral fluid-blood cannabinoid relationships. *Drug Test Anal* **8**, 690–701 (2016).

34. Patilea-Vrana, G. I. & Unadkat, J. D. Quantifying Hepatic Enzyme Kinetics of (-)-Δ9-Tetrahydrocannabinol (THC) and Its Psychoactive Metabolite, 11-OH-THC, through In Vitro Modeling. *Drug Metab Dispos* **47**, 743–752 (2019).

35. Skopp, G., Pötsch, L., Mauden, M. & Richter, B. Partition coefficient, blood to plasma ratio, protein binding and short-term stability of 11-nor-Δ9-carboxy tetrahydrocannabinol glucuronide. *Forensic Sci Int* **126**, 17–23 (2002).

36. Bouquet, E. *et al.* Adverse events of recreational cannabis use during pregnancy reported to the French Addictovigilance Network between 2011 and 2020. *Scientific Reports 2022 12:1* **12**, 1–10 (2022).

37. Young-Wolff, K. C., Adams, S. R., Wi, S., Weisner, C. & Conway, A. Routes of Cannabis Administration Among Females in the Year Before and During Pregnancy: Results from a Pilot Project. *Addictive behaviors* **100**, 106125 (2019).

38. Freeman, T. P. & Lorenzetti, V. ‘Standard THC units’: a proposal to standardize dose across all cannabis products and methods of administration. *Addiction* **115**, 1207–1216 (2020).

39. Kleinhans, N. M. *et al.* High-Potency Prenatal Cannabis Exposure and Birth Outcome Measures. *Children* **11**, 1436 (2024).

40. Westfall, R. E., Janssen, P. A., Lucas, P. & Capler, R. Survey of medicinal cannabis use among childbearing women: patterns of its use in pregnancy and retroactive self-assessment of its efficacy against ‘morning sickness’. *Complement Ther Clin Pract* **12**, 27–33 (2006).

41. Vanstone, M. *et al.* Reasons for cannabis use during pregnancy and lactation: A qualitative study. *CMAJ. Canadian Medical Association Journal* **193**, E1906–E1914 (2021).

42. Young-Wolff, K. C. *et al.* Prenatal Cannabis Use and Maternal Pregnancy Outcomes. *JAMA Intern Med* **184**, 1083–1093 (2024).

43. Corsi, D. J. *et al.* Maternal cannabis use in pregnancy and child neurodevelopmental outcomes. *Nature Medicine 2020 26:10* **26**, 1536–1540 (2020).

44. Tadesse, A. W., Dachew, B. A., Ayano, G., Betts, K. & Alati, R. Prenatal cannabis use and the risk of attention deficit hyperactivity disorder and autism spectrum disorder in offspring: A systematic review and meta-analysis. *J Psychiatr Res* **171**, 142–151 (2024).

45. Paul, S. E. *et al.* Associations Between Prenatal Cannabis Exposure and Childhood Outcomes: Results From the ABCD Study. *JAMA Psychiatry* **78**, 64–76 (2021).

46. Day, N. L. *et al.* Effect of prenatal marijuana exposure on the cognitive development of offspring at age three. *Neurotoxicol Teratol* **16**, 169–175 (1994).

47. Milligan, A. L., Szabo-Pardi, T. A. & Burton, M. D. Cannabinoid Receptor Type 1 and Its Role as an Analgesic: An Opioid Alternative? *J Dual Diagn* **16**, 106–119 (2020).

48. Vučkovic, S., Srebro, D., Vujovic, K. S., Vučetic, Č. & Prostran, M. Cannabinoids and pain: New insights from old molecules. *Front Pharmacol* **9**, 416167 (2018).

49. Kendall, D. A. & Yudowski, G. A. Cannabinoid receptors in the central nervous system: Their signaling and roles in disease. *Front Cell Neurosci* **10**, 227786 (2017).

50. Zagzoog, A., Cabecinha, A., Abramovici, H. & Laprairie, R. B. Modulation of type 1 cannabinoid receptor activity by cannabinoid by-products from Cannabis sativa and non-cannabis phytomolecules. *Front Pharmacol* **13**, 956030 (2022).

51. Bie, B., Wu, J., Foss, J. F. & Naguib, M. An overview of the cannabinoid type 2 receptor system and its therapeutic potential. *Curr Opin Anaesthesiol* **31**, 407–414 (2018).

52. Pertwee, R. G. The diverse CB1 and CB2 receptor pharmacology of three plant cannabinoids: Δ9-tetrahydrocannabinol, cannabidiol and Δ9-tetrahydrocannabivarin. *Br J Pharmacol* **153**, 199–215 (2008).

53. Hall, W. & Solowij, N. Adverse effects of cannabis. *Lancet* **352**, 1611–1616 (1998).

54. Ashton, C. H. Pharmacology and effects of cannabis: A brief review. *The British Journal of Psychiatry* **178**, 101–106 (2001).

55. Grotenhermen, F. Pharmacokinetics and Pharmacodynamics of Cannabinoids. *Clinical Pharmacokinetics 2003 42:4* **42**, 327–360 (2012).

56. Ghasemiesfe, M., Ravi, D., Casino, T., Korenstein, D. & Keyhani, S. Acute Cardiovascular Effects of Marijuana Use. *J Gen Intern Med* **35**, 969–974 (2020).

57. Hartley, J., Nogrady, S. & Seaton, A. Bronchodilator effect of delta1-tetrahydrocannabinol. *Br J Clin Pharmacol* **5**, 523 (1978).

58. Hartman, R. L. *et al.* Controlled Cannabis Vaporizer Administration: Blood and Plasma Cannabinoids with and without Alcohol. *Clin Chem* **61**, 850–869 (2015).

59. Xiong, X. *et al.* Cannabis suppresses antitumor immunity by inhibiting JAK/STAT signaling in T cells through CNR2. *Signal Transduction and Targeted Therapy 2022 7:1* **7**, 1–13 (2022).

60. Perez-Reyes, M., Timmons, M. C., Lipton, M. A., Davis, K. H. & Wall, M. E. Intravenous Injection in Man of Δ9-Tetrahydrocannabinol and 11-OH-Δ9-Tetrahydrocannabinol. *Science (1979)* **177**, 633–635 (1972).

61. Lemberger, L., Martz, R., Rodda, B., Forney, R. & Rowe, H. Comparative Pharmacology of Δ9-Tetrahydrocannabinol and its Metabolite, 11-OH-Δ9-Tetrahydrocannabinol. *Journal of Clinical Investigation* **52**, 2411 (1973).

62. Zamarripa, C. A. *et al.* Assessment of Orally Administered Δ9-Tetrahydrocannabinol When Coadministered With Cannabidiol on Δ9-Tetrahydrocannabinol

Pharmacokinetics and Pharmacodynamics in Healthy Adults: A Randomized Clinical Trial. *JAMA Netw Open* **6**, e2254752 (2023).

63. López-Pelayo, H. *et al.* Early, Chronic, and Acute Cannabis Exposure and Their Relationship With Cognitive and Behavioral Harms. *Front Psychiatry* **12**, 643556 (2021).

64. Volkow, N. D., Baler, R. D., Compton, W. M. & Weiss, S. R. B. Adverse Health Effects of Marijuana Use. *New England Journal of Medicine* **370**, 2219–2227 (2014).

65. Russell, C., Rueda, S., Room, R., Tyndall, M. & Fischer, B. Routes of administration for cannabis use – basic prevalence and related health outcomes: A scoping review and synthesis. *International Journal of Drug Policy* **52**, 87–96 (2018).

66. Cox, E. J. *et al.* A marijuana-drug interaction primer: Precipitants, pharmacology, and pharmacokinetics. *Pharmacol Ther* **201**, 25–38 (2019).

67. Ohlsson, A. *et al.* Plasma delta-9-tetrahydrocannabinol concentrations and clinical effects after oral and intravenous administration and smoking. *Clin Pharmacol Ther* **28**, 409–416 (1980).

68. Schwilke, E. W. *et al.* Δ9-Tetrahydrocannabinol (THC), 11-Hydroxy-THC, and 11-Nor-9-carboxy-THC Plasma Pharmacokinetics during and after Continuous High-Dose Oral THC. *Clin Chem* **55**, 2180 (2009).

69. Lunn, S. *et al.* Human Pharmacokinetic Parameters of Orally Administered Δ9-Tetrahydrocannabinol Capsules Are Altered by Fed Versus Fasted Conditions and Sex Differences. *Cannabis Cannabinoid Res* **4**, 255 (2019).

70. Yabut, K. C. B., Winnie Wen, Y., Simon, K. T. & Isoherranen, N. CYP2C9, CYP3A and CYP2C19 metabolize Δ9-tetrahydrocannabinol to multiple metabolites but metabolism is affected by human liver fatty acid binding protein (FABP1). *Biochem Pharmacol* **228**, 116191 (2024).

71. Elmes, M. W. *et al.* FABP1 controls hepatic transport and biotransformation of Δ9-THC. *Scientific Reports 2019 9:1* **9**, 1–13 (2019).

72. Elmes, M. W. *et al.* Fatty acid-binding proteins (FABPs) are intracellular carriers for Δ9-tetrahydrocannabinol (THC) and cannabidiol (CBD). *Journal of Biological Chemistry* **290**, 8711–8721 (2015).

73. Campbell, F. M., Bush, P. G., Veerkamp, J. H. & Dutta-Roy, A. K. Detection and cellular localization of plasma membrane-associated and cytoplasmic fatty acid-binding proteins in human placenta. *Placenta* **19**, 409–415 (1998).

74. Dutta-Roy, A. K. Transport mechanisms for long-chain polyunsaturated fatty acids in the human placenta. *American Journal of Clinical Nutrition* **71**, (2000).

75. Duttaroy, A. K. Transport of fatty acids across the human placenta: A review. *Prog Lipid Res* **48**, 52–61 (2009).

76. Kumar, A. R. *et al.* Quantification and prediction of human fetal (-)-Δ9-tetrahydrocannabinol/(±)-11-OH-Δ9-tetrahydrocannabinol exposure during pregnancy to inform fetal cannabis toxicity. *Nature Communications 2025 16:1* **16**, 1–14 (2025).

77. Ohlsson, A. *et al.* Single dose kinetics of deuterium labelled Δ1-tetrahydrocannabinol in heavy and light cannabis users. *Biol Mass Spectrom* **9**, 6–10 (1982).

78. Kemp, P. M., Cardona, P. S., Chaturvedi, A. K. & Soper, J. W. Distribution of Δ9-Tetrahydrocannabinol and 11-Nor-9-Carboxy-Δ9-Tetrahydrocannabinol Acid in Postmortem Biological Fluids and Tissues From Pilots Fatally Injured in Aviation Accidents. *J Forensic Sci* **60**, 942–949 (2015).

79. Cliburn, K. D., Huestis, M. A., Wagner, J. R. & Kemp, P. M. Cannabinoid distribution in fatally-injured pilots' postmortem fluids and tissues. *Forensic Sci Int* **329**, 111075 (2021).

80. Withey, S. L., Bergman, J., Huestis, M. A., George, S. R. & Madras, B. K. THC and CBD Blood and Brain Concentrations Following Daily Administration to Adolescent Primates. *Drug Alcohol Depend* **213**, 108129 (2020).

81. Torrens, A. *et al.* Comparative pharmacokinetics of Δ9-tetrahydrocannabinol in adolescent and adult male mice. *Journal of Pharmacology and Experimental Therapeutics* **374**, 151–160 (2020).

82. Nahas, G. G., Frick, H. C., Lattimer, J. K., Latour, C. & Harvey, D. Pharmacokinetics of THC in brain and testis, male gametotoxicity and premature apoptosis of spermatozoa. *Human Psychopharmacology: Clinical and Experimental* **17**, 103–113 (2002).

83. Gunasekaran, N. *et al.* Reintoxication: the release of fat-stored Δ9-tetrahydrocannabinol (THC) into blood is enhanced by food deprivation or ACTH exposure. *Br J Pharmacol* **158**, 1330–1337 (2009).

84. Kumar, A. R., Patilea-Vrana, G. I., Anoshchenko, O. & Unadkat, J. D. Characterizing and Quantifying Extrahepatic Metabolism of (2)-Δ9-Tetrahydrocannabinol (THC) and

Its Psychoactive Metabolite, (±)-11-Hydroxy-Δ9-THC (11-OH-THC). *Drug Metabolism and Disposition* **50**, 734–740 (2022).

85. Beers, J. L., Authement, A. K., Isoherranen, N. & Jackson, K. D. Cytosolic Enzymes Generate Cannabinoid Metabolites 7-Carboxycannabidiol and 11-Nor-9-carboxytetrahydrocannabinol. *ACS Med Chem Lett* **14**, 614–620 (2023).

86. Gaston, T. E. & Friedman, D. Pharmacology of cannabinoids in the treatment of epilepsy. *Epilepsy Behav* **70**, 313–318 (2017).

87. Eichler, M. *et al.* Heat exposure of Cannabis sativa extracts affects the pharmacokinetic and metabolic profile in healthy male subjects. *Planta Med* **78**, 686–691 (2012).

88. Tomson, T., Lindbom, U., Ekqvist, B. & Sundqvist, A. Disposition of Carbamazepine and Phenytoin in Pregnancy. *Epilepsia* **35**, 131–135 (1994).

89. Hebert, M. F. *et al.* Effects of pregnancy on CYP3A and P-glycoprotein activities as measured by disposition of midazolam and digoxin: A University of Washington specialized center of research study. *Clin Pharmacol Ther* **84**, 248–253 (2008).

90. Lemberger, L., Axelrod, J. & Kopin, I. J. Metabolism and disposition of Δ9-tetrahydrocannabinol in man. *Pharmacol Rev* **23**, 371–380 (1971).

91. Huestis, M. A. & Cone, E. J. Urinary excretion half-life of 11-nor-9-carboxy-delta9-tetrahydrocannabinol in humans. *Ther Drug Monit* **20**, 570–576 (1998).

92. Vandevenne, M., Vandenbussche, H. & Verstraete, A. Detection Time of Drugs of Abuse in Urine. *Acta Clin Belg* **55**, 323–333 (2000).

93. Goullé, J. P., Saussereau, E. & Lacroix, C. Pharmacocinétique du delta-9-tétrahydrocannabinol (THC). *Ann Pharm Fr* **66**, 232–244 (2008).

94. Mazur, A. *et al.* Characterization of Human Hepatic and Extrahepatic UDP-Glucuronosyltransferase Enzymes Involved in the Metabolism of Classic Cannabinoids. *Drug Metabolism and Disposition* **37**, 1496 (2009).

95. Patilea-Vrana, G. I., Anoshchenko, O. & Unadkat, J. D. Hepatic enzymes relevant to the disposition of (2)-δ9-tetrahydrocannabinol (thc) and its psychoactive metabolite, 11-oh-thc. *Drug Metabolism and Disposition* **47**, 249–256 (2019).

96. Patilea-Vrana, G. I. & Unadkat, J. D. Development and verification of a linked d9-thc/11-oh-thc physiologically based pharmacokinetic model in healthy,

nonpregnant population and extrapolation to pregnant womens. *Drug Metabolism and Disposition* **49**, 509 (2021).

97. Lemberger, L., Crabtree, R. E. & Rowe, H. M. 11-Hydroxy-Δ'-tetrahydrocannabinol: Pharmacology, disposition, and metabolism of a major metabolite of marihuana in man. *Science (1979)* **177**, 62–64 (1972).

98. Kelly, P. & Jones, R. T. Metabolism of tetrahydrocannabinol in frequent and infrequent marijuana users. *J Anal Toxicol* **16**, 228–235 (1992).

99. Kumar, A. R. *et al.* Understanding the Mechanism and Extent of Transplacental Transfer of (-)-Δ(9)-Tetrahydrocannabinol (THC) in the Perfused Human Placenta to Predict In Vivo Fetal THC Exposure. *Clin Pharmacol Ther* **114**, 446–458 (2023).

100. Herrick, E. J. & Bordoni, B. Embryology, Placenta. *StatPearls* (2023).

101. Li, X., Li, Z. H., Wang, Y. X. & Liu, T. H. A comprehensive review of human trophoblast fusion models: recent developments and challenges. *Cell Death Discovery 2023 9:1* **9**, 1–14 (2023).

102. Boss, A. L., Chamley, L. W. & James, J. L. Placental formation in early pregnancy: how is the centre of the placenta made? *Hum Reprod Update* **24**, 750–760 (2018).

103. Yamashita, M. & Markert, U. R. Overview of Drug Transporters in Human Placenta. *Int J Mol Sci* **22**, 13149 (2021).

104. Chen, X. *et al.* Efflux transporters in drug disposition during pregnancy. *Drug Metabolism and Disposition* **52**, 1–31 (2024).

105. Coan, P. M., Ferguson-Smith, A. C. & Burton, G. J. Developmental Dynamics of the Definitive Mouse Placenta Assessed by Stereology. *Biol Reprod* **70**, 1806–1813 (2004).

106. Uchida, Y., Ohtsuki, S., Kamiie, J. & Terasaki, T. Blood-Brain Barrier (BBB) Pharmacoproteomics (PPx): Reconstruction of In Vivo Brain Distribution of 11 P-glycoprotein Substrates based on the BBB Transporter Protein Concentration, In Vitro Intrinsic Transport Activity, and Unbound Fraction in Plasma and.... *Journal of Pharmacology and Experimental Therapeutics* **339**, 579–588 (2011).

107. Enders, A. C. & Blankenship, T. N. Comparative placental structure. *Adv Drug Deliv Rev* **38**, 3–15 (1999).

108. Ceckova-Novotna, M., Pavek, P. & Staud, F. P-glycoprotein in the placenta: Expression, localization, regulation and function. *Reproductive Toxicology* **22**, 400–410 (2006).

109. Han, L. W., Gao, C. & Mao, Q. An update on expression and function of P-gp/ABCB1 and BCRP/ABCG2 in the placenta and fetus. *Expert Opin Drug Metab Toxicol* **14**, 817–829 (2018).

110. Aleksunes, L. M., Cui, Y. & Klaassen, C. D. Prominent Expression of Xenobiotic Efflux Transporters in Mouse Extraembryonic Fetal Membranes Compared to Placenta. *Drug Metab Dispos* **36**, 1960 (2008).

111. Lee, N. *et al.* Organic cation Transporter 3 facilitates fetal exposure to metformin during pregnancy. *Mol Pharmacol* **94**, 1125–1131 (2018).

112. Smit, J. W., Huisman, M. T., Van Tellingen, O., Wiltshire, H. R. & Schinkel, A. H. Absence or pharmacological blocking of placental P-glycoprotein profoundly increases fetal drug exposure. *J Clin Invest* **104**, 1441–1447 (1999).

113. Li, Y. *et al.* Role of Human Breast Cancer Related Protein versus P-Glycoprotein as an Efflux Transporter for Benzylpenicillin: Potential Importance at the Blood-Brain Barrier. *PLoS One* **11**, e0157576 (2016).

114. Szatmári, P. & Ducza, E. Changes in Expression and Function of Placental and Intestinal P-gp and BCRP Transporters during Pregnancy. *Int J Mol Sci* **24**, 13089 (2023).

115. Imperio, G. E. *et al.* Gestational age-dependent gene expression profiling of ATP-binding cassette transporters in the healthy human placenta. *J Cell Mol Med* **23**, 610–618 (2019).

116. Hathcock, S. F. *et al.* Induction of P-glycoprotein overexpression in brain endothelial cells as a model to study blood-brain barrier efflux transport. *Frontiers in drug delivery* **4**, 1433453 (2024).

117. Miller, D. S., Bauer, B. & Hartz, A. M. S. Modulation of P-glycoprotein at the Blood-Brain Barrier: Opportunities to Improve CNS Pharmacotherapy. *Pharmacol Rev* **60**, 196 (2008).

118. Van Assema, D. M. E. *et al.* P-Glycoprotein Function at the Blood–Brain Barrier: Effects of Age and Gender. *Mol Imaging Biol* **14**, 771 (2012).

119. Eisenblätter, T. & Galla, H. J. A new multidrug resistance protein at the blood-brain barrier. *Biochem Biophys Res Commun* **293**, 1273–1278 (2002).

120. Dawson, P. A., Lan, T. & Rao, A. Bile acid transporters. *J Lipid Res* **50**, 2340 (2009).

121. Blundell, C. *et al.* Placental Drug Transport-on-a-Chip: A Microengineered In Vitro Model of Transporter-Mediated Drug Efflux in the Human Placental Barrier. *Adv Healthc Mater* **7**, 1700786 (2018).

122. Atkinson, D. E., Greenwood, S. L., Sibley, C. P., Glazier, J. D. & Fairbairn, L. J. Role of MDR1 and MRP1 in trophoblast cells, elucidated using retroviral gene transfer. *Am J Physiol Cell Physiol* **285**, 584–591 (2003).

123. Fedi, A. *et al.* In vitro models replicating the human intestinal epithelium for absorption and metabolism studies: A systematic review. *Journal of Controlled Release* **335**, 247–268 (2021).

124. Scott, R., Neeley, C. & Granchelli, J. Application properties of materials used for porous membranes in cell culture inserts. *https://www.thermofisher.com/TFS-Assets/LCD/Application-Notes/ANLSPCCINSERTMEM-Porous-membrane-materials.pdf* (2013).

125. Marchitti, S. A. *et al.* Inhibition of the Human ABC Efflux Transporters P-gp and BCRP by the BDE-47 Hydroxylated Metabolite 6-OH-BDE-47: Considerations for Human Exposure. *Toxicol Sci* **155**, 270 (2016).

126. Kurosawa, K., Chiba, K., Noguchi, S., Nishimura, T. & Tomi, M. Development of a pharmacokinetic model of transplacental transfer of metformin to predict in vivo fetal exposure. *Drug Metabolism and Disposition* **48**, 1293–1302 (2020).

127. Ni, Z. & Mao, Q. ATP-binding cassette efflux transporters in human placenta. *Curr Pharm Biotechnol* **12**, 674–685 (2011).

128. Zhang, Z. *et al.* Development of a novel maternal-fetal physiologically based pharmacokinetic model I: Insights into factors that determine fetal drug exposure through simulations and sensitivity analyses. *Drug Metabolism and Disposition* **45**, 920–938 (2017).

129. Zhang, Z. *et al.* Development of a novel maternal-fetal physiologically based pharmacokinetic model I: Insights into factors that determine fetal drug exposure through simulations and sensitivity analyses. *Drug Metabolism and Disposition* **45**, 920–938 (2017).

130. Storelli, F., Anoshchenko, O. & Unadkat, J. D. Successful Prediction of Human Steady-State Unbound Brain-to-Plasma Concentration Ratio of P-gp Substrates

Using the Proteomics-Informed Relative Expression Factor Approach. *Clin Pharmacol Ther* **110**, 432 (2021).

131. Anoshchenko, O., Storelli, F. & Unadkat, J. D. Successful Prediction of Human Fetal Exposure to P-Glycoprotein Substrate Drugs Using the Proteomics-Informed Relative Expression Factor Approach and PBPK Modeling and Simulation. *Drug Metab Dispos* **49**, 919–928 (2021).

132. Booth, J. K. & Bohlmann, J. Terpenes in Cannabis sativa – From plant genome to humans. *Plant Science* **284**, 67–72 (2019).

133. Grotenhermen, F. Pharmacokinetics and Pharmacodynamics of Cannabinoids. *Clin Pharmacokinet* **42**, 327–360 (2003).

134. Carliner, H. *et al.* Cannabis use, attitudes, and legal status in the U.S.: A review. **104**, 13–23 (2017).

135. Qian, Y., Gurley, B. J. & Markowitz, J. S. The Potential for Pharmacokinetic Interactions between Cannabis Products and Conventional Medications. *J Clin Psychopharmacol* **39**, 462–471 (2019).

136. Stout, S. M. & Cimino, N. M. Exogenous cannabinoids as substrates, inhibitors, and inducers of human drug metabolizing enzymes: A systematic review. *Drug Metab Rev* **46**, 86–95 (2014).

137. Ueda, K. *et al.* The human multidrug resistance (mdr1) gene. cDNA cloning and transcription initiation. *Journal of Biological Chemistry* **262**, 505–508 (1987).

138. Hodges, L. Very important phamacogene summary ABCB1. *Pharmacogenet Genomics* **21**, 152–161 (2011).

139. Allikmets, R., Schriml, L. M., Hutchinson, A., Romano-Spica, V. & Dean, M. A human placenta-specific ATP-binding cassette gene (ABCP) on chromosome 4q22 that is involved in multidrug resistance. *Cancer Res* **58**, 5337–5339 (1998).

140. Doyle, L. A. *et al.* A multidrug resistance transporter from human MCF-7 breast cancer cells. *Proc Natl Acad Sci U S A* **95**, 15665–15670 (1998).

141. Miyake, K. *et al.* Molecular cloning of cDNAs which are highly overexpressed in mitoxantrone-resistant cells: demonstration of homology to ABC transport genes. *Cancer Res* **59**, 8–13 (1999).

142. Aronica, E. *et al.* Localization of breast cancer resistance protein (BCRP) in microvessel endothelium of human control and epileptic brain. *Epilepsia* **46**, 849–857 (2005).

143. Fetsch, P. A. *et al.* Localization of the ABCG2 mitoxantrone resistance-associated protein in normal tissues. *Cancer Lett* **235**, 84–92 (2006).

144. Mao, Q. & Unadkat, J. D. Role of the Breast Cancer Resistance Protein (BCRP/ABCG2) in Drug Transport—an Update. *AAPS Journal* **17**, 65–82 (2015).

145. Safar, Z., Kis, E., Erdo, F., Zolnerciks, J. K. & Krajcsi, P. ABCG2/BCRP: variants, transporter interaction profile of substrates and inhibitors. *Expert Opin Drug Metab Toxicol* **15**, 313–328 (2019).

146. Tournier, N. *et al.* Interaction of drugs of abuse and maintenance treatments with human P-glycoprotein (ABCB1) and breast cancer resistance protein (ABCG2). *International Journal of Neuropsychopharmacology* **13**, 905–915 (2010).

147. Karlgren, M. *et al.* A CRISPR-Cas9 Generated MDCK Cell Line Expressing Human MDR1 Without Endogenous Canine MDR1 (cABCB1): An Improved Tool for Drug Efflux Studies. *J Pharm Sci* **106**, 2909–2913 (2017).

148. Deng, F., Sjöstedt, N. & Kidron, H. The effect of albumin on MRP2 and BCRP in the vesicular transport assay. *PLoS One* **11**, 1–15 (2016).

149. Newmeyer, M. N. *et al.* Free and glucuronide whole blood cannabinoids' pharmacokinetics after controlled smoked, vaporized, and oral cannabis administration in frequent and occasional cannabis users: Identification of recent cannabis intake. *Clin Chem* **62**, 1579–1592 (2016).

150. Busby, W. F., Ackermann, J. M. & Crespi, C. L. Effect of methanol, ethanol, dimethyl sulfoxide, and acetonitrile on in vitro activities of cDNA-expressed human cytochromes P-450. *Drug Metabolism and Disposition* **27**, 246–249 (1999).

151. Bansal, S., Maharao, N., Paine, M. F. & Unadkat, J. D. Predicting the potential for cannabinoids to precipitate pharmacokinetic drug interactions via reversible inhibition or inactivation of major cytochromes P450. *Drug Metabolism and Disposition* DMD-AR-2020-000073 (2020) doi:10.1124/dmd.120.000073.

152. US Food and Drug Administration. In Vitro Drug Interaction Studies - Cytochrome P450 Enzyme and Transporter Mediated Drug Interactions. *FDA Guidance* **1**, 1–46 (2020).

153. Zhu, H. J. *et al.* Characterization of P-glycoprotein inhibition by major cannabinoids from marijuana. *Journal of Pharmacology and Experimental Therapeutics* **317**, 850–857 (2006).

154. Loo, T. W., Bartlett, M. C. & Clarke, D. M. Drug binding in human P-glycoprotein causes conformational changes in both nucleotide-binding domains. *Journal of Biological Chemistry* **278**, 1575–1578 (2003).

155. Mi, Y. & Lou, L. ZD6474 reverses multidrug resistance by directly inhibiting the function of P-glycoprotein. *Br J Cancer* **97**, 934–940 (2007).

156. Holland, M. L., Lau, D. T. T., Allen, J. D. & Arnold, J. C. The multidrug transporter ABCG2 (BCRP) is inhibited by plant-derived cannabinoids. *Br J Pharmacol* **152**, 815–824 (2007).

157. Grotenhermen, F. & Müller-Vahl, K. Medicinal Uses of Marijuana and Cannabinoids. *https://doi.org/10.1080/07352689.2016.1265360* **35**, 378–405 (2017).

158. Borst, P. & Schinkel, A. H. P-glycoprotein ABCB1: a major player in drug handling by mammals. *J Clin Invest* **123**, 4131–4133 (2013).

159. Allen, J. D., Brinkhuis, R. F., Wijnholds, J. & Schinkel, A. H. The mouse Bcrp1/Mxr/Abcp gene: Amplification and overexpression in cell lines selected for resistance to topotecan, mitoxantrone, or doxorubicin. *Cancer Res* **59**, 4237–4241 (1999).

160. Saidijam, M., Karimi Dermani, F., Sohrabi, S. & Patching, S. G. Efflux proteins at the blood–brain barrier: review and bioinformatics analysis. *Xenobiotica* **48**, 506–532 (2017).

161. Virgintino, D. *et al.* Expression of P-glycoprotein in human cerebral cortex microvessels. *Journal of Histochemistry and Cytochemistry* **50**, 1671–1676 (2002).

162. Yeboah, D. *et al.* Expression of breast cancer resistance protein (BCRP/ABCG2) in human placenta throughout gestation and at term before and after labor. *Can J Physiol Pharmacol* **84**, 1251–1258 (2006).

163. Sun, M. *et al.* Expression of the Multidrug Resistance P-Glycoprotein, (ABCB1 glycoprotein) in the Human Placenta Decreases with Advancing Gestation. *Placenta* **27**, 602–609 (2006).

164. Gabriel, H. D. *et al.* Transplacental Uptake of Glucose Is Decreased in Embryonic Lethal Connexin26-deficient Mice. *Journal of Cell Biology* **140**, 1453–1461 (1998).

165. Chen, X., Unadkat, J. D. & Mao, Q. Tetrahydrocannabinol and its major metabolites are not (or are poor) substrates or inhibitors of human P-Glycoprotein [ATP-binding cassette (ABC) B1] and breast cancer resistance protein (ABCG2). *Drug Metabolism and Disposition* **49**, 910–918 (2021).

166. Schuhmacher, J., Bühner, K. & Witt-Laido, A. Determination of the free fraction and relative free fraction of drugs strongly bound to plasma proteins. *J Pharm Sci* **89**, 1008–1021 (2000).

167. Barker, G. *et al.* Placental Water Content and Distribution. *Placenta* **15**, 47–56 (1994).

168. Eliesen, G. A. M. *et al.* Assessment of Placental Disposition of Infliximab and Etanercept in Women With Autoimmune Diseases and in the Ex Vivo Perfused Placenta. *CLINICAL PHARMACOLOGY & THERAPEUTICS | VOLUME* **108**, (2020).

169. Karschner, E. L. *et al.* Predictive model accuracy in estimating last Δ9-tetrahydrocannabinol (THC) intake from plasma and whole blood cannabinoid concentrations in chronic, daily cannabis smokers administered subchronic oral THC. *Drug Alcohol Depend* **125**, 313 (2012).

170. Davies, B. & Morris, T. Physiological parameters in laboratory animals and humans. *Pharmaceutical research* vol. 10 1093–1095 Preprint at https://doi.org/10.1023/a:1018943613122 (1993).

171. Fujita, A. *et al.* Limited Impact of Murine Placental MDR1 on Fetal Exposure of Certain Drugs Explained by Bypass Transfer Between Adjacent Syncytiotrophoblast Layers. *Pharm Res* 1–14 (2022) doi:10.1007/s11095-022-03165-6.

172. Liao, M. Z. *et al.* P-gp/ABCBl Exerts Differential Impacts On Brain and Fetal Exposure to Norbuprenorphine. *Pharmacol Res* **119**, 61 (2017).

173. Sajid, A. *et al.* Reversing the direction of drug transport mediated by the human multidrug transporter P-glycoprotein. *Proc Natl Acad Sci U S A* **117**, 29609–29617 (2020).

174. Bauer, F. *et al.* Synthesis and in vivo evaluation of [11C]tariquidar, a positron emission tomography radiotracer based on a third-generation P-glycoprotein inhibitor. *Bioorg Med Chem* **18**, 5489–5497 (2010).

175. Grant, K. S., Petroff, R., Isoherranen, N., Stella, N. & Burbacher, T. M. Cannabis use during pregnancy: Pharmacokinetics and effects on child development. *Pharmacol Ther* **182**, 133–151 (2018).

176. Ryan, S. A., Ammerman, S. D. & O'Connor, M. E. Marijuana Use During Pregnancy and Breastfeeding: Implications for Neonatal and Childhood Outcomes. *Pediatrics* **142**, e20181889 (2018).

177. Chen, X., Unadkat, J. D. & Mao, Q. Maternal and Fetal Exposure to (-)-Δ9-tetrahydrocannabinol and Its Major Metabolites in Pregnant Mice Is Differentially Impacted by P-glycoprotein and Breast Cancer Resistance Protein. *Drug Metabolism and Disposition* **51**, 269–275 (2023).

178. Watanabe, K., Yamaori, S., Funahashi, T., Kimura, T. & Yamamoto, I. Cytochrome P450 enzymes involved in the metabolism of tetrahydrocannabinols and cannabinol by human hepatic microsomes. *Life Sci* **80**, 1415–1419 (2007).

179. Pradhan-Sundd, T. & Monga, S. P. Blood-Bile Barrier: Morphology, Regulation, and Pathophysiology. *Gene Expr* **19**, 69–87 (2019).

180. Kumar, A. R. Quantification and Prediction of Human Fetal (-)-Δ9-tetrahydrocannabinol (THC)/11-OH-THC Exposure to Inform Neurodevelopmental Toxicity of Cannabis. (University of Washington, 2023).

181. Uehara, I. *et al.* Paracellular route is the major urate transport pathway across the blood-placental barrier. *Physiol Rep* **2**, e12013 (2014).

182. St.-Pierre, M. V. *et al.* Expression of members of the multidrug resistance protein family in human term placenta. *Am J Physiol Regul Integr Comp Physiol* **279**, 1495–1503 (2000).

183. Borst, P., Evers, R., Kool, M. & Wijnholds, J. A Family of Drug Transporters: the Multidrug Resistance-Associated Proteins. *J Natl Cancer Inst* **92**, 1295–1302 (2000).

184. Samodelov, S. L., Kullak-Ublick, G. A., Gai, Z. & Visentin, M. Organic Cation Transporters in Human Physiology, Pharmacology, and Toxicology. *International Journal of Molecular Sciences 2020, Vol. 21, Page 7890* **21**, 7890 (2020).

185. Gustafson, R. A., Moolchan, E. T., Barnes, A., Levine, B. & Huestis, M. A. Validated method for the simultaneous determination of Δ9-tetrahydrocannabinol (THC), 11-hydroxy-THC and 11-nor-9-carboxy-THC in human plasma using solid phase extraction and gas chromatography–mass spectrometry with positive chemical ionization. *Journal of Chromatography B* **798**, 145–154 (2003).

186. Urakami, Y., Kimura, N., Okuda, M. & Inui, K. Creatinine transport by basolateral organic cation transporter hOCT2 in the human kidney. *Pharm Res* **21**, 976–981 (2004).

187. Müller, F., Weitz, D., Mertsch, K., König, J. & Fromm, M. F. Importance of OCT2 and MATE1 for the Cimetidine-Metformin Interaction: Insights from Investigations of Polarized Transport in Single- and Double-Transfected MDCK Cells with a Focus on Perpetrator Disposition. *Mol Pharm* **15**, 3425–3433 (2018).

188. Chufan, E. E. *et al.* Multiple Transport-Active Binding Sites Are Available for a Single Substrate on Human P-Glycoprotein (ABCB1). *PLoS One* **8**, e82463 (2013).

189. Holcberg, G. *et al.* Lack of interaction of digoxin and P-glycoprotein inhibitors, quinidine and verapamil in human placenta in vitro. *European Journal of Obstetrics and Gynecology and Reproductive Biology* **109**, 133–137 (2003).

190. Redeker, K. E. M., Jensen, O., Gebauer, L., Meyer-Tönnies, M. J. & Brockmöller, J. Atypical Substrates of the Organic Cation Transporter 1. *Biomolecules* **12**, 1664 (2022).

191. Zhou, S., Zeng, S. & Shu, Y. Drug-Drug Interactions at Organic Cation Transporter 1. *Front Pharmacol* **12**, 628705 (2021).